Performance Improvement for Wireless Mesh Networks with Renewable Energy Source

by

Peng Sun

Thesis submitted to the
Faculty of Graduate and Postdoctoral Studies
In partial fulfillment of the requirements
For the Ph.D. degree in
Electrical and Computer Engineering

School of Electrical Engineering and Computer Science
Faculty of Engineering
University of Ottawa

Abstract

Multi-radio multi-channel wireless mesh networks (WMNs) have been the focus of numerous research efforts during the past few years. These efforts aimed at extending the utilization of technologies based on the IEEE 802.11 standard in large-scale communities and even for city wide networking. However, mesh nodes in these networks are typically limited in their resources (e.g., bandwidth, power and radio interfaces). Such a limitation has led to an unsatisfactory network performance as well as users dissatisfaction. This dissertation addresses three important performance issues related to WMNs, namely, network performance enhancement, network survivability and green communications.

To address the first issue, a novel quality of service (QoS) aware joint channel assignment (CA) and routing algorithm is developed. The proposed algorithm employs both dynamic and static CA techniques and corresponding link schedules that maximize the network throughput and minimize the delay and packet loss ratio. Next, the thesis addresses the problem of network survivability and theoretically analyzes the effects of node failure probabilities on the ability of the remaining network nodes to maintain their connectivity. A tight upper bound on the node failure probabilities needed to maintain full network connectivity on the one hand is first developed. On the other hand, a lower bound, at which the system loses connectivity, is also derived. We show that these bounds are dependent only on the nodes' geometric distribution and density. Based on the premise that failure of nodes in a small area may lead to failure of dependent nodes in other areas due to the quick divergence of traffic in these areas, an efficient node failure backup scheme is presented. The scheme relies on the capacity of the surviving network components in order to find new paths that do not overload the neighbours of the failed node which reduces the probability of generating congestion.

Finally, the thesis addresses the problem of realizing energy-efficient WMNs that can operate using renewable energy sources. In these systems, batteries are often used to store and regulate the use of the supplied green energy to transmit the received data at each network router in order to overcome the problem of supply fluctuating of various energy sources. To realize these networks, the behaviour of the residual energy of the battery at a heavily loaded green wireless mesh node with a general traffic arrival and energy charging functions is first analyzed. Based on obtained theoretical results, both an online and an offline QoS aware packet scheduling schemes are proposed to minimize the probability of depleting the battery.

Each of the aforementioned contributions is supported with various experimental evaluations to demonstrate the achieved performance enhancements.

Acknowledgements

I would like to express my hearty gratitude to Professor Nancy Samaan, my Ph.D. supervisor, for her constant support and guidance through the course of my Ph.D. study. She advised me on research topics and sparkled my ideas while encouraging me to delve deeper. I am grateful to her for giving me the freedom to explore broadly, and for providing me invaluable advice and infinite patience during my research. Her extensive knowledge, insightful vision, passion in doing research has motivated me and will always inspire me to do good work in future.

Contents

List of Tables

List of Figures

Abbreviations

Acronym	Description
AF	Assured Forwarding
AP	Access Point
AODV	Ad hoc On-Demand Distance Vector Routing
BF	Best Effort
CA	Channel Assignment
CBR	Constant Bit Rate
CDF	Cumulative Distribution Probability
CoS	Class-of-Service
COR	Channel Occupancy Ratio
CSMA-CA	Carrier Sense Multiple Access with Collision Avoidance
DCF	Distributed Coordination Function
DiffServ	Differentiated Services
EF	Expedited Forwarding
ETT	Expected Transmission Time
ETX	Expected Transmission Count
MAC	Media Access Control
MANET	Mobile Ad hoc Network
MGF	Moment Generating Function
MMAC	Multichannel MAC
MRMC	Multi-Radio Multi-Channel
NIC	Network Interface Card
OLSR	Optimized Link State Routing Protocol
PDF	Probability Density Function
POC	Partially Overlapping Channel
PSM	Power Saving Mode
QoS	Quality-of-Service
SIR	Signal-to-Interference-Ratio
SINR	Signal-to-Interference-plus-Noise-Ratio
WCETT	Weighted Cumulative Expected Transmission Time
WLAN	Wireless Local Area Network
WMN	Wireless Mesh Network

Chapter 1

Introduction

Wireless mesh networks (WMNs) have gained considerable interests in expanding IEEE 802.11 networks to large-scale enterprise and community scenarios, primarily because of its capability of providing wide-band ubiquitous network access to a significant number of users. In this chapter, we summarize the features of WMNs and demonstrate our research motivation and objectives.

1.1 What is Wireless Mesh Networks

Multi-Radio Multi-Channel (MRMC) wireless networks have changed the way we communicate over the past decade. These networks enable end-users to gain access to the Internet at a low-cost while achieving ease of deployment and configuration, and flexibility of construction. These properties lend MRMC networks to be an ideal technology to serve users in remote areas, for military deployments, and emergency rescues. A WMN is usually composed of wireless mesh nodes (routers or access points) and mesh clients [4]. The Infrastructure/Backbone-based WMN is the most commonly used type, in which statically positioned wireless mesh routers form the network backbone and provide access for mesh clients. Some of the wireless mesh nodes are connected with the wired network via the high capacity cable and are called mesh routers with gateway or simply gateway nodes. This gateway functionality provides the integration of WMNs with other networks such as the Internet, cellular, IEEE 802.16, etc. This kind of back-haul network architecture is reliable, scalable, cost-effective and easy to deploy [5].

One of the most important features of WMNs is that nodes communicate through a multihop path, which meets the objective of extending the coverage range of current

wireless networks and provides non-line-of-sight (NLOS) connectivity among the users. In a traditional wireless LAN, multiple clients access the network through a direct wireless link to an access point (AP). Mesh networks have some key advantages over their single-hop counterparts, which include robustness, higher bandwidth, and spatial reuse [5].

Although a WMN is similar in concept to a mobile ad hoc network, there are some important differences between these two techniques [6]. Firstly, nodes in a WMN are fixed (i.e. not mobile). Topology changes are therefore infrequent, and occur only due to occasional node failures, node-shut-down for maintenance, or addition of new nodes. Secondly, the traffic characteristics, being aggregated from a large number of traffic flows, do not change very frequently, that permits optimization of network based on measured traffic profiles. Thirdly, the traffic distribution in a WMN is typically skewed, since most of the user traffic is directed to/from a wired network. This happens because users typically want to access resources on the Internet or on the enterprise servers, and both of them most likely reside on the wired infrastructure. Finally, to serve as an effective backbone, a WMN requires proactive discovery of paths to reduce packet delays. In contrast, in most mobile ad hoc networks, reactive routing strategies are normal since additional packet latency generated by on-demand route discovery is un-acceptable.

As shown in Fig. 1.1, there are two types of nodes in MRMC wireless networks: wireless routers and wireless clients. All of the nodes in MRMC networks act as hosts to the traffic of their directly connected wireless clients; they are responsible for relaying their flows to neighboring nodes in addition to relaying neighboring nodes' own traffic to other neighbors, until they reach their destinations. Compared with traditional wireless networks, such as ad hoc networks, MRMC wireless networks have the following main characteristics: 1) The routers are relatively stationary. Hence, once routing paths are created, they are likely to be stable. 2) Most of the traffic flows are either originating from or terminating at designated gateways which provide the Internet access to the clients. 3) The power consumption of the routers is not usually a significant issue as they have easy access to power through wires. Moreover, as these routers are located close to users, the routers must operate at low powers to avoid any health threats to end-users. Finally, security is also a critical factor.

Given all these characteristics, MRMC network technologies have attracted considerable attention in recent years due to their fast deployment and ease of maintenance compared with traditional wireless networks [4]. Furthermore, MRMC networks are highly reliable, when compared with other technologies due to the use of multiple radios and channels to increase resource redundancy. In other words, even with the presence

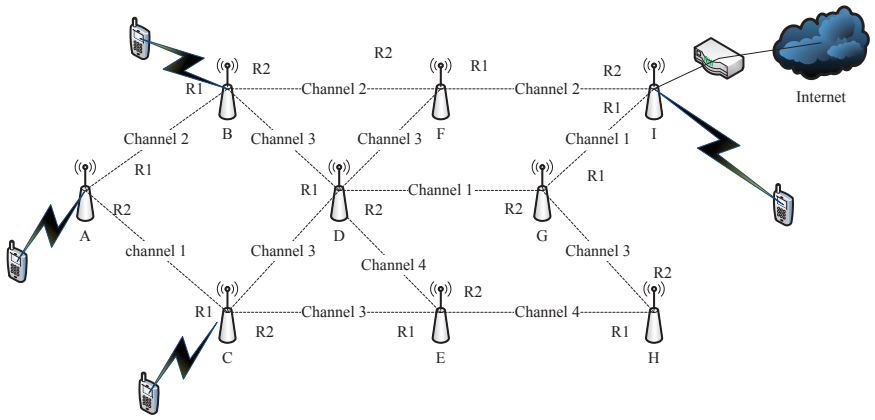

Figure 1.1: A Multi-radio Multi-Channel Wireless Networks with an initial assignment of frequency channels

of a link or node failure, nodes can still communicate with each other by using other intermediate nodes, due to the use of multiple interfaces. Hence, MRMC networks are largely considered as more stable than other single radio wireless networks. To date, MRMC wireless networks are applied in many applications such as enterprise networking, building automation, and broadband home networking [4].

1.2 Motivation and Objective

In this section, we demonstrate our research motivation and objectives. Our research focuses on three main aspects of WMNs: 1) Performance enhancement problem of WMNs. 2) Survivability analysis and backup scheme design for WMNs. 3) Energy efficient green WMNs design. These three aspects are all very important to realize the efficient WMNs. Since the end users would like receive desired services. While, the communication system operators may pay more attention to the survivability and energy efficiency of the WMNs. So, firstly, we should solve the performance enhancement problem of WMNs. Then, we need to analyse the survivability of the WMNs and design an efficient backup scheme to face the node failure problem. Finally, we need to improve the energy efficiency of the WMNs. By taking these three steps, we can have a desired WMN system that has good performance while achieving desired survivability and energy efficiency. In the following part of this section, we will demonstrate our motivation and objectives in detail.

1.2.1 Performance Enhancement

Parth *et al.* [4] provided a good survey on WMNs; generally, a limited number of mesh routers in the WMNs work as gateways to provide access to the wired backbone network. The remaining mesh routers in the system access the Internet and other services through a gateway. These routers connect to the gateway either directly or via other multiple intermediate routers (hops). Each router gathers data from end-users who are located in its coverage area. Typically, various types of data flows, such as VoIP, Video and general WWW data, are transmitted over these WMNs. Hence, one of the challenges faced when designing a WMN is that of providing services to applications with varying Quality-of-Service (QoS) requirements and WMNs must support an appropriate QoS mechanism to ensure efficient delivery of these applications. The Differentiated Services (*DiffServ*) mechanism [7] is widely used in today's networks as a principal mechanism for providing QoS. DiffServ offers a coarse granularity quality differentiation where the applications' traffic can be categorized into multiple classes (or aggregates) with QoS parameters defined for each class.

Generally, end-users mostly use WMNs to access the Internet [8]. So, the ability of these networks to support routers to deliver data through a gateway is a critical point that we address in this dissertation. Because of the limited number of gateways in the network and the variation in the number of hops from users to the gateway, it is difficult to find a way to satisfy all users' QoS requirements while maximizing the throughput of the gateways [9]. To improve the current low-throughput performance of WMNs, we need to concurrently consider three inter-dependent functionalities, namely, routing, channel assignment and data traffic scheduling.

Since most traffic converges to gateways, the links connected to a gateway always have heavier loads. When less enough transmission resources (i.e., channels and time slots) are dedicated to these critical links, congestion is created and bottlenecks are formed. On the other hand, congestion is also created in links far away from the gateway when too many resources are dedicated to links closed to the gateway [9, 10, 11]. Hence, balancing the allocated resources in the system is an important issue that must be carefully considered. Fortunately, with the aid of multiple channels and multiple radios (MCMRs), WMNs performance can be improved with effective allocation of these resources [12].

To this end, we can summarize the main goals of the design of our QoS aware joint routing, channel assignment and data traffic scheduling framework in WMNs as follows: 1) The developed techniques must enable differentiation among users and provide a

flexible control for fair partitioning of the transmission resources (i.e., time and channels) between different classes-of-service (CoS) [13]. Each CoS must be delivered at the level that satisfies its target market. 2) Spatial fairness between routers must be ensured in order to guarantee deterministic access to the Internet service to end-users. 3) The scheme running at the gateway should be reasonably simple. Hence, the proposed work functions in a semi-distributed manner taking advantage of the ability to have a global view of the system as is the case for centralized schemes while operating in a reduced complexity as achieved by distributed approaches.

1.2.2 Survivability Analysis and Backup Scheme Design

Due to the heterogeneity of the traffic loads and the fluctuation of the wireless link conditions, preserving the required performance of MRMC WMNs is still a challenging problem. For example, some nodes of the MRMC WMN may experience significant interference from other coexisting wireless networks' components (e.g., during a jamming attack). Some parts of the network might not be able to support the increasing bandwidth demands from new users and applications. Furthermore, links in a certain area (e.g., a hospital or a police station) might not be allowed to use some frequency channels because of spectrum etiquette or regulations. Also, a blackout of the power supply may cause some nodes of the system to lose functionality. A dramatic real-world example of a power related cascade of router failures is the electrical blackout that affected much of Italy on 28 September 2003 [2]: the shutdown of power stations directly led to the failure of nodes in the communication network, which, in turn, caused a further breakdown of more power stations.

Because of its destructive impact on the performance of wireless networks, the node failure problem has been explored extensively. Many of the existing research efforts aim at improving the robustness and survivability of MRMC WMNs by designing efficient routing and channel assignment algorithms. Wellons and Xue in [14] showed a routing formulation for multi-radio, multi-channel networks to handle the unexpected traffic demand changing (caused by jamming attack or link failure) by exploiting traffic demands which fell into a predicted region based on the knowledge of the historical traffic demand. In [15], the authors designed a graph routing approach to construct reliable routing graphs which satisfied the required reliability. In this scheme, the intermediate devices on a path could be pre-configured with multiple neighbours to help transmitting packets without using a fixed path which started from a source. Other robust routing algorithms

and anti-collision protocols can be found in [16, 17, 18].

In addition to recovery schemes, several studies have been dedicated to the design of failure-resilient networks. In [3], the authors tested the resilience of networks with topologies following Exponential (Erdos-Renyi model) and Power-Law (scale-free model) distributions, which represented homogeneous and inhomogeneous networks, respectively. Buldyrev *et al.* [2] analysed the cascade of failures in interdependent networks. In [19], the authors designed a model to measure the cascading failure probability based on the given component failure probability.

Meanwhile, it is evident that all of these studies did not consider an interesting but more fundamental question that is whether a cascade of node failures is related to the nodes' density and their geometric distributions. In this dissertation, we theoretically analyse the connectivity of MRMC WMNs based on a given node failure probability and nodes' geometric distributions. More precisely, we analyze the effects of node failures on the ability of network nodes to maintain their connectivity. We present a tight upper bound on the node failure probabilities needed to maintain full network connectivity on the one hand and a lower bound at which the system loses connectivity on the other hand. Using these bounds, one can design more efficient wireless networks that consist of as small number of routers as possible but are guaranteed to achieve their required reliability.

1.2.3 Energy efficient Green WMNs Design

MRMC Wireless Networks have changed the way we communicate over the past decade [20]. These networks enable end-users to access the Internet at a low cost while achieving ease of deployment and configuration. Such properties lend MRMC wireless networks to be an ideal technology to serve users in remote areas, in military deployments and in emergency rescue situations. An MRMC wireless network is composed of wireless mesh nodes (routers or access points), each serving a number of clients. The routers are mostly stationary and form a multi-hop network with or more of the wireless mesh nodes connected to a backbone network to provide Internet access to all the mesh clients. Over the past few years, various research efforts have addressed important issues such as channel assignment, routing and data traffic scheduling with the aim of increasing the capacity of these networks [4] or to maximize the routers' energy usage efficiency and the network's overall energy utilization [21, 22, 23] have also been discussed in the literature. Most of these efforts assumed the continuous availability of permanent

electricity sources. However, this assumption may not be always valid; on the one hand, electricity is mostly generated from limited and non-reusable natural resources, such as coal and oil that are very costly and unfriendly to the environment. On the other hand, some deployment scenarios of WMNs, such as those that take place in rural communities or during battlefields, cannot rely on fixed utility infrastructures.

Green WMNs that rely only on renewable energy sources (e.g., sunlight, hydrogen and wind) have been recently considered in [24, 25, 26, 27, 28] with focus on developing functionalities (e.g., routing and scheduling) that minimize the energy consumption. However, it is essential for these approaches to have a good estimate of the available energy in the routers' batteries and, in turn, their expected lifetimes. However, this is not a straightforward task since, unlike permanent electricity sources, the supply of green energy sources is irregular and fluctuates over time. For instance, a solar energy source provides varying energy levels across the time of the day and the season of the year and is affected by weather conditions and geography. As a result, the unreliable nature of the green energy source will affect the wireless node availability. Hence, it is necessary to analyse the wireless node's residual energy changing process and find out which parameter may affect the lifetime of the battery.

1.3 Contributions

1.3.1 A QoS Aware Joint Algorithm For Wireless Mesh Networks

To the best of our knowledge, the presented work is the first that adopts the DiffServ mechanism to realize QoS differentiation in WMNs. The key goal in our design is to maximize the capability of WMNs to deliver multiple CoSs of data through the gateway. This differentiates our solution from many early solutions which are limited to use only data rates to represent the QoS requirements [29, 30]. Our work has been published in [31].

The main contributions of our work are listed below:

- A minimum expected delay routing algorithm that finds the paths with small delays to the gateway while balancing the traffic load between the network routers.
- A weight-aware channel assignment algorithm that balances the traffic loads between the communication links in the network.

- A novel distributed QoS-aware traffic scheduling algorithm that achieves real-time traffic differentiation and improves the flexibility and robustness of the system.
- A new reduced tree topology construction mechanism that reduces the computational complexity and circumvents the disadvantage of centralized schemes.

1.3.2 Theoretical Analysis of the Properties of Random Node Failure in Wireless Networks

We analyze the effects of node failures on the ability of network nodes to maintain their connectivity. More precisely, we present a tight upper bound on the node failure probabilities needed to maintain full network connectivity on the one hand and a lower bound. On this probability, after which the system loses connectivity. We show that these bounds are dependent only on the nodes' geometric distribution and density. We also verified these theoretical results against those obtained via experimentation. This work has been published in [32].

1.3.3 A New Random Node Failure Recovery Scheme

There are many approaches that have been proposed to recover a MRMC WMN from link/node failures; generally, these approaches are categorized into three main classes: protection schemes, restoration schemes and hybrid ones [33, 7]. The majority of these schemes rely on the use of additional transmission resources (i.e., wireless channels) or introduce more frequent channel switching. The limited number of available wireless channels and the ineluctable channel switching delays lend these schemes difficult to adopt in a practical wireless network. Also, these schemes mostly re-route the backup traffic flows to their neighbourhood which in turn generates congestion at these nearby routers.

Our work overcomes the above limitations by first investigating the effects of random node failures on the connectivity of MRMC WMNs and then developing a new recovery (backup) scheme to improve the robustness of these networks against these random failures. At its core, the proposed scheme employs a local redistribution of traffic loads that maximizes the recovery possibility while minimizing the possibility of congestion generation that may lead to further node failures. More precisely, the proposed recovery scheme first searches for feasible local-to-end re-routing plans which generate new

paths to avoid the faulty area. Then, by considering current network settings as constraints, the proposed scheme redistributes the traffic loads in the local area to satisfy the Quality-of-Service (QoS) requirement of each data flow. The scheme optimally chooses reconfigurations that introduce the smallest amount of modifications.

The main advantages of the proposed recovery scheme are as follows: 1) Per-flow QoS requirements are guaranteed: Each data flow is guaranteed a specific level of fault-tolerance according to its QoS requirements. 2) Fast failure recovery: The service disruption time of a connection caused by failures is minimized. 3) Small recovery overhead: The amount of additional overhead resources required by the fault recovery is small. 4) Robust failure handling: Failures are always handled robustly; even though failure occurrences may exceed the hypothesised failure threshold, as many faulty flows as possible should be recovered. 5) Interoperability/scalability: The proposed scheme is inter-operable with various existing and future routing and channel assignment protocols. Also, it scales well in a dynamic environment where (short-lived) flows are set up and torn down frequently. This work is published in [34]

1.3.4 Optimal Energy Efficient Packet Scheduler Design for Green Wireless Networks

Our work solves the aforementioned lifetime problem of the green energy powered battery (section 1.2.3) by providing a rigorous theoretical analysis of the behaviour of the battery's residual capacity while assuming general distributions for the traffic arrival and the battery charging rates. For the two scenarios of a battery with finite and infinitely large capacities, we answer the following questions: what is the probability that the battery will run out of charge? what are the parameters, related to the traffic arrival and transmission, that can affect this probability? how can the transmission behaviour of the node be adjusted in order to prolong the battery's lifetime? Based on obtained theoretical results, both an online and an offline scheduling schemes are proposed to minimize the probability of depleting the battery. To this end, this work has been submitted as [35]. The contributions of this work can be summarized as follows.

- *Theoretical analysis of the residual energy of the wireless node battery*: We develop a novel theoretical framework to analyze the behaviour of the residual energy of the wireless router's battery when it has an infinitely large, as well as a finite, capacity. In these two scenarios, we model the battery's residual energy using two general queuing models, namely, G/G/1/∞ and G/G/1/N, respectively. Hence,

in contrast to traditional approaches that are limited to a specific traffic arrival or energy charge patterns (e.g., Poisson arrival [36]), the model works with general distributions. The residual energy variations, reflected by changes in the queue length, are then approximated by a continuous-time and -state Markov process, referred to as the diffusion process [37]. The probability distribution function of this new process is then modelled by the well known Fokker-Planck differential equation [37] with appropriate boundary conditions to reflect the behaviour of both the infinite and finite capacity batteries.

- *Quantification of the effects of transmission rate variance on the depletion probability*: A closed form solution for the aforementioned equation is obtained and employed to calculate various critical parameters such as the probability distribution of the residual energy, the length of the wake up and operational periods of the router and the battery's depletion probability. We formally show that the probability of depleting the battery can be minimized by reducing the variance of the energy discharge rate. This is achieved by controlling the variance in the transmission rate of the router.

- *Development of novel QoS aware packet scheduling schemes*: Using the obtained theoretical results, we propose two energy efficient packet scheduling schemes that minimize the node energy depleting probability while achieving the required service quality. The first is an off-line scheme employs the traffic's lag autocorrelation metrics to find an optimal schedule that minimizes the energy usage variance but assumes knowledge of future traffic demands. The second scheme relaxes this assumption but employs a heuristics to find an energy efficient schedule that satisfies the traffic delay constraints.

1.4 Dissertation Organization

Chapter 2 focuses on the performance enhancement problem and survivability problem in WMNs and presents in-depth surveys of the related approaches addressing both of problems. Chapter 3 describes our joint QoS aware algorithm for the MRMC WMNs in detail. Chapter 4 theoretically analyses the properties of random node failure in MRMC WMNs. Chapter 5 proposes our random node failure recovery scheme for the MRMC WMNs. In Chapter 6, we present our optimal energy efficient packet scheduler for the green energy powered MRMC WMN that based on the theoretical analysis results of

the residual energy changing process of the battery. Chapter 7 concludes this thesis and discusses future research directions.

Chapter 2

Research Background

In parallel, there are ongoing efforts in both academia and industry to address the capacity issues through the use of multiple radios and multiple channels in a multi-hop wireless network. Also, the issue of improving network survivability has been studied. In this chapter, we first discuss the related work on WMN performance related issues (i.e., channel assignment, routing, scheduling, etc.). Then the work on addressing the network survivability are introduced. Finally, we survey the research efforts about green energy powered WMNs.

2.1 Performance Related Design Issues

2.1.1 Channel Assignment

In [8, 38, 39, 12], the channel assignment problem was studied extensively. Alicherry *et al.* [8] presented a centralized channel assignment algorithm based on a linear program describing the constraints in the WMN, such as channel interference and link capacity constraints. In [38], Brzezinski *et al.* introduced the conflict graph method to solve the channel assignment problem and proposed a centralized channel assignment algorithm. These approaches mostly suffer from their computational complexity because of the need to decompose and solve an NP-hard optimization problem. In [12], Subramanian *et al.* designed a distributed channel assignment algorithm based on the interference constraints. The distributed algorithm can quickly adapt to traffic variation and link failures; thus, robustness can be achieved, but they do not take into consideration of the optimality of the throughput performance of the gateway.

Selvakennedy *et al.* [1] provided a good survey of the existing channel assignment

Channel Assignment Approaches for MRMC WMNs				
Centralized			Distributed	
Graph Based	Network Flows	Network Partitioning	Gateway Oriented	Peer Oriented
CLICA [40]	LA-CA [41]	MCI-CA [42]	Hyacinth [6]	PCU-CA [43]
INSTC [44]	BSCA&PDCA [45]	MCCA [46]	DMesh [47]	JOCAC [48]
BFS-CA [49]	RCL [8]		CoMTaC [50]	SC-CA [51]
CTA [52]				DGA [52]
				SS-CA [53]

Table 2.1: Classification of Channel Assignment approaches for MRMC WMNs [1]

(CA) methods. As shown in the Table.2.1, the authors classified all the Channel Assignment approaches into two categories: centralized and distributed. For the centralized approaches, a central control is assumed and it has the complete knowledge about mesh networks. Thus, the formulated CA problems can be solved at a single place. After the result of CA is calculated, it is distributed to the nodes to accomplish. Altogether, we have seen three types of such problems being formulated: the graph-based problem, the network flows problem, and the network partitioning problem. Accordingly, the centralized approaches are classified into three categories using the above problem formulations respectively.

For the distributed approaches, no central control is assumed and each node runs its own copy of the algorithm to assign the channels. They are further classified into two categories according to the traffic pattern being considered: gateway-oriented Channel Assignment approaches and peer-oriented Channel Assignment approaches. The former one assumes that the main network traffic is to or from the gateways, so the Channel Assignment can exploit the heuristic that the near-gateway links should be given relatively high bandwidth. The latter one assumes that the network traffic can occur between any pair of nodes with no fixed pattern, so the CA approaches have to be as general as possible to accommodate various kinds of network traffic.

Besides the classification of the Channel Assignment Approaches that was introduced in [1]. In [52], channel assignment protocols can be broadly classified in static, dynamic and hybrid schemes. We will review several channel assignment protocols in each class in next few sections.

2.1.1.1 Static Channel Assignment

Static channel assignment is a fixed assignment of channels to the radios of nodes which remains unchanged over the course of network operation. Such mechanisms are often less adaptive to change wireless conditions like external interference and traffic. On the other hand, such mechanisms are simpler and do not incur channel switching delays.

In some of the earlier efforts to utilize multiple channels for network capacity enhancements, [54] proposed a multi-radio unification protocol (MUP). MUP assigns different channels to different radios of a node and this assignment is identical for all nodes of the network. A node uses the best quality channel out of its all radios for communicating with its neighbor. Though it improves performance with respect to the single channel assignment, the number of channels utilized in the network is still restricted by the number of radios at nodes. Channel assignment problem can be modeled as edge-coloring of the network graph and related well-known heuristics and algorithms can be applied for the solution. Along the same lines, [40] proposes a channel assignment algorithm CLICA (Connected Low Interference Channel Assignment) based on edge-coloring of the links in the connectivity graph. In the first phase of CLICA, every node greedily chooses colors for edges incident to it in a way that the network connectivity is maintained. This choice is assisted by a weighted conflict graph so that the choice of link color minimizes the interference with conflicting links. The second phase handles multiple edges between the nodes and the unassigned radios at nodes which can be later utilized as per offered load using dynamic assignment. Like link scheduling, conflict graph can also be used for channel assignment to incorporate interference relationship between the links. When dealing with multi-radio mesh nodes, the notion of conflict graph can be further extended to a per-radio case instead of per-node. The study of [52] provides channel assignment algorithms for multi-radio WMNs with the objective of minimizing the co-channel interference while adhering to the interface assignment constraints. It uses conflict graph representation to capture the interference based conflicts between the links. This way, channel assignment problem of network graph turns out to be a vertex coloring problem in the corresponding conflict graph. Presented centralized algorithm tries to find such a coloring with condition that the number of distinct channels assigned to the links incident to a node is no more than the number of interfaces available at the node. Distributed version of the algorithm tries to resolve the same using greedy heuristics of Max-K-cut problem (problem of assigning k colors to the vertices in such a way that the number of edges with endpoints of different colors is maximal). The efficiency of optimization

algorithms are proved with semi-definite programming formulation. The study of [55] shows that the link interference graphs (conflict graphs) belong to a special family of graphs called Overlapping Double-Disk (ODD) graphs. Such graphs can be created by having both endpoints of a link to possess a disk of radius half their interference range. If ODDs of two links intersect, it can be concluded that corresponding links interfere with each other. The channel assignment is performed by finding the independent sets using Polynomial-time Approximation Scheme (PTAS) in such ODD-based link interference graphs. Changing the channel of a radio may cause several other nearby nodes to change the channels on their respective radios to maintain the symmetric links and channel dependencies. This is often referred as the ripple effect and it is an important design constraint addressed in the [56]. It proposes the design of a logical topology from the actual physical topology while adhering to design constraints like channel dependency, ripple effect and hop count. Channel dependency constraint mentions that if multiple links are chosen in logical topology for the same radio at a node, all such links should be assigned the same channel. The choice of only a certain set of links out of the actual physical topology should also be carefully balanced to avoid long routing paths. Though there is no implicit consideration of interference, once all other constraints are formulated, actual radios are assigned channels based on the solution of the logical topology. The study of [57] models the relation between channel assignment and radio assignment as binary vectors. Using link conflict graph for interference relationship, it models the achievable link rates as a function of these binary vectors. The joint problem is formulated as a non-linear maximization problem and the solution to which has been provided with two design schemes.

Similar to K-hop model of interference, [58] presents a novel edge coloring based channel assignment algorithm. The motivation is based on the observation that active links which are at the distance of one hop from each other should be assigned different channel to avoid interference. By this way, the channel assignment problem becomes Distance-1 edge coloring problem, which finds minimum number of colors that any two active links at one hop distance are assigned different color. The problem is NP-complete, [58] provides a heuristic for solution and describes a relevant MAC scheduling protocol based on the proposed solution.

Though most of static channel assignment algorithms depend on graph coloring, there have been a few other efforts also. The study of [59] motivates the importance of component-based channel assignment in single-radio multi-channel ad-hoc networks. It proposes the use of the same channel for all links of a flow whenever multiple flows

intersect at a node in the network. Different intersecting or contending flows may operate on different channels. Such design has merits of simplicity and lower switching delay. A combinatorial technique is used in [60], named Balanced Incomplete Block Design (BIBD), for channel assignment. Specifically in BIBD, all nodes are assigned the same number of distinct channels and each channel is assigned to same number of nodes. In this way the network topology turns out to be a regular graph which has a good connectivity property. The algorithm presented in [60] assigns channels that certain connectivity is maintained and interference between same channel links are minimized.

A localized superimposed code based channel assignment algorithm is presented in [51] where nodes use the channel code (list of primary and secondary channels) to derive interference-free channel allocation. The approach taken in [61] holds practical importance in terms of scalability and deployment where every node is equipped with two physical radios. It divides the mesh nodes into clusters, and cluster-head decides the best intra-cluster channel to be used by detecting energy on every channel. Another radio at every node is dedicated for inter-cluster communication to handle the control and management messages. The study of [62] presents an ILP formulation for the channel assignment problem where the objective is to maximize the total number of simultaneous transmissions on links while meeting the interference constraints. As one can see, all static policies discussed here can be used as a solution in network deployment and design phase but their inflexibility to adopt to changing conditions often requires dynamic mechanisms of channel assignment which we will discuss next.

2.1.1.2 Dynamic Channel Assignment

Such channel assignment changes dynamically based on considerations like current interference, traffic demands, power allocation etc. This results in a more challenging design problem and also adds overhead of channel switching. Such mechanisms can be further classified into per link, per packet and per time-slot based mechanisms. These channel assignment policies pose novel design problems like multi-channel hidden terminal, sporadic disconnections etc. but if carefully designed, they have the potential to achieve better system capacity.

Since every node in the network changes channels of its radios dynamically, nodes often require tighter coordination between them to avoid disconnections, deafness problems and the multi-channel hidden terminal problem. Such issues make dynamic channel assignment mechanisms more and more complicated.

The multi-channel hidden terminal problem [63] arises when channel selection is made

during RTS/CTS exchanges. When a transmitter and a receiver choose their channel for data transfer in RTS/CTS, it is possible that hidden terminal is listening on the other channel. Such hidden terminal can never receive the choice of channel between sender and receiver, and may end up selecting the same channel for its communication to some other node. This can result in collision at the receiver. To solve the problem of multi-channel hidden terminal, [63] proposes a multichannel MAC protocol (MMAC) which uses time synchronization between nodes in the network just like IEEE 802.11 Power Saving Mode (PSM) using BECON intervals. In MMAC, in initial ATIM window all nodes tune to predefined control channel. All nodes having data to send, send ATIM message using control channel and also provide their preferred list of channels for data communication. Receivers choose a channel and send back ATIM-ACK message. All other nodes hearing the channel choice choose their preferred channels different from each other to avoid the collision. After completion of ATIM window, actual data transfer takes place.

Sometimes it is not feasible to dedicate a separate control channel due to lesser number of available orthogonal channels especially in standards like IEEE 802.11. Slotted Seeded Channel Hopping (SSCH) [64] improves on MMAC by eliminating the need of such a control channel. In SSCH, each node switches channels in every slot based on its pseudo-random channel hopping schedule. Nodes have knowledge about other's channel hopping schedule. A sender wishing to send data designs its channel schedule in such a way that in some slot it achieves an overlap with receiver schedule. Such slotted design with switching channels can also benefit from the fact that distinct links can be active on different channels to avoid interference and increase network performance by simultaneous communication. It is shown that such a random schedule can sometimes suffer from deafness problem (missing receiver problem) that transmitting node does not find the intended receiver during the slot of communication. Both SSCH and MMAC protocols require tight time synchronization between the nodes in the network. To avoid this problem, [65] proposes xRDT (Extended Receiver Driven Transmission) protocol which extends RDT [66], where sender switches to well-known fixed receiver channel for data transfer. xRDT uses additional busy tone interface to mitigate multichannel hidden terminal problem which can still happen in RDT. Proposed Local Coordination based Multichannel MAC [65] uses control and data window similar to MMAC [63] without the need of global synchronization and busy tone interface. Senders use 802.11 based channel access mechanism in default channel to negotiate local schedules and channel usage during the control window.

CSMA-CA has been previously shown to be unfair even in single-cell infrastruc-

ture 802.11 networks. The study of [67] first points out two fundamental coordination problems which cause flow starvation and unfairness in single-channel multi-hop CSMA networks - Information Asymmetry (IA) and Flow-in-the-middle (FIM) (details in [68]). Multi-channel MAC can address these issues if designed carefully but it may lead to problems like multi-channel hidden terminals or missing receiver problem [68]. Described Asynchronous Multi-channel Coordination Protocol (AMCP) uses one dedicated control channel. Nodes use the control channel to contend for preferred data channel by using 802.11 DCF mechanism. Be different from other previous protocols, in AMCP nodes can contend for data channels anytime without any specific synchronization. Selected data channel by sender-receiver is announced in RTS/CTS to other nodes which mark the channel to be unavailable for that data communication time. Several approaches rely on a central authority for performing the channel assignment and also try to accommodate real-time channel quality measurements. The study of [49] makes a significant contribution by developing a dynamic channel assignment algorithm which requires a centralized entity (gateway and channel assignment server). The proposed algorithm requires one radio at every mesh router to be dedicated for a common channel throughout the network. This is to maintain a connected back-bone topology which is near optimal routing paths and non-interrupted flows of communication. It utilizes real-time measurements of all available channels to prioritize them based on their quality and effects of other co-located active networks (external sources of interference) on channel utilization. Based on this estimated co-channel interference, it develops a Multi-radio Conflict Graph (MCG). The MCG is built by the communication graph in which each of its radios is presented with vertex instead of every mesh router. This way, the number of assigned channels to a node is automatically restricted by the number of radios it has. Gateway, being central entity, initiates a breadth-first search for the channel assignment based on the MCG and the information of channel priorities.

Because of its complexity in derivation and maintenance, only a few approaches have attempted to perform the channel assignment in distributed fashion. One of these [69] proposes a channel assignment heuristic (SAFE-Skeleton Assisted Partition Free) which assigns channels in a distributed fashion. With every node having K radios and N available channels in the network, if $N < 2K$ and every node randomly chooses K channels, they will lead to at least one common channel at every node. Nodes then communicate and choose different channels if their adjacent links have common channels. With $N > 2K$, SAFE finds a spanning subgraph of the network to maintain connectivity and assigns a default channel on it. As before, regarding their choices, nodes choose a

random set of channels and communicate with each other. Default channel is only used when other choices are not available without violating the interference limitations or the connectivity constraint.

All the approaches discussed, to the point, do not take traffic demands at nodes into consideration for the channel assignment. Most of the times, it is very difficult to derive a completely interference-free channel assignment solution. In such cases, if there exists a heuristic which can prioritize the links based on their importance, such a ranking of links can be helpful to perform the channel assignment. The study of [70] is motivated by such need for traffic aware channel assignment in which partial or full information of current traffic is required. Such channel assignment ensures that nodes with high traffic demands are definitively assigned non-overlapping channels. Though presented algorithm is designed for WLANs, it can be applied to WMNs which also have the high-traffic links near the gateway. Dynamic mechanisms are likely to incur higher overhead of control messages and are also more prone to ripple effect kind of real-time issues due to their fast adopting nature. The study in [71] uses routing control messages to propagate the information about the channel assignment in K-hop neighborhood. It tries to assign non-conflicting channel to nodes during the Route Discovery and Reply processes to avoid any extra overhead. On the other hand, [72] defines a framework for self-healing mesh network where network reconfigures itself minimally when faults like link failure occur. For example, in the case of high interference on a particular link, it forces to use minimal reconfiguration of the channel assignment and avoids network-wide ripple effects. Similar mechanism has also been proposed in [73].

2.1.1.3 Hybrid Channel Assignment

In hybrid channel assignment schemes, some of the radios are assigned fixed channels while others switch their channels dynamically. These policies benefit from their partially dynamic design while inheriting simplicity of static mechanisms. As shown in [74], in hybrid assignment all nodes try to assign a different channel to their fixed radio. Node is wishing to communicate by switching its switchable radio to the channel used by the fixed radio of the receiver. IEEE 802.11 b/g standard provides 11 channels whose center frequencies are separated by 5 MHz and each channel spreads around the center for 30 MHz. Though this results in only 3 non-overlapping channels, other partially overlapping channels can also be utilized for simultaneous communications if the interference caused between them is within a tolerable margin. [75, 76] present first analytical reasoning about how partially overlapped channels can increase the spatial reuse.

In WMNs, assigning a partially overlapping channel (POC) to a node can help bridge the communication between nodes with entirely non-overlapping channels. The study of [75] and [76] prove with examples that if designed carefully, POC can provide routing flexibility as well as significant throughput enhancements. The study of [77] provides an evaluation of the usefulness of POC using testbed experiments and confirms that when utilized carefully, POCs can improve network capacity by the factor of 2 in typical 802.11 b/g case. It provides a LP formulation for achievable network capacity in multi-hop networks using POCs. It also presents an interference model which captures the effects of partial interference of POCs. The interference range of POCs is much smaller than that of non-overlapping channels. This enables more simultaneous communications leading to a better spatial reuse as described in [75, 76, 77]. With advancements in directional antennas and cognitive radio technologies, it is important that channel assignment mechanisms intelligently accommodate their characteristics. The study of [47] uses directional antennas at every mesh router while designing a mesh network. It incorporates the spatial separation provided by directional antennas in a channel assignment algorithm which improves on spatial reuse drastically. CogMesh [78] tries to address common control channel problem in cognitive radio based mesh network where spectrum access is dynamic. It tries to cluster the nodes on the basis of their detected spectrum hole and assigns it a control channel. With evolution of cognitive radio and software defined radio and their increasing usage in mesh, decisions of channel assignment and opportunistic access can become more and more complicated [79]. Because such adaptive radio technologies have capabilities to achieve true heterogeneity, their integration to mesh networks is imminent.

2.1.2 Routing

Just as in any other networks, finding out high throughput routing paths is a fundamental problem in WMNs. Routing metrics and protocols of wireless multi-hop networks differ from other traditional routing protocols due to the dynamic and unpredictable nature of the wireless medium. WMNs display relatively stable topological behavior due to the lack of mobility but still underlying issues of link quality and the interference remain the same. This has motivated design and development of various new routing metrics and protocols for WMNs. In this section, we will discuss some of the routing metrics that have been proposed for WMNs firstly and then review some existing routing approaches.

2.1.2.1 Routing Matrics for Wireless Mesh Networks

Only utilizing the hop-count as routing metric in mesh has proven to be inefficient [80] as it does not take dynamic characteristics of wireless medium (such as link quality, interference etc). into consideration. As mentioned in [81], WMNs differ from other wireless ad-hoc networks in terms of their static nodes. Though inherent wireless medium is similar, the links between nodes are fairly stable and display relatively higher constant characteristics. These properties require exclusive routing metric and protocol design for WMNs. Considering the routing metrics first, [81] provides a detailed explanation of characteristics that a mesh routing metric should possess. It shows that the metric should provide stable, good performance (in terms of throughput or delay), computationally efficient and loop-free routing paths. Though it has been shown that topology-dependent routing metrics are more stable in relatively static environments like mesh, many recent metrics still consider dynamic wireless conditions. Below, we present some of metrics proposed in literature for routing in WMNs. A more detailed comparison between a very few of them can be found in [81].

1. ETX [82]: Expected transmission count (ETX) is the estimated number of transmissions (including retransmission) required to send a data packet over the link. In this terms, if link has a forward delivery ratio d_f(probability that data packet successfully arrives at receiver) and a backward delivery ratio of d_r (probability that ACK is received by sender), its ETX value can be defined as follows

$$ETX = \frac{1}{d_f \times d_r} \tag{2.1}$$

   $d_f \times d_r$ shows that packet is transmitted with success in forward direction and ACK is also successfully received in backward direction. The total ETX of a path is summation of ETX of all links on the path.

2. ETT [83]: Expected transmission time (ETT) improves over ETX by considering bandwidth also while assigning metric to a link. If S is the size of the packet and B is bandwidth of the link then ETT can be defined as follows

$$ETT = ETX \times \frac{S}{B} \tag{2.2}$$

   This way, ETT of the link captures the time taken for successfully transmitting a packet on the link.

3. WCETT [83]: Weighted cumulative ETT improves over ETT by considering the channel diversity along the path. As different links on paths might have different channels assigned to it, it is important to capture the effect of sum of transmission times of links on every channel. Let X_j be the sum of transmission times of links on channel j as follows

$$X_j = \sum_{link\ i\ is\ on\ channel\ j} ETT_i\ ,\ 1 \leq j \leq k \tag{2.3}$$

Now, WCETT can be defined as follows

$$WCETT = (1-\beta) \times \sum_{i=1}^{n} ETT_i + \beta \times \max_{1 \leq j \leq k} X_j \tag{2.4}$$

Thus, WCETT finds routing paths with the least ETT values and the highest channel diversity. WCETT is proven to be non-isotonic [81] (a metric has isotonic property if it ensures that order of weights of two paths are preserved if they are appended or prefixed by a common third path) which requires very efficient algorithms to find minimum weight paths. The study of [84] discusses how to use iterative line search technique to efficiently find WCETT based optimal or near-optimal paths using Dijsktra's algorithm [7].

4. MIC [85]: Metric of interference and channel switching improve over ETT by considering inter-flow and intra-flow interference using IRU (Interference-aware Resource Usage) and CSC (Channel Switching Cost) components of links. IRU of a link ij operating on channel c also includes its ETT and can be defined as below

$$IRU_{ij}(c) = ETT_{ij}(c) \times |N_i(c) \cup N_j(c)| \tag{2.5}$$

$|N_i(c) \cup N_j(c)|$ is the number of neighboring nodes interfered due to activity of a link ij on channel c. To consider intra-flow interference, every node on the routing path is assigned CSC value to it. CSC of a node x is lesser if previous link where x was receiver and next link where x is sender are on different channels. CSC value us higher if both incoming and outgoing links are on the same channel as it introduces more intra-flow interference. MIC of a routing path p can be expressed as below

$$MIC(p) = \alpha \times \sum_{link\ ij \in p} IRU_{ij} + \sum_{node\ i \in p} CSC_i \tag{2.6}$$

Here, $\alpha = \frac{1}{N \times \min(ETT)}$ which tries to balance the load in the network.

5. MCR [43]: *Multi-channel routing* metric improves over WCETT by considering switching costs required for channel switching on different links along the path. WCETT does not capture the effect of switching delay for links that active on different channels on a path. MCR adds switching delay to metric so that switching delay at every link does not take away the benefits achieved from hybrid channel assignment [74]. Let $SC(c_i)$ be the switching cost of ith hop on a path, operating on channel c_i, then MCR combines the effect of channel quality, diversity and switching delay as follows

$$MCR = (1-\beta) \times \sum_{i=1}^{n} (ETT_i + SC(c_i)) + \beta \times \max_{1 \leq j \leq k} X_j \tag{2.7}$$

6. WCCETT [86]: Weighted Cumulative Consecutive ETT also proposes a way to extend WCETT for better consideration of intra-flow interference. If we refer consecutive hops of a path which are operating on same channel as segment then WCCETT can defined as below

$$Y_j = \sum_{link\ i\ is\ on\ segment\ j} ETT_i\,,\ 1 \leq j \leq k \tag{2.8}$$

$$WCCETT = (1-\beta) \times \sum_{i=1}^{n} ETT_i + \beta \times \max_{1 \leq j \leq k} Y_j \tag{2.9}$$

   This way, WCCETT selects a path with more channel diversity (smaller segments) compared to WCETT yielding lesser intra-flow interference.

7. iAWARE [87]: WCETT does not capture the inter-flow interference and may end up choosing congested routing paths. iAWARE uses physical interference model for calculating inter-flow interference. The study of [87] defines *Interference Ratio* (IR_l) for link l from u to v where $IR_l = \min(IR_i(u), IR_i(v))$ and $IR_i(v) = \frac{SINR_i(v)}{SNR_i(v)}$. iAWARE is defined as below

$$iAWARE = \frac{ETT_l}{IR_l} \tag{2.10}$$

   iAWARE of path is calculated in similar way as ETT.

8. ETOP (Expected number of Transmissions On a Path) [88, 89]: As mentioned in [88, 89], ETX metric does not take into account that practically if certain number of link layer transmissions are unsuccessful, packet is dropped and transport layer

at the source node re-initiates the end-to-end transmission. In this case, if the lossy link is closer to the destination than source, most of the link transmissions from source to the lossy link are often wasted in unsuccessful end-to-end attempts. ETOP can be defined as expected number of transmissions required for delivering a packet over a path. ETOP takes into account the effect of relative position of links on path together with number of links and link quality.

9. METX [90]: *Multicast* ETX (originally $C(s,d)$ [91]) captures the total expected number of transmissions required by all nodes along the source-destination path so that destination receives at least one packet successfully. It is formally defined as follows
$$METX = \sum_{l=1}^{n} \frac{1}{\prod_{i=l}^{n}(1 - Perr_i)} \tag{2.11}$$
where l denotes lth link on $n - hop$ path and $Perr_l$ is the error rate of the link.

10. SPP [90]: *Success Probability Product* (originally EER in [92]) is proposed for multicast routing in WMNs. It is similar to METX and can be defined as $SPP = \prod_{i=l}^{n} d_{fl}$ where $d_{fl} = 1 - Perr_l$. Considering link layer broadcast in multicast, SPP reflects the probability that destination receives the packet without error. Routing protocol should choose the path which has minimum $1/SPP$.

2.1.2.2 Traditional MANET-like routing protocols

The MANET routing protocols are designed for mobile wireless nodes, intermittent links and frequently changing topologies. Such protocols often rely on flooding for route discovery and maintenance. Direct employment of such protocols is not suitable for relatively static mesh networks for various reasons.

Traditional MANET-like protocols can be largely classified in reactive and proactive routing protocols. AODV [93], DSR [94] etc. are **reactive routing** protocols in which a route discovery is initiated only on demand from any source nodes. Links in WMNs are fairly stable over a longer period of time and likely to carry relatively stable backbone-like traffic. Flooding messages for on-demand route discovery can induce high unnecessary overhead in WMNs [81]. Also, such protocols mostly use hop-count as routing metric which is not suitable for wireless medium because it can lead to shorter yet low throughput routing paths [80, 81].

Proactive routing protocols are table-driven protocols which require flooding in case of link failure and use hop-count as the primary metric for routing. They do not

take link quality or any other dynamic wireless characteristics like intermediate packet losses in consideration. Many of the proactive routing protocols have been adopted or specifically designed for WMNs. As an example, OLSR [95] has recently accommodated feature for link quality sensing and it is being adapted for mesh implementations. Similarly, Babel [96] is also a proactive routing protocol based distance vector routing and utilizes link ETX values for maintaining better quality routes. Hop-by-hop forwarding (e.g. opportunistic routing) is better suited for mesh than table-driven routing protocols due to its simplicity and possible adaptation to link dynamics [81]. B.A.T.M.A.N. (Better Approach To Mobile Ad-hoc Networking) routing protocol [97] tries to adopt such forwarding ideology in which every node maintains logical direction towards the destination and accordingly chooses the next-hop neighbor while routing. A useful empirical comparison of these proactive routing protocols can be found in [98]. Instead of developing new routing protocols for WMNs, many researchers have proposed modifications to the above mentioned MANET-like routing protocols. Most of such protocols try to adapt to the characteristics of WMNs such as lower mobility, stable routes etc. Also, variety of such protocols utilizes previously discussed routing metrics. Following are a few examples of such protocols:

- AODV-ST [99]: provides AODV-ST (spanning tree) routing protocol which improves on AODV in several ways to adapt to WMN characteristics. To avoid repetitive reactive route discovery with flooding, AODV-ST maintains spanning tree paths rooted at gateway from the nodes. It can incorporate high throughput metrics like ETT, ETX etc. for high performance spanning tree paths. AODV-ST also uses IP-IP encapsulation for avoiding large routing tables at relay nodes and can also perform load balancing for gateways.

- AODV-MR [87]: presents multi radio extension for AODV protocol where each node has multiple radios and channel assignment is performed with some predetermined static technique. AODV-MR uses iAWARE metric with bellman-ford algorithm to find efficient low interference paths. Links on such paths display low intra-flow and inter-flow interference together with good link quality.

- ETOP-R [88, 89]: ETOP-R routing protocol uses ETOP routing metric described earlier for finding the shortest path by using Dijkstra's shortest path algorithm. Practically, ETOP-R has been implemented with modified source routing protocol DSR.

- THU-OLSR (Timer-Hit-Use OLSR) [86]: An interval optimization algorithm is presented in [86] which adaptively adjusts control message intervals of OLSR based on the mobility. The hello interval and topology control interval of OLSR are set based on neighbor's status and multi-point relay (MPR) selector's status. This informed values of intervals are then utilized in THU-OLSR.

- PROC [100]: In Progressive ROute Calculation (PROC) protocol, source node first establishes a preliminary route to destination using broadcast. Destination then initiates building of a minimum cost spanning tree to source with the nodes around the preliminary route. The source uses this optimal route for future data transfer.

2.1.2.3 Opportunistic Routing Protocols

As we discussed previously that traditional shortest path routing and traditional ad-hoc routing protocols may not be sufficient for mesh. Recently, opportunistic routing protocols have been proposed to exploit the unpredictable nature of the wireless medium. Boukerche *et al.* proived a good survey about the opportunistic routing protocols [101]. Unlike all previous approaches, opportunistic routing protocol defers the next hop selection after the packet has been transmitted. Meaning, if a packet fortunately makes it to a far distant node than expected, such useful transmissions should be fully exploited. Though there are many advantages of such mechanisms like faster progress towards the destination, it requires complex coordination between the transmitters regarding the progress of the packets. Many protocols have been developed based on this idea which we discuss below.

- Ex-OR [102]: An important opportunistic routing protocol is proposed in [102] which displays its direct applicability in WMNs. In proposed routing protocol (called Ex-OR), sender broadcasts batch of packets to a list of potential forwarders in order to increase their chances to reach destination. The highest priority forwarder forwards the packets from its buffer and each packet has a copy of sender's estimation of the highest priority node which should have received the packets. To avoid blind flooding, it maintains information about which packets have been received by the intermediate nodes. The packets which are not received and acknowledged by higher priority forwarders are forwarded by the other forwarders in the list. The process continues until the batch of packets reaches the destination.

- SOAR [103]: Simple Opportunistic Routing Protocol (SOAR) proposed in [103] improves on Ex-OR in certain ways and efficiently supports multiple flows in WMNs. First, it requires the nodes forwarding packets to be near the shortest path (least ETX) from source to destination to avoid packets being misdirected. Second, it adds a timer based low overhead distributed mechanism to coordinate between the forwarders regarding when and which packets to forward. Higher priority nodes having smaller timer values forwards first upon their expiration. Other forwarders, listening to it, discard the redundant packets which avoid unnecessary flooding without any extra coordination overhead.

- MORE [104]: Ex-OR requires high amount of coordination between the forwarders and inherently cannot take advantage of spatial reuse. MORE [104] (MAC-independent Opportunistic Routing and Encoding) extends the Ex-OR with network coding. Here, packets are randomly mixed before forwarding to avoid the redundant packet transmissions without any needs of special scheduling or coordination. Similar approaches are presented in [105, 106].

- ROMER [107]: Similarly, in Resilient Opportunistic Mesh Routing (ROMER) [107] protocol, a packet traverses through the nodes only around long-term and stable minimum cost path. These nodes build a dynamic forwarding mini-mesh of nodes on the fly. Each intermediate node opportunistically selects transient high throughput links to take advantage of short-term channel variations. In this way, ROMER deals with node failures and link losses, and also benefits from opportunistic high throughput routing.

2.1.2.4 Multi-path Routing and Load Balancing

As mentioned in [108], using traditional routing approaches and metrics, many mesh routers may end up choosing already congested routing paths to reach the gateway nodes. This can lead to low performance due to highly loaded routing paths. The study of [108] proposes a routing protocol called MMESH (Multipath Mesh), in which every node derives multiple paths to reach the gateway node using the source routing. It then performs load balancing by selecting one of the least loaded paths. A large set of multi-path routing protocols are reviewed in [109].

Other multi-path routing mechanisms have been previously proposed in [110, 111] for ad-hoc networks. Interestingly, [112] claims that unless and until very large number of paths (infeasible in practice) are used in multi-path routing, single path routing performs

almost as good as multi-path routing. In such cases, more routes to the destination do not help much in balancing the load throughout the network. This is in line with the common belief of generation of hot-spots in multi-hop wireless networks. When the shortest path or straight line routing is used, most of the routing paths passing through a certain region (e.g, the center of a network) creates a highly congested, security prone area. Nodes in such area have to relay disproportionate amount of traffic for other nodes and often suffer from severe unfairness. Recently, [113] shows that relay load on the network mainly depends on the offered traffic pattern. When the shortest path routing is used with random traffic pattern, it can give rise to different load distributions and generate hot-spot at different places in the network.

Problem of modeling the relay load of nodes in a network has been addressed by a few research efforts. In uniform topologies, relay load is often modeled as a function of node's distance from the center [114, 115]. Recently, relay load of a node has also been modeled probabilistically as a function of perimeter of node's Voronoi cell [113]. Though such modeling works in uniform topologies and traffic, relay load estimation in arbitrary topologies is still an open problem. Similarly, finding ways to evenly distribute the relay load in the network is also an open research issue and is being actively investigated. Current approached for relay load balancing depends mainly on transforming Euclidean network graph on symmetric spaces like sphere or torus which do not show such crowded center characteristics. Many divergent, center-avoiding routing mechanisms described below have been proposed by researchers to try to balance the relay load among the nodes.

- Curve-ball Routing: [114] and [116] present an approach for load balancing in which stereographic projection is used to map the Euclidean node positions on a sphere. The routes between the source and destination are then found using great circle distance on sphere and then they are mapped back to the actual plane in the network. Such routes often result in circular arc shaped forwarding which is claimed to be distributing the load in the network since they intentionally avid passing through the center.

- Outer-space Routing: [117] proposes the concept of routing in outer space in which original network space is mapped onto a symmetric outer space (torus). The shortest routing paths between nodes in such outer space will symmetrically distribute the relay load in the entire network. Such paths are then used for routing in the original network to avoid routing via hot-spots.

- Manhattan routing: [118] proposes a divergent routing scheme in which source forwards the packet to an intermediate node which is near the intersection of horizontal/vertical lines passing through the source and destination.

Similarly, Several other similar load balancing mechanisms are described and analyzed in [119]. As shown in [120] and [121], such routing mechanisms display trade-off between stretch-factor of routing paths and actual load balancing.

2.1.2.5 Geometric Routing Approaches

According to the two surveys [122, 123], there are plenty of approaches that apply geometric routing on wireless networks. The geometric graphs adopted by those approaches mainly include the *relative neighborhood graph* (RNG), *Gabriel graph* (GG), *Yao graph* (YG), and *Delaunay triangulation*. Despite using different kinds of graphs, most of these approaches have the following common characteristics.

First, the wireless network environment is modeled by the *unit disk graph* (UDG), in which all network nodes use omni-directional antennas with an identical transmission range and two nodes have a link between them if their distance is no more than the transmission range. Thus, there exists significant interference among links that are near each other, which makes the routing protocols solely based on position information not appealing.

Second, the geometric graphs used as the network topology needs to be established and maintained by exchanging control messages among the nodes, which incurs significant overhead.

Finally, in routing a packet to the destination, if the processing node does not have a neighbor closer to the destination than itself, *face routing* is used to overcome this communication void phenomenon and to guarantee the packet delivery [123]. Though face routing can not generate loops in static networks, it can do so in dynamic networks.

For example, face routing will fall in a loop in the dynamic network scenario depicted in Fig. 2.1, where the source s has a packet P destined for t, and the link ac is temporarily broken. We assume that a combined greedy-face routing algorithm is used here. In the beginning, s will send P to u according to the greedy forwarding algorithm. At u, since no neighbor is closer to t than u, u will start the face routing process. Without loss of generality, here we assume that u uses the left-hand rule to forward P. Thus, P will traverse nodes a, b, c sequentially. When P arrives at c, supposing the link ac becomes available, in this new topology, P will be trapped in the loop b-c-a-b, since in a face

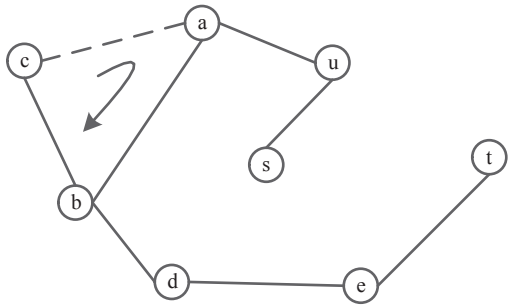

Figure 2.1: A dynamic network scenario where face routing generates loops

routing algorithm, loops are detected by remembering the first edge that the current face has been traversed [124]. In this example, the face routing algorithm will remember the edge *u*-*a*, so it will not be able to discover the loop *b*-*c*-*a*-*b*.

2.1.2.6 QoS Aware Routing Approaches

A number of research approaches are dedicated to address to the problem of QoS aware routing in WMNs. For example, in [29], Liu *et al.* design a call admission control scheme to protect the existing flows from QoS violations while fully utilizing the transmission resources (channels) in the network. Their scheme is based on the channel available bandwidth estimation. However, their solution only focuses on finding feasible paths for newly injected flows and does not consider the problem of network performance optimization. In [125], the same authors propose a distributed interference aware QoS routing algorithm. In their paper, QoS is limited to data rates specifications. Based on both inter- and intra-flow contentions, the authors calculate the maximum available bandwidth in each segment (link) of the path and employ it to represent the path bottleneck value. Based on this calculated value, they choose the best available path which has the best path bottleneck value. A similar algorithm can be found in [30] where Hou *et al.* propose a scheme using weighted paths which also captures the available path bandwidth information. The path with the largest available bandwidth is assigned the highest weight. Based on the path bandwidth information, they propose a hop-by-hop routing algorithm. On the other hand, in [126], Javadi *et al.* propose a QoS aware resource management algorithm which uses end-to-end delay requirements to represent QoS. Their algorithm choose the path with the best end-to-end delay condition to satisfy the demand of each data stream. The above approaches do not consider the priority of different data streams. Hence, higher priority data is dropped if the available bandwidth is not sufficient in the

path. Although these solutions attempt to maximize the network performance, they assume that the channel assignment is fixed. In other words, their performance depends on the underlying channel assignment mechanism. An energy-aware data-centric routing is proposed in [127]. A number of other routing algorithms are discussed in three surveys [128, 129, 130]. These solutions attempt to improve the one-hop capacity of the network but still they cannot guarantee the end-to-end bandwidth requirements of flows, which is the main obstacle in supporting QoS.

2.1.3 Scheduling

Link scheduling estimates the interference conflicts between the links that have transmission demands (based on the interference model) and tries to achieve a conflict-free feasible transmission schedule. The first generation of scheduling algorithms [131, 132, 133] for multi-hop wireless networks are based on simplified graph models. Such algorithms mainly follow characteristics like the network topology graph and often fail to capture the issues of dynamic wireless medium such as interference. The study of [134] indicates that the graph-based scheduling does not take full interference knowledge in account while performing the link scheduling. It might be too optimistic by allowing few unintended transmissions nearby the receiver which may cause collisions or can be too pessimistic by not allowing such a transmission which can cause tolerable interference at the receiver. Compared with the physical-model type SINR-based scheduling, it achieves lower network performance. Along the same line, [135] concludes that transmission scheduling based on the maximal independent set in graph-based interference model may suffer from intolerable SINR at the receivers, yielding low network capacity. Even maximizing the cardinality of the independent sets does not yield any better performance. Similarly, [136] prove with theoretical examples and experimentation that such graph-based models can undermine the achievable capacity even for simple settings of the network. They conclude the need of protocol design based on more realistic SINR-based physical interference model.

CSMA-CA and TDMA are two MAC protocols commonly used in the wireless networks [7, 137]. Both protocols have their pros and cons which make them viable choice for WMN MAC. CSMA is a simple, robust and scalable medium access technique. It does not require any time synchronization. Also, addition or removal of nodes from the network can be handled in the distributed fashion. The Distributed Coordination Function (DCF) of 802.11 is an implementation of CSMA with binary exponential back-off

[7, 137]. In DCF, a node wishes to transmit first senses no matter the medium is busy or not. If the medium is not busy, the node proceeds with the transmission but if the medium is found busy, node chooses a random back-off time and waits for that duration until the next retry. Since such carrier sense only works among one-hop neighbors, transmissions of two nodes which can not listen to each other can collide at the receiver. Such a problem is typically referred as hidden terminal problem and is a critical problem with 802.11 MAC. RTS/CTS (Ready to send/ Clear to send) are two messages which are used to alleviate the problem but they incur higher overhead. On the other hand, TDMA does not suffer with MAC collisions in its ideal implementation because each node only transmits in its dedicated slot which does not conflict with its interfering nodes. When traffic is relatively stable (non-sporadic), TDMA can achieve maximum system capacity but there are several issued with TDMA too. Its distributed implementation is substantially difficult and requires tight time synchronization. Also, it is relatively inflexible to dynamic changes to the topology.

Since interference can be caused by many nearby nodes in mesh networks, medium access and link layer protocols are much more complicated to design. CSMA-CA based MAC protocols often suffer from lower throughput in multi-hop mesh due to their conservative design but still offer advantages of their distributed nature and standardized implementation (802.11). On the other hand, TDMA based MAC protocols are known to be more efficient due to their work-conserving nature which is better suitable for relatively stable traffic pattern of mesh backbone. The problem with TDMA based MAC protocols is that their actual implementation requires thorough engineering efforts, which is often outside the scope of research [7, 137]. Due to this reason, TDMA scheduling protocols can be classified into coarse-grained and fine-grained protocols. In coarse-grained TDMA protocols, emphasize is given to link scheduling with various valid assumptions of interference model, traffic demands and centralized control. To realize their potential in practice, they often have to depend on existing link layer technologies for framing, link layer acknowledgments etc, while handling medium access and transmission control at upper layers. Fine-grained TDMA protocols often handle all link layer functions at MAC layer, which makes them increasingly difficult to implement in practice. For brevity, we do not distinguish between the two kinds of TDMA protocols and discuss them together next.

2.1.3.1 TDMA-based Link Scheduling Protocols

Recently, CSMA-CA is shown to be not suitable for multi-hop wireless networks because of its conservative medium access and hidden/exposed terminal problems [137]. On the other hand, TDMA based link scheduling can achieve better spatial reuse in case of WMNs where traffic demands between routers are assumed to be relatively stable. Along the first step towards designing realistic scheduling protocols, [138] provides LP formulation for node-based and edge-based spatial reuse TDMA scheduling for physical interference model. The study of [139] provides traffic controlled schedule generation algorithm but the computational complexity of [138, 139] can be of a high order.

It is important to model interference relationship between links based on respective interference model before they can be scheduled. The problem of link scheduling can be represented as the problem of finding the maximum independent set in the conflict graph. Vertices connected to each other in the conflict graph represent those links of communication graph which interfere with each other and cannot be scheduled simultaneously. The study of [140] first designs conflict graph for protocol interference model indicating which set of links interfere with each other and cannot be scheduled together. Conflict graph in physical interference model has vertices which correspond to edges in the communication graph. There is a directed edge between two vertices (edges in communication graph) whose weight indicates the fraction of the maximum permissible noise at the receiver of one link by activity on another link. This conflict graph based on interference model adds interference constraints to the LP formulation which optimizes the throughput for a single source-destination pair. The LP formulation requires calculating all possible transmission schedules and it is shown to be computationally expensive.

To avoid the complex edge-based conflict graph of [140, 141] proposes a method to simplify the design of conflict graph in the physical interference model. The node-based conflict graph is designed by keeping the vertex set same as the communication graph and adding a directed edge uv between vertices u and v whose weight corresponds to the received power at v of the signal transmitted by u. The only constraint in this case is that a node cannot transmit and receive on different links simultaneously. So, feasible schedule of links in physical interference model forms a matching in the communication graph and should comply with SINR constraint. With non-uniform link demands and uniform random node distribution, [141] provides computationally efficient polynomial-time scheduling algorithm for which an approximation factor relative to the optimal schedule has been proved. The algorithm is not distributed and still

requires a central entity to perform schedule calculation. Similar algorithm for double disk based interference model is presented in [142]. The computational complexity of spatial TDMA scheduling is known to be very high especially when using the physical interference model. In such cases, it becomes increasingly difficult to estimate or even bound the optimal scheduler performance and compares it with the proposed strategy. The study of [143] derives a column generation method using set covering formulation which efficiently solves the scheduling problem. The method is also used to derive tight bounds on the optimal scheduling performance which can be very useful as a benchmark for performance comparison.

To enhance the performance of TDMA, [144] considers a problem of designing minimum delay schedules via intelligent ordering of link transmissions in TDMA MAC which ensures lower node-to-gateway delays. For example, if the outgoing link is assigned the slot before the incoming link in a TDMA frame, the end-to-end delay may become significantly high. Instead, [144] formulates the TDMA scheduling problem as a network flow problem on the conflict graph, solution to which minimizes the delay on a routing tree rooted at the gateway. First, low delay transmission ordering of links is found and then it can be used with the link conflict information. Bellman-ford algorithm is used to find feasible TDMA schedule in polynomial time. The study of [145] extends the work of [144] by providing a distributed scheduling algorithm. It is first shown that TDMA scheduling problem is equivalent to finding the shortest paths in augmented partial conflict graph which is available at nodes based on their local information. Using distributed Bellman-ford algorithm, conflict-free and feasible schedule can then be derived.

Cross-layer optimization problem has also attracted researchers to derive resource allocation solutions for multi- hop wireless networks. Starting out, seminal work of [146] coins throughput-optimal scheduling. It shows that scheduling mechanism is throughput optimal if it maximizes queue-weighted sum of rates and also characterize maximum attainable throughput region. Scheduling policy proposed in [146] is centralized and suffers from a higher computational complexity. The study of [147] shows that relaxing scheduling component in cross-layer design can actually open up many chances for new distributed, simpler and provably efficient algorithms. The imperfect scheduling (also known as greedy scheduler or maximal weight scheduler) policy determines the schedule by choosing links in decreasing order of the traffic backlog at every node. As described in [148], such greedy maximal scheduler often performs near optimal empirically but the known bounds of its performance are still very loose. It is known that such maximal scheduler is guaranteed to achieve at least half of the maximum throughput region for

node exclusive interference model [149]. Such efficiency ratio is shown to be dependent on interference degree of the network in [150]. It is shown that with bidirectional equal power geometric (double disk) interference model, such scheduling can achieve 1/8 of the maximum throughput region. Similarly, it is shown in [151], when $K \geq 2$, greedy maximal scheduler can achieve the efficiency ratio of 1/49. The study of [152] shows that network topologies that satisfies local pooling condition can achieve maximum throughput in case of longest-queue first scheduling. Using this result, it is proven in [148] that greedy maximal scheduler can achieve full system capacity in tree networks under K-hop interference model and has efficiency ratio between 1/6 to 1/3 in geometric network graphs. Such an imperfect scheduling [153] has led the way to many joint algorithms for scheduling [154], congestion control [155], channel assignment [156] and routing [157]. A good survey for such approaches can be found in [147]. One interesting extension of the TDMA scheduling problem is to design collision-free link scheduling of the broadcasts. Network wide broadcasting of messages is one fundamental operation in ad-hoc networks and several upper layer protocols depend on such functionality. As outlined in [158], broadcast scheduling with link interference conflicts incurs a latency which is calculated as duration between time of first broadcast and time at which all nodes receive the broadcast. The objective is to compute a broadcast schedule which requires less number of slots (minimum latency) and fewer numbers of retransmissions. The study of [158] first proved that minimum latency broadcast scheduling is also NP-hard and provides approximation algorithm for it. The latency of approximation algorithms are subsequently improved by [159, 160, 161, 162, 163].

2.1.3.2 CSMA-CA Based Scheduling Protocols

Several research approaches try to modify CSMA-CA based MAC to make it suitable to multi-hop mesh networks. Such ideas hold practical importance because they can be implemented using existing available 802.11 systems. A proposed MAC named DCMA (Data-driven Cut-through Medium Access) [164] allows a packet to be forwarded from the Network Interface Card (NIC) by only using MPLS like label-based forwarding. Such forwarding does not require IP route lookup or any other assistance from the forwarders CPU. Packets next hop is decided based on the label in RTS/ACK packet and the MAC-label table lookup in NIC. Due to combined RTS/CTS mechanism and pipeline kind of MAC-forwarding, DCMA reduces the number of channel access attempts and end-to-end latency. The study of [165] extends such the label switching based MAC design for multi-radio multi-channel WMNs. It shows that with link layer forwarding in cut-

through MAC, it is possible to make channel reservations in advance for packets next hop simultaneously while receiving them from previous hop on a different channel. It provides modified channel access/reservation mechanism for this label-switched forwarding similar to 802.11 DCF which can reduce the end-to-end delay in multi-hop communication.

The RTS/CTS mechanism of 802.11 is often disabled in WMNs because of their over-conservative nature. In such cases, hidden terminal and exposed terminal problems can increase MAC collisions. The study of [166] first proposed measurement based technique to mitigate the exposed terminal problem and improve spatial reuse. In the first phase, interference estimation technique of [167] is extended for detecting all potential exposed terminal combinations. Such information is then propagated in the network. Special control messages (RTSS C Request to Send Simultaneously, CTSS C Clear to Send Simultaneously) are then used whenever such transmissions with probable exposed terminals are encountered. This improves the overall simultaneous transmissions but requires large overhead of message transfers in the initial learning phase. The study of [168] proposes the use of location information to avoid exposed terminal problem in 802.11 MAC protocol which can lead to better spatial reuse in mesh. Similarly, [169] and [170] outline a busy-tone based solution for avoiding hidden terminal problem without interfering with data signals.

Other issues of CSMA-CA like rate control, fairness and carrier sense are also addressed for multi-hop networks. The study of [171] studies effectiveness of 802.11, 802.11e and 802.11n MACs on multi-hop mesh with different rate adaptation mechanisms. The study of [172] proposes spatial back-off algorithm which controls transmission rate and carrier sense threshold for current transmission to allow more number of other concurrent transmissions resulting in better spatial reuse. 802.11 MAC can be inherently unfair when used in multi-hop environment. Maxmin model for per-flow fair bandwidth assignment to prevent such unfair MAC performance is provided in [173].

2.1.4 Other Related Approaches

In [41], a centralized joint channel assignment and routing algorithm is designed to improve the throughput of the system. In this algorithm, a link with higher load is given a higher priority to be assigned a channel. The algorithm also considers the traffic balance in the whole system. In [10], channel assignment and routing decisions are made based on the calculation of logic topology constraints, interference constraints and radio constraints. On the other hand, Huang *et al.* [9] propose an approach to improve the system

throughput in the gateway using a tree topology. Their centralized algorithm assigns a channel to every link in the system. When the number of the routers in the system increases, the control overhead becomes noticeable and reduces the network performance significantly. The tree topology is also used in [174], but only for transmitting multi-cast data. More related approaches can be found in [175, 176, 177, 178]

Unfortunately, to the best of the author's knowledge, no previous work has addressed the problem of improving the gateway throughput while achieving fairness and supporting QoS differentiation for end-users. In Chapter 3, we explore the capacity of WMNs to serve multiple CoSs with different QoS requirements.

2.2 Survivability of Wireless Mesh Networks

As shown in Fig. 1.1, there are two types of nodes in MRMC wireless networks: wireless routers and wireless clients. All of the nodes in MRMC networks act as hosts to the traffic of their directly connected wireless clients; they are responsible for relaying their flows to neighboring nodes in addition to relaying neighboring nodes' own traffic to other neighbors, until they reach their destinations. Compared to traditional wireless networks, such as ad hoc networks, MRMC wireless networks have the following main characteristics: firstly, the routers are relatively stationary, hence, once routing paths are created, they are likely to be stable. Secondly, most of the traffic flows are either originating from or terminating at designated gateways which provide the Internet access to the clients. Thirdly, the power consumption of the routers is not usually a significant issue as they have easy access to power through wires. Moreover, as these routers are located close to users, the routers must operate at low powers to avoid any health threats to end-users. Finally, security is not a critical factor since routers usually belong to a single domain.

Given all these characteristics, MRMC network technologies have attracted considerable attention in recent years due to their fast deployment, ease of maintenance compared to traditional wireless networks. Furthermore, MRMC networks are highly reliable, when compared to other technologies due to the use of multiple radios and channels to increase resource redundancy. In other words, even with the presence of a link or node failure, nodes can still communicate with each other by using other intermediate nodes, due to the use of multiple interfaces. Hence, MRMC networks are largely considered as dynamic self-organizing and self-configuring species of networks. To date, MRMC wireless networks are applied in many applications such as enterprise networking, building

automation, and broadband home networking.

2.2.1 Node and Link failures Wireless Mesh Network

2.2.1.1 Classification of link failure problems

Link-quality degradation: Unfortunately, similar to other wireless networks, the quality of wireless links in MRMC networks can degrade due to severe interferences from other co-located wireless networks. For example, Bluetooth devices, cordless phones, and other coexisting wireless networks operating on the same or adjacent channels may cause varying degrees of losses or collisions with transmitted packets. By switching the tuned channel of a link to other interference-free channels, the quality of the wireless link can be recovered.

Link congestion: Links in some areas may not be able to accommodate increasing quality of service (QoS) demands from end-users, depending on the spatial or temporal locality. For example, links around a conference room may have to relay too much data/video traffic during the session. Likewise, relay links outside the room may fail to support all attendees' Voice-over-IP (VoIP) calls during a session break. By re-associating their radios with under-utilized channels that are available, links can avoid such service degradation.

Heterogeneous channel availability: Links in some areas may not be able to access wireless channels during a certain time period due to the spectrum etiquette or regulation. For example, some links in an MRMC are forced to vacate some channels if they are being used for an emergency response near the wireless links (e.g., hospital and public safety operations). Such links can seek and identify alternative channels available in the same area.

2.2.1.2 Classification of node failure problems

Since an MRMC can be made up of hundreds of components, their failures or misbehavior put additional burden on neighboring components and may even cause them to fail if their resulting traffic-loads exceed a given threshold. This may happen recursively and can lead to a cascade of failures. In general, we can classify node failures into three categories as follows:

Failure of Regular Nodes: In this case, the failed node is a regular node in a given MRMC. As shown in Fig. 2.2, if an intermediate wireless node D fails, all the data flows

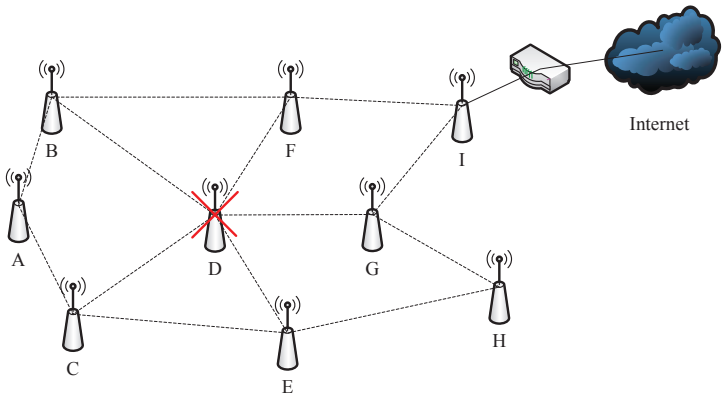

Figure 2.2: Failure of regular Nodes

through it will be affected. In order to keep the system working, these data flows must be moved to other nodes in the system. So, the extra traffic load burdens are added to those backup nodes and this in turn may lead to traffic congestion in those nodes. In addition, some delay sensitive data flows may be dropped in this process. Accordingly, the performance of the system may be degraded depending on the location and criticality of the failed node. Hence, it is necessary to have a good recovery scheme that is able to find congestion free detour paths for the affected data flows while maintaining a balanced traffic load in the affected system.

Failure of Gateway Nodes: In MRMC networks, some of the nodes in the system are chosen to be gateways which connect to the wired networks and provide Internet access service to end-users. As shown in Fig. 2.3, nodes B, I, J are working as gateways, if node J fails, the nodes connecting to it may lose their connection to the Internet. So, it is necessary to design a node failure recovery scheme which can build backup routes to alternate gateways for the affected nodes.

Failure of Boundary Nodes: Many MRMC networks exploit modularity as a way of coping with complexity. Modules in MRMC networks are clusters of wireless nodes that are highly interconnected within and loosely connected outside the cluster. Fig. 2.4 depicts an MRMC wireless network that is composed of five tightly coupled clusters, each of which is loosely connected to the other clusters. In this case, Node A, B, C, D, E can be considered as boundary nodes. All the data flows between the two clusters will go through them. If one of these boundary node fails, the whole system may separate into multiple clusters and lose connections between each other. As shown in Fig. 2.4, if node C fails, the system becomes separated into three isolated parts: two mid-sized

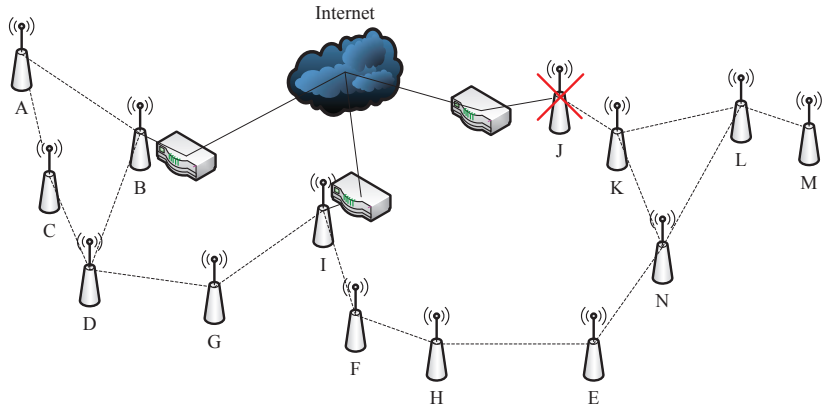

Figure 2.3: Failure of gateway Nodes

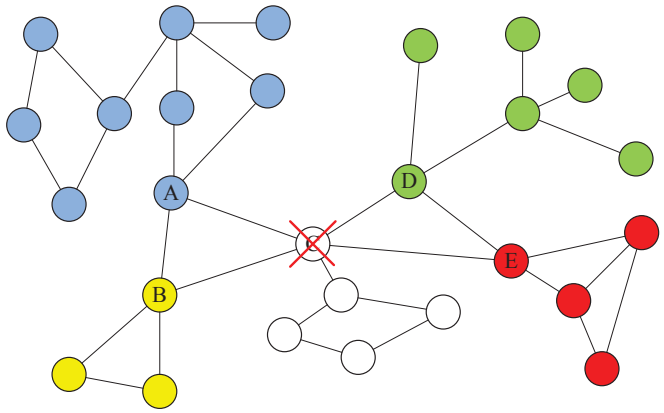

Figure 2.4: Failure of boundary Nodes

clusters (cluster $A-B$ and $D-E$) and a small size cluster C.

Node Failure in Interdependent Networks: Besides working as a wireless backbone network, MRMC networks are also employed in the power grid control networks. These two networks are interdependent: the power grid supplies power to the MRMC wireless network and the MRMC transmits the essential control messages for the power grid. In this case, if a node fails in one of these two networks, the whole system may malfunction. As shown in Fig. 2.5, there are two interdependent networks. A is the power grid and B is the MRMC wireless network. In step a, an attack occurred in one of the nodes of A. In step b, the attacked node is lost and the dependent node in B is also lost because it lost the power supply from A. In step c, more links fail because the communications between those nodes failed. At the end of this recursive process, the system is separated into multiple small clusters.

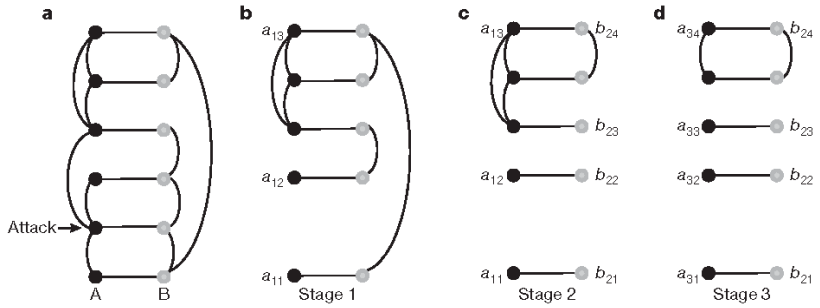

Figure 2.5: An example of node failure in interdependent networks [2]

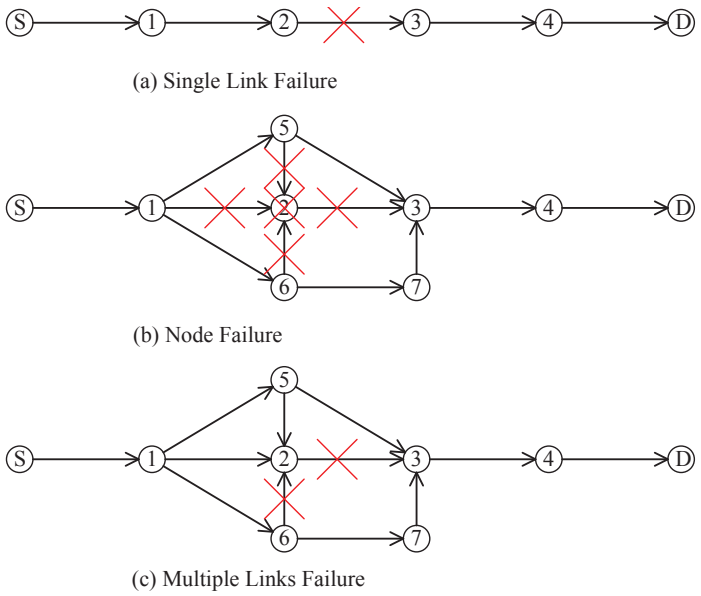

Figure 2.6: Illustration of the link and node failure

2.2.1.3 Causes of link failures

Since MRMC wireless networks are typically used as wireless backbones, they have the nature that the wireless transmission is not stable. However, the nodes in MRMC wireless networks do not move, and the route failure is most probably caused by power-off or system failure. Generally, there are two types of failures: node failure and link failure. Link failure happens more frequently than node failure. While node failure always contains multiple link failures since the links will fail on a failed node, which is shown in Fig. 2.6.(b).

Link failure can be classified into two categories based on the number of the failed

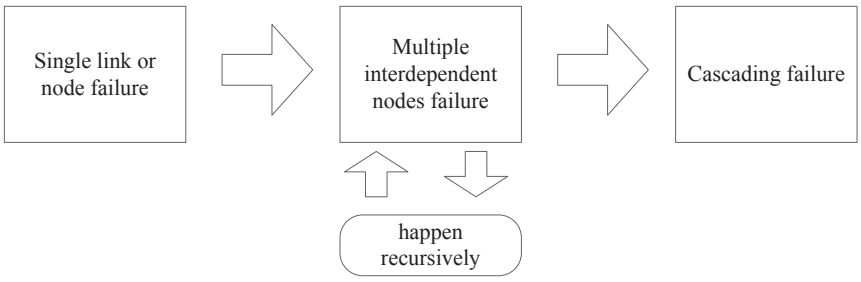

Figure 2.7: The illustration of the generation of the cascading failure

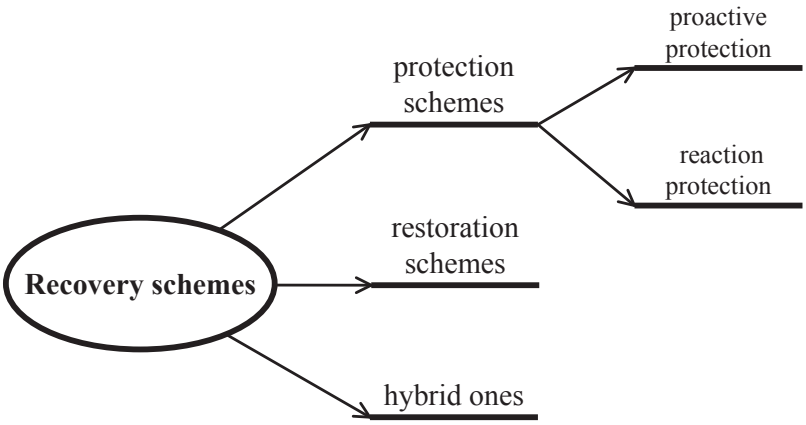

Figure 2.8: The classification of the recovery schemes

links: single-link failure and multiple-link failure, which are shown in Fig. 2.6.(a) and (c) respectively. Moreover, according to the recovery time from the link failure, they can be classified as permanent failure and transient failure [179]. If a failure cannot be recovered automatically within a short time, we call it a permanent failure. And if a failure lasts for a very short duration, we call it a transient failure. Temporary failures are more frequent than permanent ones.

2.2.2 Failure Recovery Approaches

As described before, there are three main classes of approaches focusing on link and node failure recovery (as shown in Fig. 2.8), namely, protection schemes, restoration schemes and hybrid ones [33, 7].

In the *protection scheme*, two (or more) link-disjoint paths are selected between a

source and a destination node. The source node forwards the data on all of the selected paths. If there is a link on one of the paths which is broken, the destination can still receive the data for the other paths. Currently, most mentioned protection schemes are referred to be 1+1 protection schemes. The protection schemes can be classified into two categories: *the proactive protection* [33, 180] and *the reaction protection* [181]. The major difference between these two classifications is that data is transmitted to the destination along the selected paths at the same time in the proactive protection. Hence, this activity needs at least as twice as many resources, which is hard to realize. In reactive protection, there are a primary path and a backup path. The backup path is not used until a failure occurs. *Restoration approaches* are more capacity-efficient, and they are used in [179, 182, 183]. When a failure is detected, the restoration approach switches the failed path to a backup path dynamically. Many data flows can share the links which will be used in a backup route. However, since restoration introduces delay in the recovery process, the capacity-efficiency and recovery speed must be balanced. There are two kinds of restoration algorithms, dynamic and pre-planned. In dynamic ones, message flooding is needed to recompute the route. They have quick responses to addressing frequent failures, but these algorithms introduce high cost of resource usage and a higher delay. The other ones, the pre-planned algorithms, recover from the failure more quickly but are not as robust to various failures. *Hybrid schemes* are similar to protection schemes but resort to restoration when the protection fails.

2.2.2.1 Protection Schemes

The proactive protection: Such schemes can be found in [33, 180]. In [33], the authors proposed an proactive protection approach which is based on the network coding. They claimed that the approach created n+1 paths from n data units and then forwarded these combinations. Hence, when a path was loss due to link failure, the destination could be recovered. In [180], a coding scheme is designed to tolerate the maximum number of failures in the worst case, which may sacrifice network throughput when the average number of failures is much smaller than the maximum number of failures in the worst case. The authors used the scheme to encode data packets in the source and send them in multiple disjoined paths. The destination works as a decoder to decode the received packets back to the original data. Similar work can be found in [184], the authors proposed a multi-path transport protocol, based on a carefully crafted (encoded) set of enhancements to TCP data.

The reaction protection: Many routing protocols addressed that they can cope

with the node (link) failures (or disconnections) without incurring high overhead. Existing routing approaches can be roughly divided into two categories: topology-based and position-based [122]. Topology-based protocols do not assume that each node can determine its position. Such protocols usually employ global flooding to distribute either topology information (e.g., DSDV [185]) or queries (e.g., AODV [93], DSR [94], TORA [186], and ZRP [187]). In [188], the author designed a QoS aware multi-path routing scheme to achieve high fault-tolerance. In this scheme, multiple paths are selected based on both channel load and interference on wireless links. Then the traffic split allocated to each path from a source to a destination which are determined using the congestion feedback provided by intermediate nodes along the path. Javadi *et al.* [189] proposed another multi-path routing protocol that utilized the mesh connectivity of WMNs in order to enhance the delay and reliability. The designed protocol discovers one primary path and multiple mini-paths between a source and a destination. Whilst the former connects the source to the destination, the latter connects pairs of intermediate nodes along the primary path. Multiple copies of packets are simultaneously routed through the mini-paths to compensate for possible outage at intermediate nodes along the primary path or their corresponding links. Routing along these mini-paths is performed in a way that redundant copies do not cause an excessive congestion on the network. In [190], authors also designed a multi-path routing protocol to improve the reliability of WMNs. In this protocol, the interference and load of each link is determined based on which a combined routing metric is designed. Multiple shortest paths are then established and the path with least combined metric is chosen as primary path. In case of any failures in primary path, the data transmission can be rerouted through the backup path. Some other multi-path routing protocols can be found in [191, 192]. [193] developed a Fault Tolerant HAWAII (FT-HAWAII) protocol and investigate the performance in Tree and partial Mesh routing topologies. This protocol modified the RIP (Routing Information Protocol) in order to achieve fault tolerance. Topology-based protocols do not assume that each node can determine its position. Such protocols usually employ global flooding to distribute either topology information or queries, and hence suffer from limited scalability [122, 194]. By assuming that each node can determine its location, position-based protocols achieve better efficiency and scalability than topology-based ones [122]. Position-based protocols differ from each other mainly in how many location servers store each node's location. Li *et al.* [194] have proposed the Grid Location Service (GLS), which stores each node's location at small number of nodes. They have shown that this approach, achieves good tradeoff between reliability and load: each node updates its lo-

cation at small number of nodes without flooding the network, and location queries incur a reasonable overhead. The authors also shown that in a small network, GLS tolerates intermittent node disconnections well. However, as shown in [195], in large networks, GLS's fault-tolerance greatly degrades. Li *et al.* [181] proposed an reactive protection scheme to achieve the desired robustness of the wireless network. The proposed scheme reserved partial bandwidth for backup paths disjoint from the primal paths. It considered the path overlapping allocation of backup paths for different receivers to take advantage of network coding, and took into account the robust multi-path rate-control and bandwidth reservation problem for scalable video multi-cast streaming when possible link failures of primary paths existed. Similar schemes about the reliable multi-cast and broadcast can be found in [196, 197]. In [198], authors proposed a fault tolerance technology to support emergency information transmission in WSN by selecting alternative path after fault detection.

The aforementioned protection schemes exploited the multi-path property of the wireless mesh networks and increased the robustness of the MRMC wireless network to the unexpected transmission failures based on the link failure. But, this kind of schemes is achieved by using more transmission resources (wireless channels) and more frequently channel switching. Due to the limited number of the wireless channels and ineluctable channel switching delay, this kind of schemes is difficult to be adopted in a practical wireless network.

2.2.2.2 Restoration Schemes

The restoration approach is more capacity-efficient (resource-efficient) than the protection schemes. Because the restoration scheme do not need to reserve the transmission resources for the works data stream. In [179], Wu *et al.* proposed a restoration scheme called Hybrid Fast Restoration Scheme (HFRS) in which local and global restorations were used. Its main idea was the recovery strategy called local recovery for local failure. Further, Jiang and Xue in [182] proposed a joint routing, channel assignment and scheduling algorithm to face the jamming happened in the wireless mesh network. The authors used a greedy scheduling algorithm to schedule both jamming traffic and regular traffic. Also, they adopted both global and local restoration to achieve desired tradeoff between the restoration latency and the network throughput after restoration. In order to quantitatively evaluate the impact of jamming attacks during and after restoration, the authors also defined two performance degradation indices, the transient disruption index (TDI) and the throughput degradation index. Another link recovery scheme can be

found in [183] which is designed for the wireless mesh networks. This work describes an autonomous network reconfiguration system (ARS) that enabled a multi-radio wireless networks to autonomously recover from local link failures while preserving their performance. In order to recover from failures, the proposed scheme generates necessary changes in local radio and channel assignments by exploiting channel and radio diversities in MRMC wireless networks. Then, based on the generated configuration changes, the system cooperatively reconfigured network settings among local mesh routers.

2.2.3 Survivability Against Failures by Design

2.2.3.1 Survivable Wireless Network Designs

In the recent years, several studies have been dedicated to the design of failure-resilient networks. For example, in [19], the authors designed a model to measure the cascading failure based on the given component failure probability in a network, such as wireless MRMC network. In this proposed model, the traffic load on the faulty node is redistributed to its neighbours. This activity increases the traffic load of its neighbor and the new total traffic load may exceed the given threshold value and cause the new node failure. When this process keeps going, the cascading failure happens. As an improvement, in [199], the authors designed a "probabilistic" region failure model to capture the key features of a region failure and applied it for the reliable assessment of wireless networks. Further, based on the failure probability, multiple algorithms are designed to improve the robustness of the network.

Currently, there is a number of existing works that aim at improving the robustness and survivability of MRMC networks by designing a new routing and channel assignment algorithms. In [200], a distributed potential-field-based routing scheme is proposed to face the sudden traffic and network perturbations. The basic idea of this algorithm is that the potential of a node failure increases as the traffic load increases and hence they try to redirect the traffic in order to avoid the area with high failure potential. This algorithm cooperates with the local re-routing scheme to achieve its goals. Wellons and Xue in [14] showed a routing formulation for multi-radio, multi-channel networks to handle the unexpected traffic demand changing (caused by the jamming attack or the link failure) by exploiting traffic demands that fall into a predicted region based on the knowledge of historical traffic demands. They showed that the robustness of MRMC wireless networks to the uncertainty of traffic demands could be improved. In [15], the authors designed a graph-based routing approach to construct reliable routing graphs which satisfy the

given reliability requirements. In this scheme, the intermediate devices on the path can be pre-configured with multiple neighbors to help transmitting packets without using a fixed path starting from a given source. Another robust routing algorithm is designed by Xiang in [16]. In this work, a deadlock-free routing scheme for meshes is proposed based on a new virtual network partitioning scheme, called channel overlapping. This algorithm is designed for an n-dimensional virtual network, but MRMC wireless networks can adopt it by reducing the dimensions to two. Similar design can be found in [201]. In [202], the authors designed a centralized channel assignment algorithm to face the given Quality-of-Service requirements. In this algorithm, a rank value for each node is computed based on the aggregate traffic, weighted cumulative expected transmission time (WCETT) from the gateway, and the number of radios per node. The proposed channel assignment algorithm enhanced the robustness of the MRMC wireless networks by improving the network throughput and by the utilization of channels to a large extent. In [203], the authors proposed an similar scheme to achieve the desired robustness and load balance of wireless networks by channel assignment and router selection. But this scheme is again purely centralized and thus lacks scalability and agility. In [204], authors designed a new sensing technique to improve the accuracy of the wireless channel condition measurement. Based on this technique, the wireless sensor networks could make more accurate decision for the routing and channel assignment. So, the reliability of the system could be improved. In [205], Deng and Yang proposed a multi-cast MAC layer control scheme to improve the system reliability and robustness based on network coding technique and IEEE 802.11 Distributed Coordination Function (DCF). Also, some approaches tried to improve the system reliability by carefully designing the connectivity or topology of wireless backbone networks. Paper [206] addresses the problem of fault tolerant deployment of wireless ad-hoc networks. The authors present a method for determining the probability that a backbone network graph is k-connected, based on the transmission range. In [207, 208], authors proposed a a localization-based method to achieve fault-tolerant radio coverage of wireless mesh networks in dynamic propagation environments. The idea is to use radio signal strength measurements from the mobile stations, find their positions with localization and use this information to automatically calibrate a radio propagation model to the real environment. This model is then used to automatically detect radio coverage errors at run-time and to repair them before the radio coverage fails. A fault-tolerant base station planning scheme in wireless mesh networks proposed in [209]. The algorithm determines a close-to-minimal number and the positions of base stations to be installed such that the radio coverage is correct in the

presence of faults (base station crash or link outage). The algorithm also considers both the connectivity of the multi-hop backbone and the connectivity of the mobile stations. Similar scheme can be found in [210]. In this design, the redundant wireless sensors are employed, of which one can fail and the other supplies the needed data. Chen and Son [211] presented a fault-tolerant topology control by adding necessary redundant nodes to the network's simple communication backbone with a distributed algorithm. But it may not always be possible to add redundant nodes to the existing network. Li and Hou [212] presented the fault-tolerant topology control algorithm in which all nodes compute a spanning subgraph locally, where an edge is added to the local spanning subgraph if the two endpoints of the edge are not k-connected, and prove that the global network is k-connected. In [213], it is argued that mobility resilient topology control protocol should require little maintenance in the presence of mobility. In [213], Topology control protocols are classified into two types: P1 and P2. In protocol P1 the nodes builds the topology in the distributed manner and set their own transmission power according to their own requirement. In protocol P2 every node tries to maintain some number of neighbors in its vicinity according to some criteria. The algorithm presented by Li and Hou [212] is an example of protocol P1, whereas the algorithm presented by Bahramgiri *et al.* [214] is an example of protocol P2. The reconfiguration procedure for protocol P1 is more complicated than that for protocol P2. Maintaining the Minimum Spanning Tree in mobile scenario demands the algorithm to run frequently, as the absence of one edge from the topology graph may make the topology disconnected. On the other hand maintaining a number of neighbors at a particular cone as done in [214] is easier than protocol P1. As a result, though the algorithm presented by Li and Hou [212] is very efficient for static network, it is not advantageous in mobile scenario. [215] proposed a distributed algorithm for assigning minimum possible power to all the nodes in a static wireless network such that the resultant network topology is k-connected. In this algorithm, a node collects the location and maximum power information from all nodes in its vicinity, and then adjusts the power of these nodes in such a way that it can reach all of them through k optimal vertex-disjoint paths. The algorithm ensures k-connectivity in the final topology provided the topology induced when all nodes transmit with their maximum power is k-connected. Some more works can be found in [216, 217, 218, 219, 220, 221].

2.2.3.2 Survivable Interdependent Networks Designs

Besides the MRMC wireless networks, some works are proposed for the interdependent networks that incorporate MRMC networks. In [222],the authors introduced a Combina-

tion of Cognitive Wireless Network (CWN) and Satellite System for Disaster Information System to realize a Never Die Network (NDN) which supposed to be unaffected by any changes in environment after severe disaster. In [223], authors designed a survivable hybrid Wireless-Optical Broadband-Access Network (WOBAN). In this paper, the proposed survivable network achieved desired survivability by using pre-configured Optical Network Units (ONUs) to serve as a backup gateway and redistribute their local traffic through the connected wireless backbone. Similar work can be found in [224]. The authors designed a fault aware routing scheme to enhance the network resiliency in the hybrid WOBAN. In [225, 226], authors used the wireless network to improve the robustness of the given smart-grid network. In [227], the authors proposed a unified definition of the Self-healing of the MR-MC wireless networks. In [228], authors designed a fault-tolerant event detection scheme in order to detect the node failure accurately, which is important in structural health monitoring (SHM) and volcano monitoring. Some other efforts targeting the survivable and reliable networks design can be found in two surveys [229, 230].

2.2.4 Theoretical Analysis of Node Failure Problem

In some cases, repetitive single failures may lead to a cascade of network failures as illustrated in Fig. 2.7. Hence, this type of failures must also be considered by any efficient recovery scheme. A dramatic real-world example of a cascade of failures is the electrical blackout that affected much of Italy on 28 September 2003, as shown in Fig. 2.9: the shutdown of power stations directly led to the failure of nodes in the Internet communication network, which in turn caused further breakdown of power stations. In general, research efforts targeting link and node failure recovery can be also considered as efforts that can eliminate or reduce the effect of the cascading failure.

In the light of the inevitability of link and node failures and their detrimental consequences, several studies have been dedicated to address the properties of cascading failures, particularly those caused by node (component) failure. We summarize these research efforts in three main fields:

1) Research focusing on system resiliency to the cascading failure based on different network topologies. For example, in [3], the authors test the resilience of the networks in the topologies following Exponential ($Erdös - Rényi$ model) and Power-Law (scale-free model) distributions, which represent homogeneous and inhomogeneous networks respectively, as shown in Fig. 2.10. The authors concluded that exponential networks

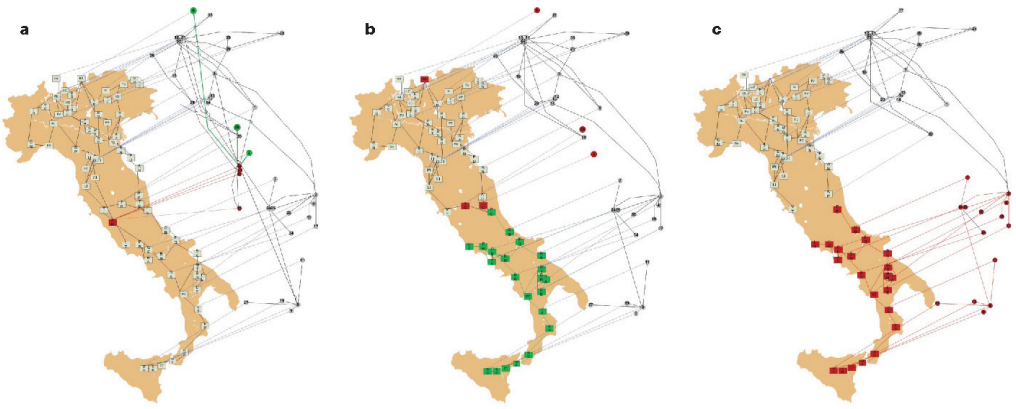

Figure 2.9: Modelling a blackout in Italy [2]

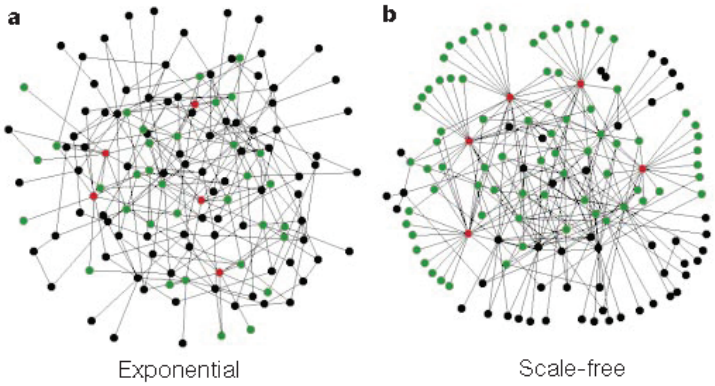

Figure 2.10: Illustration of the exponential and the scale free network [3]

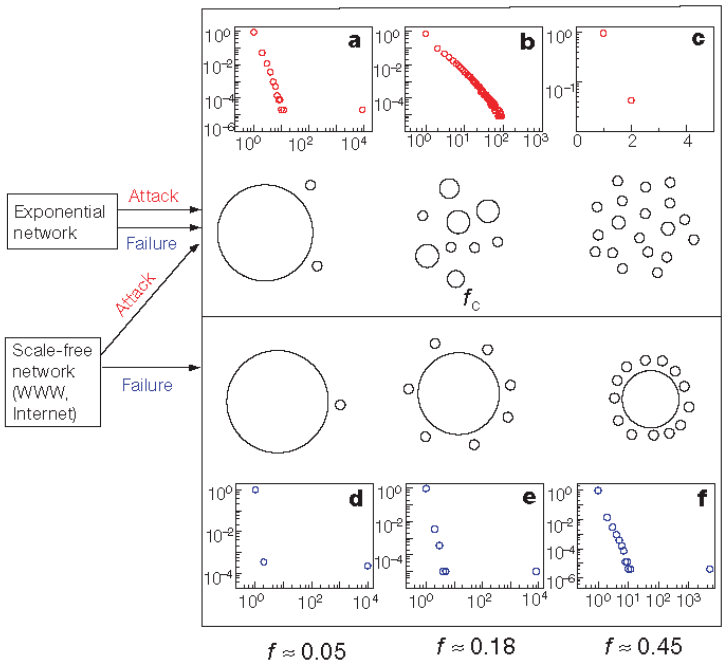

Figure 2.11: Summary of the response of a network to node failures or attacks [3].

had similar performance under failures or attacks while scale free networks are more robust to failures but had worse performance under attacks. The results are summarized in Fig. 2.11. In sub-figures (a-f), the cluster size distribution for various values of f (the fraction of the failed nodes) when a scale-free network is subject to random failures (a-c) or attacks (d-f). Upper panels, exponential networks under random failures and attacks and scale-free networks under attacks behave similarly. For small f, clusters of different sizes break down, although there is still a large cluster. This is supported by the cluster size distribution: although we see a few fragments of sizes between 1 and 16, there is a large cluster of size 9,000 (the size of the original system being 10,000). At a critical f_c the network breaks into small fragments between sizes 1 and 100 (b) and the large cluster disappears. At even higher f (c) the clusters are further fragmented into single nodes or clusters of size two. Lower panels, scale-free networks follow a different scenario under random failures: the size of the largest cluster decreases slowly as first single nodes, then small clusters break off. Indeed, at $f = 0.05$ only single and double nodes break off (d). At $f = 0.18$, the network is fragmented (b) under attack, but under failures the large cluster of size 8,000 coexists with isolated clusters of sizes 1 to 5 (e). Even for an unrealistically high error rate of $f = 0.45$ the large cluster persists, the size of the broken-off fragments not exceeding 11 (f). From the upper part of the

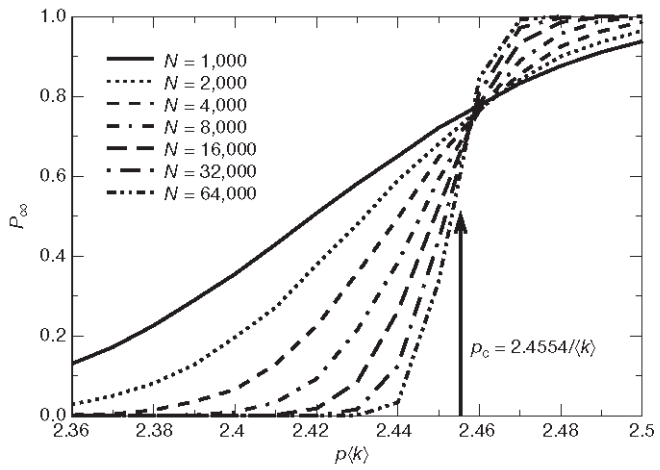

Figure 2.12: Numerical simulations of coupled $Erdös - Rényi$ networks [2]

figure, we can see that both the exponential and scale free networks were separated into small unconnected clusters due to an attack on few nodes in the system. The scale free networks were more robust than the exponential networks in the random failure case. Based on these conclusions, it is clear that network topologies must be considered as an essential factor when we design a MRMC networks.

2) Mathematical modeling of cascading failures in different types of practical networks, such as power grids, transport networks and wireless MRMC networks. In [231], the authors designed a mathematical model for the cascading failure in complex networks which is based on local load distributions; this model can be easily adopted in MRMC networks. Similar work can be found in [232].

3) Research about cascading failures in interdependent networks. For example, in [2], the authors showed that cascading failures often happen in a mixed power grid and communication networks, as has been discussed before. In Fig. 2.12, numerical simulations of coupled $Erdös - Rényi$ networks with average degree $\langle k \rangle = \langle k_A \rangle = \langle k_B \rangle$ and a finite number of nodes, N. The probability of existence of the giant mutually connected component, P_∞, is shown as function of p for different value of N. As $N \to \infty$, the curves converge to a step function. The theoretical prediction of p_c is shown by the arrow. Fig. 2.13 depicts the simulation results for P_∞ as a function of p for coupled scale-free (SF) networks with $\lambda = 3$, 2.7, 2.3, coupled $Erdös - Rényi$ (ER) networks and coupled random regular (RR) networks, all with an average degree $\langle k \rangle = 4$ and $N = 50,000$.

Based on these simulation results, we can see that only a small percentage of nodes in

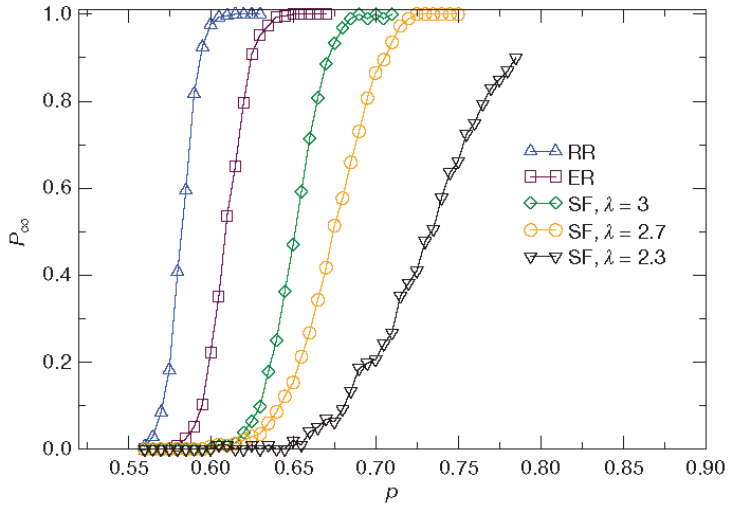

Figure 2.13: Numerical validation of theoretical results [2]

the system when losing their function can cause a whole network failure. Because these results where obtained for some general types of networks, MRMC networks are also expected to have the same behavior. In [233],the authors conducted a systematic study of human initiated cascading failures in critical inter-dependent societal infrastructures (i.e. transport network and communication network), which again lead to similar results.

2.3 Research Efforts about Green Energy Powered Wireless Mesh Network

As energy savings and environment protection became global demands and inevitable trends, researchers and engineers gradually shifted their focus to developing energy-efficient MRMC wireless networks solutions. To date, various research efforts have generated efficient solutions to minimize the overall network energy consumption [234] or to maximize the routers' energy efficiency or the overall energy utilization of the network [21, 22, 23].

Unfortunately, these design efforts have mainly focused on increasing the network capacity and enhancing its performance while assuming that electricity sources are readily available to provide the mesh routers with a continuous power supply with no stringent usage limit. However, this assumption may not be always valid. On the one hand, electricity is mostly generated from limited and non-reusable natural resources, such as coal,

natural gas, and petroleum that are very costly and unfriendly to the environment. On the other hand, in some deployment scenarios of MRMC wireless network, such as those that take place in rural communities or during battlefields, these networks may represent the only feasible means of communication in areas with no utility infrastructures. These two limitations motivate the use of green energy sources to power wireless networks. These sources produce energy harvested from natural resources, that can be replenished without compromising the energy requirement of future generations like solar, wind, etc., are expected to be widely used in next-generation wireless networks. The sustainable and environment-friendly characteristics of these sources can help in meeting the ever-increasing user demand, while reducing the detrimental effects of conventional energy production.

Recently, some research efforts have focused on the use of the green energy to power wireless network [25, 26, 27] with focus on efficient functionalities such as scheduling and routing [28] with the objective of minimizing the consumed power. The study of power-optimized routing in multi-hop wireless networks has received a considerable interest in the literature. For example, the authors in [147] considered the problem of energy-aware routing without explicitly allocating transmission powers to the wireless devices. A joint optimal routing and power allocation scheme has been presented in [235]. The authors employed the Bellman-Ford algorithm to calculated shortest paths satisfying one of two objectives, namely, sum-power minimization or maximum power minimization.

Other energy efficiency and spectrum efficiency routing algorithms can be found in [21, 22, 23]. In addition to energy-optimized routing schemes, several studies have been dedicated to investigate energy efficient communication through cooperation. Zou *et al.* [236] investigated the use of user terminals that can cooperate with each other in transmitting their data packets to the base station (BS), by exploiting the multiple network access interfaces. In [237] a joint planning and energy management framework for MRMC wireless networks was proposed. Several energy aware scheduling algorithms were introduced in the literature; for example, in [238], the authors designed a joint energy efficient packet scheduling and fair queuing for wireless communication systems. Yang and Ulukus [239] designed an optimal long-term scheduling policy to minimize the time by which all packets are delivered to the destination, under causality constraints on both data and energy arrivals. Similar approaches can be found in [240, 241].

The general framework of the proposed work also relates to efforts targeting energy usage minimization while transmitting data by users' mobile devices. For example, the work presented in [242] seeks to find an the optimal rate-control policy in order to mini-

mize the needed transmission energy given additional constraints such as the transmission deadline. The authors employ the cumulative curves methodology to find an admissible departure curve with the least energy expenditure. In [25], Lin *et al.* consider a wireless mesh network with renewable energy sources and aimed at minimizing the overall network consumption of energy while guaranteeing a minimum maximum power allocation of each node according to its residual energy. The problem developed a mixed-integer nonlinear program that finds the optimal routes and link rates in order to achieve their objective. A heuristics based algorithm is then employed to solve the problem. However, the solution does not guarantee that one ore more nodes in the system might be eventually depleted of energy.

The main limitation of the aforementioned research efforts is that they typically assumed that the routers or access points are permanently connected to a sustainable energy supply such as the electric grid.

Recently, several research efforts have been dedicated to considering wireless networks operating solely on rechargeable energy supply sources. For example, the sustainable performance of a wireless mesh networks powered by renewable energy sources has been analyzed in [234]. The authors developed a routing scheme that minimizes the depletion probability of a mesh node rechargeable battery. Similarly, in [28] the authors considered a mesh network in a disaster situation. A two stage routing scheme that delivers the clients traffic to the gateways is then developed by the authors. The scheme is based on an Integer linear program that finds the paths that maximize the throughput while minimizing the throughput. The proposed work in this thesis assumed that the instantaneous harvested energy is known.

The authors in [243] consider a time period that has a fixed amount of harvested energy and develop various transmission policies to maximize the short term throughput. The authors also address the problem of minimization of the transmission completion time for a given amount of data as well given a fixed amount of energy. Two deadline aware scheduling schemes for the green energy powered wireless system can also be found in [244, 245]. In [26] the authors focused on solar systems as green energy sources. Historical data were used in order to determine the optimal size for a solar panel powering an access point in order to reduce the outage probability while minimal the cost. Closest to our work is the routing scheme developed in [234]. The authors share the same objective of the minimizing the battery depleting probability. However, the authors focus on developing an efficient routing scheme.

2.4 Summary

This chapter discussed various issues related to the performance enhancement and survivability problems in WMNs. In summary, with respect to channel assignment, existing approaches mostly suffer from their computational complexity because of the need to decompose and solve an NP-hard optimization problem. On the other hand, simplified approaches that are based on heuristics fail to find optimal solutions. Furthermore, none of the previous approaches have addressed the problem of improving the gateway throughput while achieving fairness and supporting QoS differentiation for end-users during the channel assignment process. In Chapter 3, we explore the idea of improving the capacity of WMNs through efficient channel assignment and scheduling while serving multiple classes of services with different QoS requirements. The chapter also discussed the problem of network survivability in the face of node and link failures. We noted that existing studies did not consider an interesting but more fundamental question for WMNs that is whether a cascade of node failures is related to the nodes' density and their geometric distributions. In Chapter 4, we address that question. Also, in Chapter 5, a novel backup scheme is proposed. Finally, this chapter surveyed the research efforts about the energy efficient WMNs' design and green energy powered WMNs. In Chapter 6, we theoretically analysed the residual energy behaviour of the wireless node battery. Based on the theoretical results, we propose an optimal energy efficient packet scheduling scheme to prolong the battery life in green WMNs nodes.

Chapter 3

A QoS Aware Design for Wireless Mesh Networks

As described in Chapter 1 section 1.1 and section 1.2.1, WMNs provide Internet access to remote areas and wireless connections on a metropolitan scale. In this chapter, we focus on the problem of improving the gateway throughput in WMNs while achieving fairness and supporting quality-of-service (QoS) differentiation for end-users. To address this problem, we propose a new distributed dynamic traffic scheduling algorithm that supports different QoS requirements from different users. We also develop a joint weight-aware channel assignment and minimum expected delay routing mechanism. Simulation results demonstrate the performance of the proposed work in terms of the achieved throughput and minimized packet loss ratio and delay [31].

3.1 System Model and Problem Formulation

3.1.1 System Model

We consider a WMN comprised of multiple static wireless routers and can be represented by an undirected graph $G = (V, E)$. The set V represents the set of routers and E is the set of communication edges in the system. The wireless routers form the wireless backbone network to relay the traffic from end-users to the gateway. The gateway in the system is used to connect these users to the backbone network.

Each router $v_i \in V$ has a set of wireless radio interfaces, which is represented by $R(v_i)$. Each radio $r \in R(v_i)$ can operate on a single channel selected from K orthogonal channels

with identical maximum capacity [10, 9, 174, 11]. The number of radios employed in each router v_i, can not exceed K, which means that the size of set $R(v_i)$ is typically smaller than K. Also, we assume that a router has at least two radios (one for uplink and the other for downlink communication). Each router v_i in the system aggregates the data from all end-users associated with it. The local traffic load at v_i is denoted by $ld(v_i)$. Because we are focusing on maximizing the throughput in the gateway, we are only concerned with the outgoing traffic from the routers to the gateway. So the load $ld(v_i)$ represents only the local outgoing traffic load. Also, we assume that $ld(v_i)$ follows a random distribution with a fixed long-term mean value [30, 8, 9]. Similar to [30], we assume that $ld(v_i)$ consists of a mix of constant bit rate (CBR) and variable bit rate (VBR) traffic.

3.1.2 Traffic Model

Based on the definition of *DiffServ* [7], we adopt three classes of services: CoS1, CoS2 and CoS3. CoS1 represents low-loss, delay-sensitive Expedited Forwarding (EF) services, which typically provides for CBR VoIP data. CoS2 data represents Assured Forwarding (AF) services. It is suitable for non-delay sensitive, bandwidth guaranteed VBR video/data. Finally, CoS3 represents Best Effort (BE) services, which requires no bandwidth commitment from the system and is suitable for WWW data [7].

3.1.3 Wireless Interference Model

Two wireless routers can communicate if they are within the communication range of each other when a common channel is assigned to their radios. We use Ri to denote the interference range; the routers that use the same channel and are located in each other's interference range may interfere with each other. Let Rt be the transmission range common to all routers and let $d(v_i, v_j)$ denote the physical distance between routers v_i and v_j. An edge $e(v_i, v_j) \in E$ exists if and only if $d(v_i, v_j) \leq Rt$, which means that router v_i can communicate with router v_j directly. Since we only consider outgoing traffic, we only focus on traffic originating from one router v_i to another router v_j that is closer to the gateway and not vice versa. In this case, v_j is considered as the *parent* of v_i and is represented by $P(v_i)$. The transmission rate, $r_{trans}(v_i, v_j)$, from router v_i to v_j is chosen by the parent router v_j based on the SINR of the received data from router v_i, which is introduced in IEEE 802.11 standards [246]. For simplicity, we assume that the transmission rate $r_{trans}(v_i, v_j)$ is based only on the distance $d(v_i, v_j)$ [8].

Notation	Description
N	number of routers in the system
$R(v_i)$	the set of radios in router v_i
K	number of available channels in the system
$ld(v_i)$	local outgoing traffic load in router v_i
$e(v_i, v_j)$	the physic link between router v_i and v_j
Rt	transmission range
Ri	interference range
$r_{trans}(v_i, v_j)$	transmission rate from router v_i to v_j
$d(v_i, v_j)$	the distance between routers v_i and v_j
$L^r_{v_i}$	the set of links share radio r of router v_i
$C^r_{v_i}$	the children set of radio r of router v_i
$\mathcal{C}$	the set of children sets in the system
$\mathcal{L}$	the set of meta-links in the system
$S(v_i)$	aggregated traffic load in v_i
$P(v_i)$	parent router of router v_i
$\mu(v_i)$	relative weight of router v_i
$\mu(L^r_{v_i})$	relative weight of link set $L^r_{v_i}$
T	length of scheduling interval
$t(L^r_{v_i})$	time fraction assigned to link set $L^r_{v_i}$
$p(L^r_{v_i})$	priority of link set $L^r_{v_i}$ based on transmission history
$p(v_i)$	priority of router v_i based on its transmission history
$f^c_{v_i}$	the predefined percentage of data in CoS c of router v_i
$t^c_{v_i}$	time fraction for router v_i to transmit data in CoS c
$b(L^r_{v_i})$	observed average $Mbps$ of data transmission through $L^r_{v_i}$ and received in v_G
$b(v_i)$	observed average $Mbps$ of data transmitted by v_i and received by its parent
D	frequency reuse distance measured in hops
$Path(v_i)$	the set of intermediate routers on the path from router v_i to the gateway
$Del(v_i, v_j)$	expected delay to transmit one unit of data from v_i to v_j
$EXD[v_i]$	estimated delay from router v_i to the gateway

Table 3.1: Adopted notations and their definitions

It is important to note that *our developed schemes are independent of the used interference model*. Hence, both the physical interference model [11] and the protocol interference model [4, 30, 9] can be employed in our algorithm. Definitions of the variables used in the proposed work are summarized in Table.3.1.

In the next section, we will propose a novel efficient joint routing, channel assignment and scheduling mechanism.

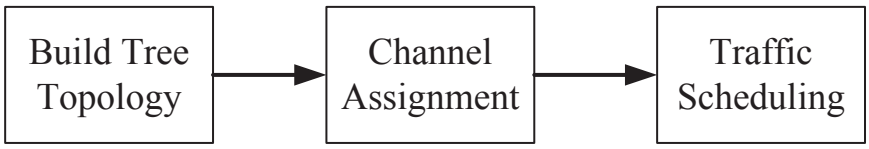

Figure 3.1: Steps involved in the execution of proposed schemes

3.2 Proposed Work

The proposed work performs the following three steps: 1) *Topology building*: the proposed minimum expected delay routing algorithm first chooses a path to the gateway for all the routers in the system. After this step, the original topology of the network is reduced to an efficient tree topology. 2) *Channel assignment*: we propose a channel assignment algorithm to assign both a channel and a number of time slots to different links in the tree topology based on the calculated links' relative weights. The channel and time assignment is adjusted periodically based on the transmission history. 3) *QoS-aware traffic scheduling*: in this step, each parent router distributes the transmission time to different children based on their transmission requirements dynamically.

The steps of our algorithm are shown in Fig. 3.1 and described in detail in the following sections.

3.2.1 Topology Building

We assume that the time in the system is well slotted and that the system works in synchronous mode [8]. Because longer, frequency diversified paths often yield worse performance than shorter paths [49], the routers in the system are separated to different levels based on the minimum hops count from the gateway [9]. Here, level l_1 denotes the lowest level, in which the routers are directly connected to the gateway.

In this section, we show how the tree topology is built using our minimum expected delay routing algorithm. In our work, we only consider the uplink transmission from routers to the gateway. In the proposed algorithm, the expected delay is estimated based on the aggregated traffic load in each router. At the end of this step, each router v_i will be associated with a $Path(v_i) = (v_i, v_j, \cdots, v_G)$ that defines the sequence of the intermediate routers to the gateway v_G.

The first step of the topology establishment starts at the gateway v_G. For level l_1 routers (i.e., routers at a one hop distance from v_G), the gateway is their only possible

parent. Thus, v_G chooses the transmission rate for each router based on their distance, as we mentioned before. Then, a router v_i at level l_1 calculates the expected delay to transmit one unit of data to its parent, v_G, based on its transmission rate. This delay is represented by $Del(v_i, v_G)$, and is given by

$$Del(v_i, v_G) = \frac{1}{r_{trans}(v_i, v_G)} \tag{3.1}$$

Then the expected delay to the gateway ($EXD[v_i]$) can be estimated as follows:

$$EXD[v_i] = Del(v_i, v_G) \times S(v_i) \tag{3.2}$$

where $S(v_i)$ is the total aggregated traffic load from all children in router v_i. Initially, since no router at level l_2 has selected a parent at level l_1 yet, we set $S(v_i) = ld(v_i)$. The gateway v_G is saved as an element in v_i's path set, i.e., $Path(v_i) = (v_i, v_G)$.

For the other levels (i.e., from level l_2 to the highest level), a router v_i needs to request information from all the lower level routers which the router can directly communicate with. The lower level router that provides the minimum estimated expected delay to a gateway, is chosen as the parent router. Then, router v_i's approximate expected delay to the gateway through the potential parent router v_j can be updated as follows:

$$\begin{aligned} EXD[v_i] &= Del(v_i, v_j) \times S(v_i) \\ &+ \sum_{v_p \in Path(v_j)} Del(v_p, P(v_p)) \times (ld(v_i) + S(v_p)) \end{aligned} \tag{3.3}$$

The second term of Eq. (3.3) is the total delay of all intermediate routers on the path of v_i to the gateway after adding the load of v_i to these routers. $P(v_p)$ represents the parent router of v_p. When the router v_i receives all the required information from the lower-level routers, v_i chooses the parent node which provides the minimum $EXD[v_i]$ and sends the feedback information to the lower-level routers. The selected parent router v_j and all the elements in its own path set $Path(v_j)$ are saved in v_i's path set $Path(v_i)$. The aggregated load $S(v_p)$ of each router v_p (including v_j) in $Path(v_i)$ is then updated based on the traffic load in v_i as follows:

$$S(v_p) = S(v_p) + ld(v_i), \forall v_p \in Path(v_i) \tag{3.4}$$

Next, the parent router re-calculates the expected delay to the gateway based on the new aggregated traffic load and then send the new value to its children to update their local

Algorithm 1

1. **For** (each level l) **do**
2. **For** (all v_n in level l) **do**
3. send a request to all level $l-1$ routers v_j
4. **For** (all v_j in level $l-1$) **do**
5. choose transmission rate $r_{trans}(v_n, v_j)$, based on distance $d(v_n, v_j)$
6. calculate unit data transmission delay to parent, Del_{v_n}
7. calculate expected delay to gateway $EXD(v_n)$ and send it back to v_n
8. **End**;
9. choose the parent with minimum $EXD(v_n)$, send the confirm information to parent v_i
10. parent v_i updates traffic load $S(v_i) = S(v_i) + ld(v_n)$
11. parent v_i sends new delay information to its other children (line 10 and 11 need to repeat in higher level routers)
12. **End**;
13. **End**;

Figure 3.2: Minimum expected delay routing algorithm

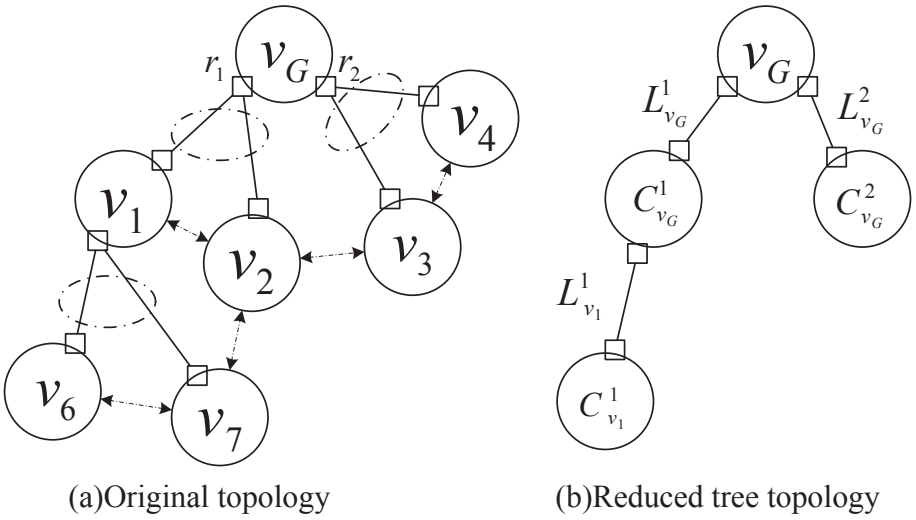

Figure 3.3: Illustration of the reduced tree topology

information. In order to avoid a deadlock, the parent router can only serve one higher level router's request at one time. A Pseudo-code of this process is depicted by Fig. 3.2.

After all routers in the system have chosen a parent, each parent, including the gateway, starts to distribute a list of its children to its radios. Each parent maintains a list of its current children ordered in a decreasing order of their aggregate traffic load $S(v_p)$. Then, the parent assigns the first child in the list (i.e., child with heaviest traffic load) to the radio with the smallest aggregated traffic load and remove it from the list until the list is empty. In this manner, the traffic load is fairly distributed between different radios.

After the above step, the original topology of the WMN is converted to a reduced tree topology. Due to the radio constraints, a set of edges must share a common radio in a router v_i. We use a meta-link, $L^r_{v_i}$, to represent the set of edges sharing a radio $r \in R(v_i)$ of router v_i. The routers connected to a radio r of a parent router v_i are represented by a children set $C^r_{v_i}$. Fig. 3.3 depicts an example of a WMN and its reduced tree topology after this step. The original topology is shown in Fig. 3.3(a), where router v_G represents gateway. Here, v_1 and v_2 share radio r_1 of v_G, v_3 and v_4 share the radio r_2 of v_G. Similarly, v_5 and v_6 share the radio r_1 of v_1. The dotted lines indicate the physical links in the original topology. As shown in Fig. 3.3(b), edges $e(v_1, v_G)$ and $e(v_2, v_G)$ are represented by link $L^1_{v_G}$ and $\{v_1,v_2\}$ is represented by the children set $C^1_{v_G}$. Similarly, $\{v_3, v_4\}$ and $\{v_5, v_6\}$ are represented by $C^2_{v_G}$ and $C^1_{v_1}$, respectively. The reduced tree topology is shown in Fig. 3.3(b).

The original graph $G = (V, E)$ is now converted to a reduced tree topology $T = (\mathcal{C}, \mathcal{L})$ with the gateway representing the root of the tree. $\mathcal{C}$ denotes the set of children sets in the system and $\mathcal{L}$ represents the set of meta-links in the system. In the next step, the channels and time slots are assigned to each meta-link $L^r_{v_i}$ which is shared by the children in $C^r_{v_i}$. Because the number of meta-links in the reduced tree topology must be less than the number of edges in the original topology, the computational complexity of our centralized channel and time slot assignment algorithm are greatly reduced. The interference relationship among the meta-links in the reduced tree topology is stored in the gateway.

After the tree topology is built, each meta-link $L^r_{v_i}$ will be associated with a traffic load. Because the gateway possesses a global view of the system, it first calculates a relative weight $\mu(L^r_{v_i})$ for each link $L^r_{v_i}$ as follows,

$$\mu(L^r_{v_i}) = \frac{\sum_{v_n \in C^r_{v_i}} S(v_n)}{\sum_{v_j \in V} S(v_j)}, \ \forall L^r_{v_i} \in \mathcal{L} \tag{3.5}$$

The relative weight $\mu(L^r_{v_i})$ represents the ratio between the traffic load in link $L^r_{v_i}$ and the total traffic load in the network.

An example is shown in Fig. 3.4, with 10 routers (1 to 10) in the system. We assume that the outgoing traffic load in each router is 0.1. The traffic load of each link is calculated (the value above the link). In Fig. 3.4(b), we can see that the relative weights are ratios of their own traffic load over total system traffic load. The denominator (the value 2) represents the total traffic load in the system, which is the sum of the weights of all links. The numerator represents the traffic load in each link.

Also, each child router v_i in each of the children set $C^r_{v_n}$ is assigned a relative weight $\mu(v_i)$

$$\mu(v_i) = \frac{S(v_i)}{\sum_{v_j \in C^r_{v_n}} S(v_j)}, \ \forall C^r_{v_n} \in \mathcal{C} \tag{3.6}$$

which represents the traffic load for the router v_i relative to the total traffic load of the children set $C^r_{v_n}$.

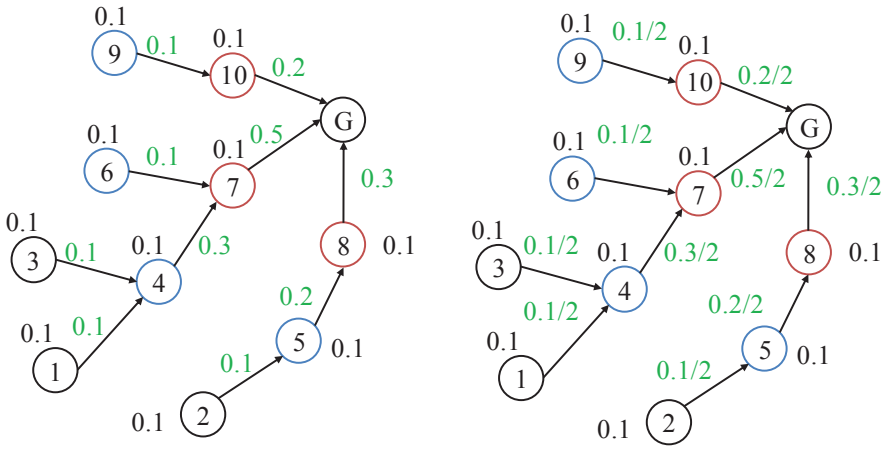

(a) Traffic Load **(b) Relative Weight Calculation**

Figure 3.4: An example of links weights calculation

3.2.2 Weight-aware Meta-Link Scheduling and Channel Assignment Algorithm

In this section, we introduce our weight-aware link scheduling and channel assignment algorithm. Based on the tree topology we obtained in the previous step, the proposed weight-aware link scheduling and channel assignment algorithm distributes the transmission resources (i.e., channels and time slots) to the meta-links in the tree topology. Because the transmission resources (i.e., channels and time slots) are assigned to meta-links based on their weights, a global traffic balance is achieved.

The link scheduling and channel assignment processes consist of two cycles. In the first cycle, the channels are assigned to links based on their relative weights. This assignment will not change if there are no changes in topology. In the second cycle, the algorithm assigns extra time slots to the meta-links that did not receive enough resources based on their relative weight and their transmission history. The second cycle of the algorithm runs periodically. Details of these two cycles are described below.

All the links in the system are stored in a list in a decreasing order according to their relative weights calculated using (3.5). The scheduling length, T, is fixed. It reflects the number of time slots to be allocated in each scheduling interval. More precisely, T is calculated as follows:

$$T = \left\lceil \frac{|\mathcal{L}|}{K} \right\rceil \times D \tag{3.7}$$

The first component in Eq. (3.7) is used to calculate the minimum number of time slots

which can ensure that all the links are active at least once in each scheduling interval and is referred to as the basic scheduling interval where $|\mathcal{L}|$ is the number of meta-links in the tree topology. The second term is used to extend the basic scheduling interval to a reasonable length by which the algorithm can allocate a different number of slots to different links according to their relative weights $\mu(L^r_{v_i})$. If the scheduling interval is too small, links with heavy traffic loads may not get enough transmission resources. On the other hand, if the scheduling interval is too large, the schedule will not be able to meet the real time traffic requirements of the system. So we use D to extend the basic scheduling interval to a reasonable length. The frequency reuse distance [9] can be used as a good candidate value for D. If we draw a circle centered at the gateway and take D as the radius, all the links outside the circle can reuse the frequency resources which are used inside the circle. This circle is called the non-reuse-circle. In the 2-hop interference model, D is set to 3 [9]. In the physical interference model, D is the ratio of the radius of the non-reuse-circle to the maximum transmission range. Usually, the sensing range of a node is about twice as large as its transmission range. Therefore, in the physical interference model, D may also be set to 3. Hence, in a proper channel assignment, links outside the non-reuse-circle are always able to reuse some frequency resources which are used by the inside links. This frequency reuse separation remains valid no matter what the real topology is.

At the beginning of the channel assignment stage, all channels are available to all links in the system. In the first cycle, in each slot of the scheduling interval, the assignment starts from the first meta-link in the list. Based on the link weight $\mu(L^r_{v_i})$, the gateway calculates the expected number of time slots for that link as follows,

$$t(L^r_{v_i}) = \left\lceil \mu(L^r_{v_i}) \times T \right\rceil \tag{3.8}$$

The gateway then assigns an available channel to this link in the time slots. In each time slot, the link can be assigned only one channel. If the link has been assigned a channel in a time slot, it is moved to the end of the list. Also, one link can only use the same channel in the contiguous time slots to avoid the delay resulting from switching the channel [247]. If the number of slots assigned to the link has reached the expected number $t(L^r_{v_i})$ obtained in Eq. (3.8), the link is excluded from first cycle and moved out of the list. Otherwise, the link is moved to the end of the list. Then the algorithm checks the next link in the list, and so on. If the link is not conflicting with the existing assigned links, the link is assigned an already used channel. Otherwise, the algorithm checks if there are any unused channels left. If there is still an available channel, the

link is assigned this new channel. If there are no unused channels left, the algorithm checks the next link in the list. If all the links in the waiting list are already checked, the assignment for this time slot is stopped and the assignment for next time slot starts. This process is summarized by Algorithm 2 in Fig. 3.5. When the link waiting list is empty, the first cycle of channel assignment is terminated.

In the second cycle, the links are stored in a list in an increasing order according to a priority value, $p(L^r_{v_i})$, that reflects the relative change in the priority of each meta-link according its transmission history. The priority value is given by

$$p(L^r_{v_i}) = \frac{1}{\mu(L^r_{v_i})} \times \left(\frac{b(L^r_{v_i})}{\sum_{L^r_{v_j} \in \mathcal{L}} b(L^r_{v_j})} - \mu(L^r_{v_i})\right) \tag{3.9}$$

where $b(L^r_{v_i})$ is the observed average data transmission rate through link $L^r_{v_i}$ and received by gateway v_G. The scheduling processing is similar to the first cycle; each time, before the second round of the algorithm, the priority value $p(L^r_{v_i})$ is calculated.

3.2.3 QoS Aware Traffic Scheduling Algorithm

Our traffic scheduling algorithm operates in a dynamic and distributed manner. As we mentioned before, links adjacent to the same router and sharing the same radio will share a common meta-link. Parent routers need to schedule the traffic for their own children who share common meta-links. The parent router assigns a different access-time length to the child based on the child's relative weight and transmission requirements. The gateway is also considered as a parent. In our design, every router employs a different queue for each CoS. The proposed dynamic transmission time distribution system within each parent is demonstrated by Fig. 3.6.

As shown in the figure, a parent router v_p calculates two relative weights for children routers. One is the long-term relative weight $\mu(v_i)$ which is calculated in Eq. (3.6); the other is the relative weight $\varphi^c_{v_i}$ for each different CoS c ($c \in \{1, 2, 3, \cdots\}$) of router v_i, which is given by

$$\varphi^c_{v_i} = \frac{f^c_{v_i} \times \mu(v_i)}{\sum_{v_j \in C^r_{v_p}} (f^c_{v_j} \times \mu(v_j))} \tag{3.10}$$

where $f^c_{v_i}$ is the the predefined percentage of data in CoS c allowed in router v_i.

Similar to the channel assignment mechanism, traffic scheduling is carried out in two cycles.

Algorithm 2

First Round:

```
1.  For (each slot i in Scheduling Interval T) do
2.    While (not all links are checked) do
3.      choose the first link in the waiting list
4.      If (conflict with existing assigned links) then
5.        If (there is no available channel) then
6.          move the link to the end of waiting list
7.        Else
8.          assign a new channel to the link; decrease
    number of available channels by one
9.           increase number of assigned slots to the
    link by one
10.       End;
11.     Else
12.       assign a used channel to the link
13.       increase number of assigned slots for the
    link by one
14.     End;
15.     If (achieve expected number of assigned slots)
    then
16.       remove the link from the waiting list
17.     Else
18.       move the link to the end of the waiting list
19.     End;
20.   End While;
21. End;
```

Figure 3.5: Weight aware joint meta-Link scheduling and channel assignment algorithm

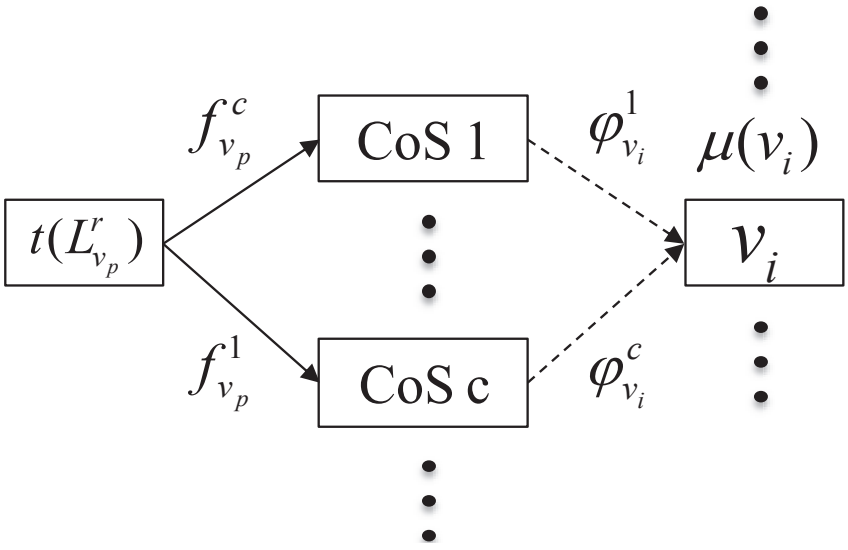

Figure 3.6: Proposed dynamic transmission time distribution system in parent router

In the first cycle, each parent v_p separates the total available transmission time into different parts for each CoS based on its predefined percentage $f^c_{v_p}$. Then, the parent assigns the time length to different child v_i in each CoS c based on their requirements. The maximum time length for each child v_i in the first scheduling round is calculated as follows

$$t^c_{v_i} = t(L^r_{v_p}) \times f^c_{v_p} \times \varphi^c_{v_i} \tag{3.11}$$

After all the children are assigned a *transmission time*, the first cycle is terminated. Then, the parent checks if there is any available transmission time left in the system. If there is, the parent starts the second cycle. Otherwise, the scheduling is terminated. The transmission time assignment process for each CoS is summarized by Algorithm 3 depicted in Fig. 3.7.

The second cycle is used to assign extra transmission time to children who did not receive enough service in the past. The children nodes are stored in an increasing order based on the value $p(v_i)$, which reflects the child transmission history. This value is given by

$$p(v_i) = \frac{1}{\mu(v_i)} \times \left(\frac{b(v_i)}{\sum_{v_j \in C^r_{v_p}} b(v_j)} - \mu(v_i)\right) \tag{3.12}$$

where $b(v_i)$ is the observed average throughput from router v_i to the parent router v_p. The second scheduling round is similar to the first cycle.

Algorithm 3

First Round:

```
1.  For (CoS1 to CoS3) do
2.    While (waiting list is not empty) do
3.      choose the first child in the waiting list
4.      If (required resources > predefined portion)
    then
5.        assign predefined portion of resources to
    the child
6.        subtract this part of resources from the
    total available resources
7.      Else
8.        assign required resources to child
9.        subtract this part of resources from the
    total available resources
10.     End;
11.     remove the child from the waiting list
12.   End;
13. End;
```

Figure 3.7: QoS aware traffic scheduling algorithm

3.2.4 Computational Complexity of The Proposed Work

As described in the pervious sections, the proposed algorithm consists of three steps: *Topology building, Channel assignment, and QoS-aware traffic scheduling*. So we calculate the computation complexity in three parts. 1) Topology building: this is an interactive process. The computational complexity of the topology building process is $O(N^2 - l * N)$, where l is the number of levels and N is the number of nodes. In the tree topology each node has only one link to its parent. So the number of links is equal to N. When $l << N$, the complexity is $O(N^2)$. 2) Channel assignment: this step also works in a centralized manner. Generating the channel assignment plan incurs $O(N)$ computational steps. 3) QoS-aware traffic scheduling: this scheme is distributed; all the scheduling decisions are made by the parent nodes and broadcasted to the children through their associated links. So the computational complexity is $O(|\mathcal{L}|)$ where $|\mathcal{L}| << N$. In general, the total computation complexity of proposed joint algorithm is $O(N^2)$. We note that the first and second steps which have the highest cost, are only triggered when there are major changes in the network. On the other hand, the last step is triggered more frequently in response to smaller variations in the traffic loads of different CoSs. This step, due to its distributed nature as a very small cost $O(|\mathcal{L}|)$.

3.2.5 Support of Multiple Gateways

In this section, we outline how the proposed work can be extended to consider a network with multiple gateways. When there are several gateways in the field, the proposed algorithm also works in the same three steps: topology building, channel assignment, and QoS-aware traffic scheduling which can be modified as follows. 1) Topology building: each node chooses a parent based on the minimum expected delay to the gateway. No matter how many gateways exist in the system, the node only chooses one parent that offers the minimum expected delay to a gateway. If there are multiple gateways providing the same minimum delay, the node chooses the one who has a lower level. If the level is also similar, the node can choose any one randomly. 2) Channel assignment: in this case, the gateways, connecting through the wired network, exchange their channel assignment information in any interfering areas of their tree topologies constructed in the previous step. Based on the received information, each gateway can adjust its own channel assignment to avoid interference. 3) QoS-aware traffic scheduling: this step is not affected by the existence of multiple gateways. If there are multiple gateways connecting to the Internet, a WMN can provide more transmission resources for the end-users and

a larger coverage area.

3.3 Performance Evaluation

In this section, we conduct different simulation experiments to demonstrate the performance of our proposed schemes. We employ three performance metrics, namely, the *gateway throughput*, *delay* and *packet loss ratio*.

3.3.1 Simulation Setup

Based on the protocol interference model introduced in [4, 30, 9], the transmission range Rt and the interference range Ri are set to $90m$ and $180m$, respectively. We simulate a WMN of 50 routers ($N = 50$) that are uniformly distributed in $500m \times 500m$ area with a gateway at its center [9]. Similar to [8], we assume that the transmission rates when two routers are within $30m$, $32m$, $37m$, $45m$, $60m$, $69m$, $77m$, $90m$ are $54Mbps$, $48Mbps$, $36Mbps$, $24Mbps$, $18Mbps$, $12Mbps$, $9Mbps$, $6Mbps$, respectively. The number of available channels is 12, and the number of radios per router is set to 3. For simplicity, we assume that the gateway has sufficient wired back-haul capacity and that the bit error rate of each channel is zero [8].

The data rate of CBR CoS1 data is $64Kbps$ with $120bytes$ packet based on the G.711 codec [248]. We use an ON-OFF source to generate traffic for each of CoS2 and CoS3. The two sources have identical parameters. For each source, the ON and OFF (silent) intervals are drawn according to a *Pareto distribution*, which has been widely used to model self-similar traffic in the Internet [249]. The Pareto distribution is a heavy-tailed distribution characterized by a shape parameter and a location parameter. This distribution has a finite mean and infinite variance when the shape parameter is chosen in the interval $[1, 2]$. We set the shape parameter for the ON and OFF intervals to 1.4 and 1.2, respectively [11]. Based on these values, the aggregate traffic load $ld(v_i)$ in router v_i can follow the long-term mean value with short-term traffic bursts. We assume that CoS3 traffic load is *twice* as that of CoS2 traffic. The relative weight $\mu(v_i)$ based on the traffic long term mean value is calculated for each router v_i and is used to provide spatial fairness between routers in order to guarantee a deterministic access to the Internet service. We set the buffer size of each router to be $5Mbytes$. The buffer is shared by all the CoSs' queues. All the packet loss happens in the router's buffer. Because there are three radio interfaces in the gateway with $54Mbps$ maximum transmission rate

each, the maximum throughput in the gateway equals to $3 \times 54Mbps = 162Mbps$. This value will be used to measure the system load ratio ρ. We assume that all the routers have identical input traffic loads which are given by

$$ld(v_i) = \frac{162Mbps \times \rho}{N} \tag{3.13}$$

and we vary ρ from 0.1 to 1.0. In the simulation, we will test our algorithm in two different scenarios. In the Scenario I, similar to [126, 250], we compare our algorithm with the Shortest Path Routing Algorithm with perfect scheduling (SP). In this comparison, both algorithms follow the *Strict Priority Rule* [7]. Following this rule, the data within high priority class is always served first. In the Scenario II, we will give a specific predetermined transmission resources for CoS2 and CoS3 to test whether our algorithm can easily dynamically adjust its behaviour to face varying QoS requirements for each CoS. In this scenario, we expect that CoS2 and CoS3 achieve the same performance. Finally, we will demonstrate the performance of the the proposed algorithm with different system size (i.e., number of routers in the system). We expect that increasing the size of the system does not degrade the performance of the proposed algorithm.

3.3.2 Performance Analysis

3.3.2.1 Scenario I

According to Fig. 3.8, Fig. 3.9 and Fig. 3.10, we can see that our proposed algorithm achieves much better performance than the shortest path routing algorithm. From Fig. 3.8, we can see that there are no lost packets for CoS1 traffic in both algorithms. For CoS2 and CoS3, the packet loss ratio increases with the increase in the system traffic load. Fig. 3.9 shows that when the system load ratio is higher than 0.5, there is a decrease in CoS3's throughput in both algorithms. The reason for this phenomenon is that we follow the strict priority rules in this comparison. CoS2 data occupies the majority of transmission resources, which results in insufficient transmission resources for CoS3 data. In order to avoid this problem, our algorithm can allocate different transmission resources to different CoSs according to a predetermined percentage. Fig. 3.10 also shows that the proposed algorithm achieves a much smaller packet delay for both CoS2 and CoS3.

3.3.2.2 Scenario II

In the following experiments, we set the predetermined transmission resources percentage of CoS3 to twice as that allocated to CoS2. Recall that we assumed that CoS3 data is

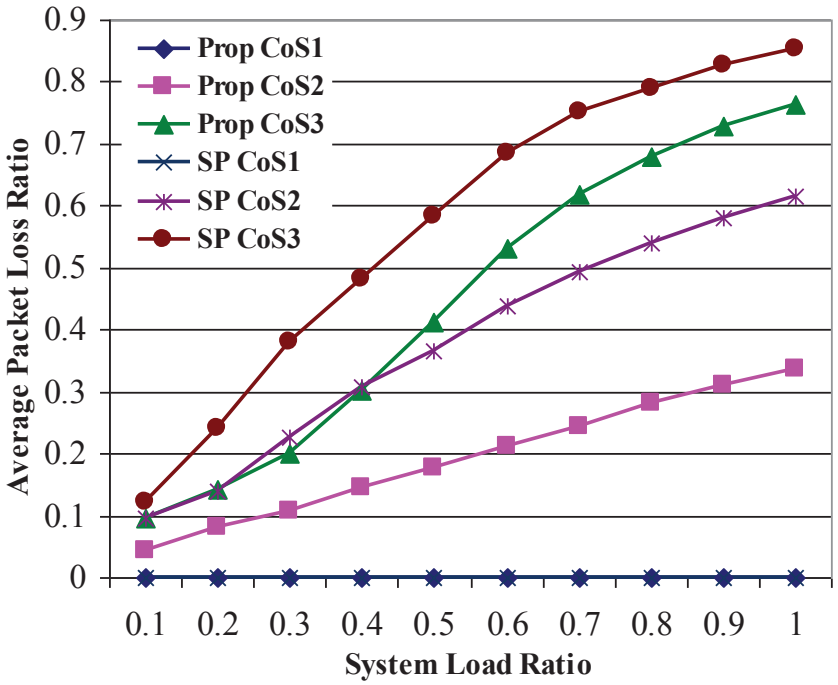

Figure 3.8: The comparison of average packet loss ratio

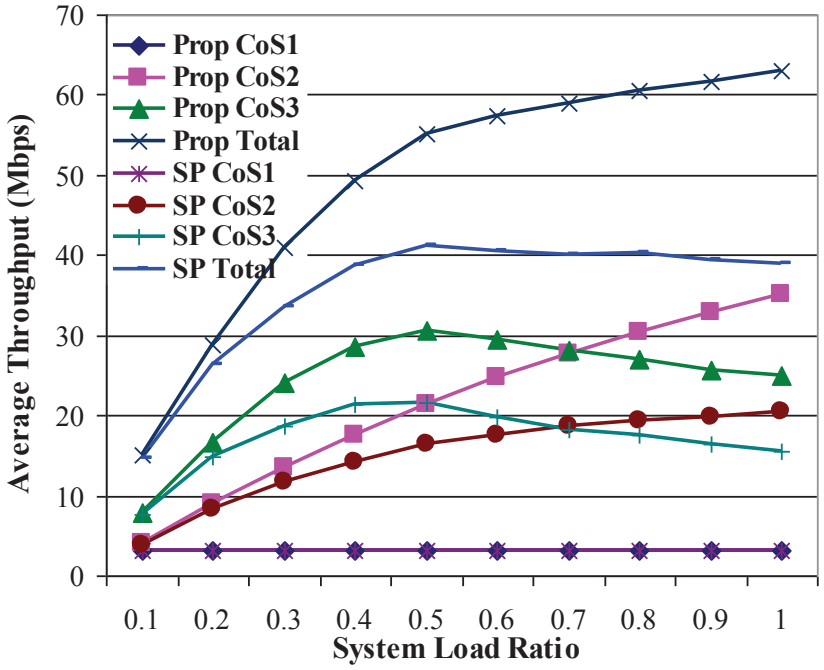

Figure 3.9: The comparison of average throughput in gateway

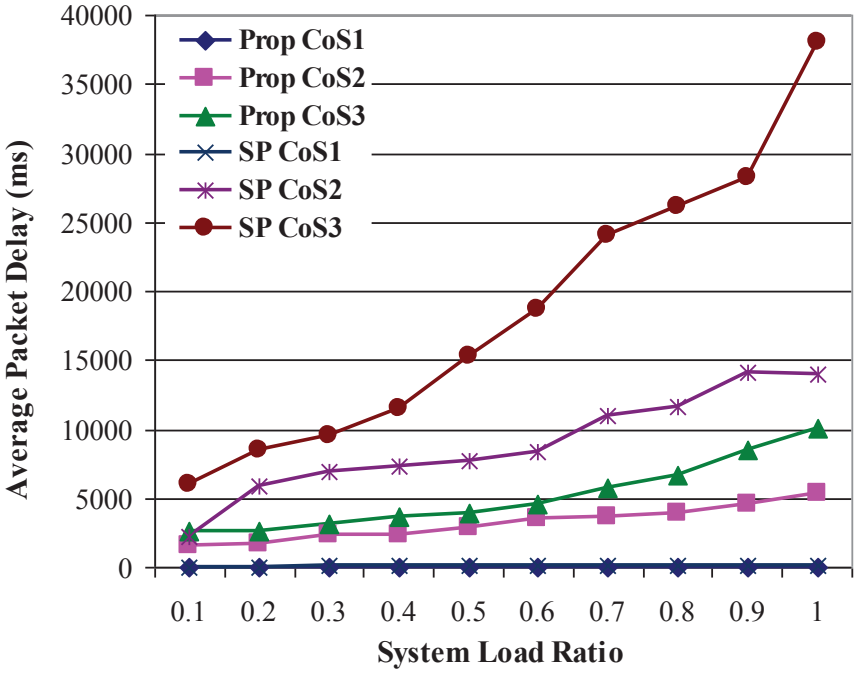

Figure 3.10: The comparison of average packet delay

system load	0.1	0.2	0.3	0.4	0.5
delay(ms)	31.2	35.2	38.5	39.1	32.3
system load	0.6	0.7	0.8	0.9	1.0
delay(ms)	39.5	38.9	37.5	37.8	34.9

Table 3.2: The average delay of CoS1 data

set to twice as that of CoS2. Hence, we can expect that CoS2 and CoS3 will receive a similar packet loss ratio performance.

Fig. 3.12 shows the average packet loss ratio of the proposed algorithm with predetermined proportion of transmission resources. From Fig. 3.12, we can see that CoS1 data achieves a very low packet loss ratio, and it gets almost the same performance under different system loads, which means that the performance of CoS1 will not be degraded by other CoSs transmissions. CoS2 and CoS3 obtain a similar packet loss ratio, which reaches our anticipatory aim.

Table 3.2 indicates the average delay experienced by CoS1 data for different system loads. From Table 3.2, we can see that CoS1 data achieved stable delay results; the average delay of CoS1 slightly fluctuates as the system load increases. Overall, the aver-

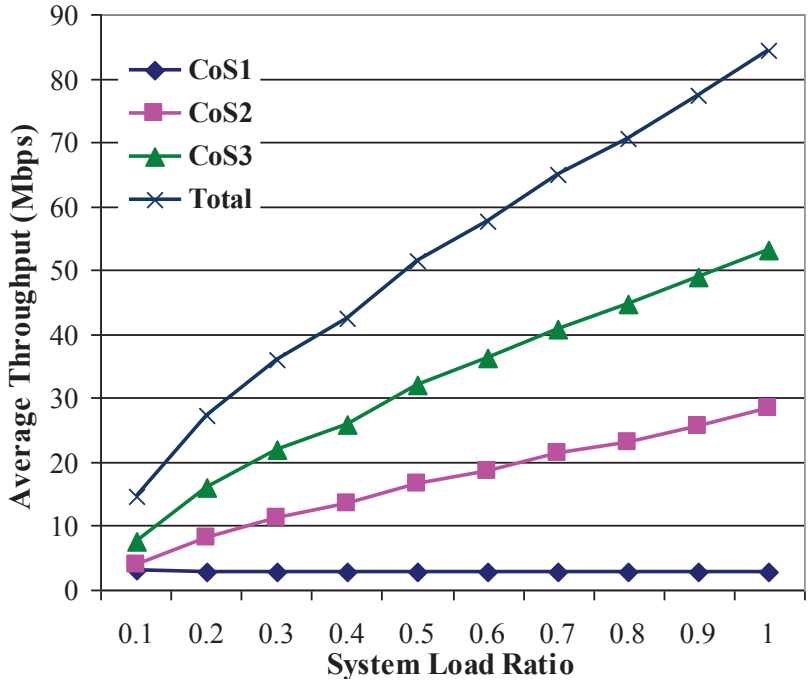

Figure 3.11: Average throughput in gateway

age delay of CoS1 falls in the interval [31ms,40ms]. Fig. 3.11 illustrates our algorithm's performance with respect to the average throughput of each CoS in addition to the total throughput. From Fig. 3.11 and Fig. 3.12, we can see that CoS2 and CoS3 traffic have a similar packet loss ratio and that the throughput of CoS3 traffic is twice as that of CoS2. This behaviour exactly matches our predictions. At this point, we can draw a conclusion that our algorithm can easily dynamically adjust its behaviour to face varying QoS requirements for each CoS.

3.3.2.3 Effects of the system size

Fig. 3.13, Fig. 3.14 and Fig. 3.15 show the performance of the proposed algorithm as the number of routers in the network increases, with 100% system load ($\rho = 1.0$). Based on these three graphs, we can see that our algorithm achieves a relatively stable performance as the network increases in size. The packet loss ratio and the packet delay for each CoS increases slightly as the number of routers increases. The system throughput is maximized when the number of routers is 60. After that, the throughput performance remains fairly constant. From these results we can see that different system conditions will not negatively impact the performance of our proposed algorithm.

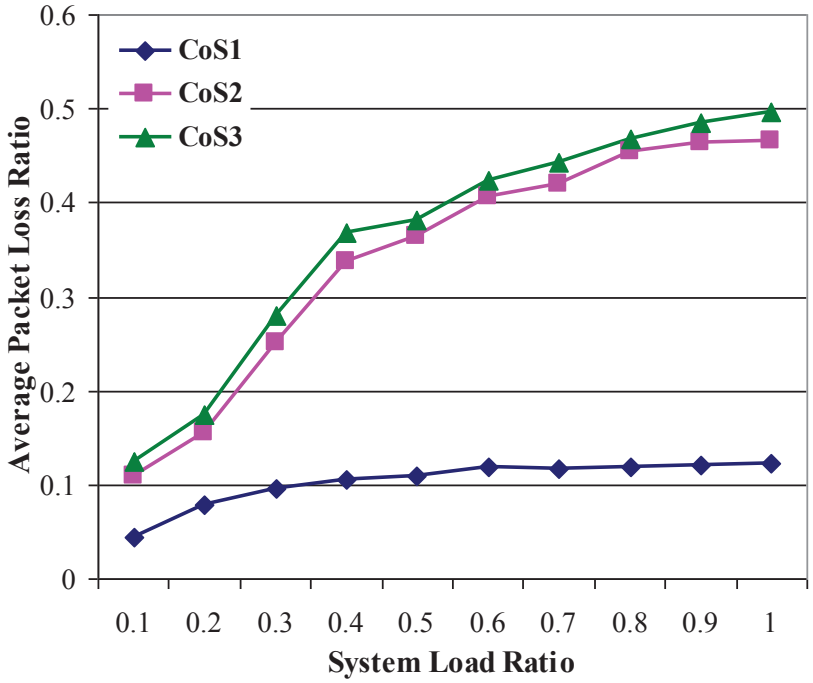

Figure 3.12: Average packet loss ratio

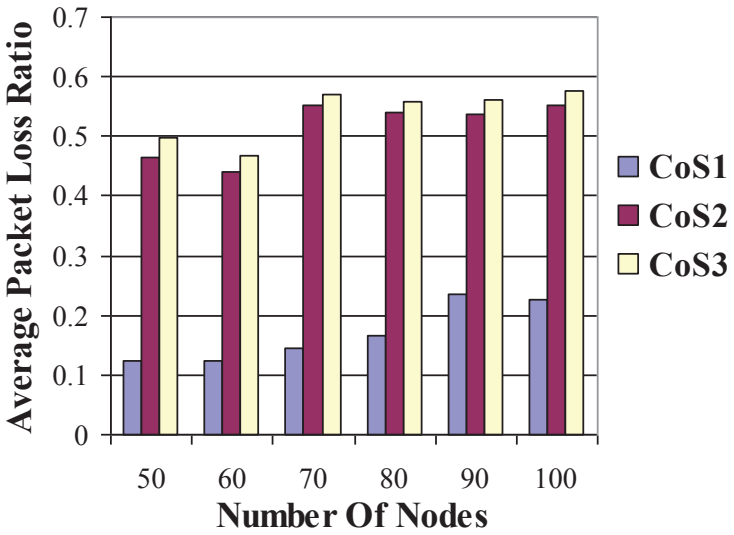

Figure 3.13: Impact of the number of routers on the average packet loss ratio when system load is 100%

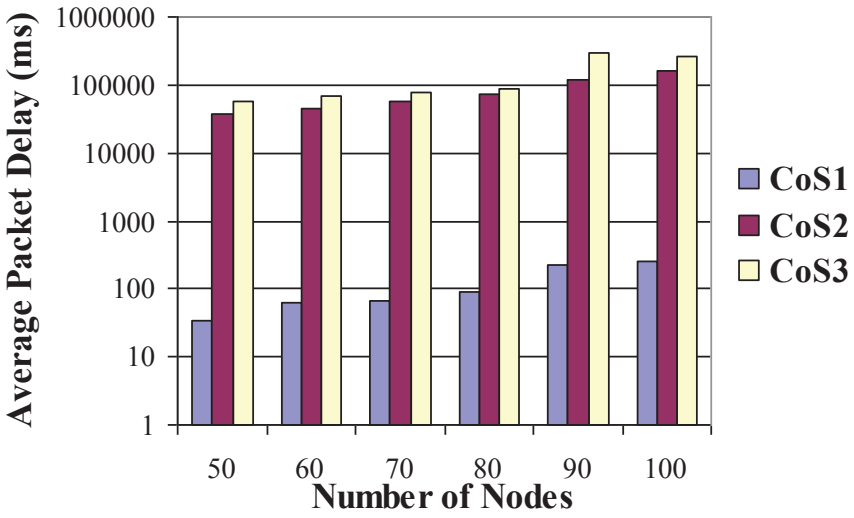

Figure 3.14: Impact of the number of routers on the average packet delay when system load is 100%

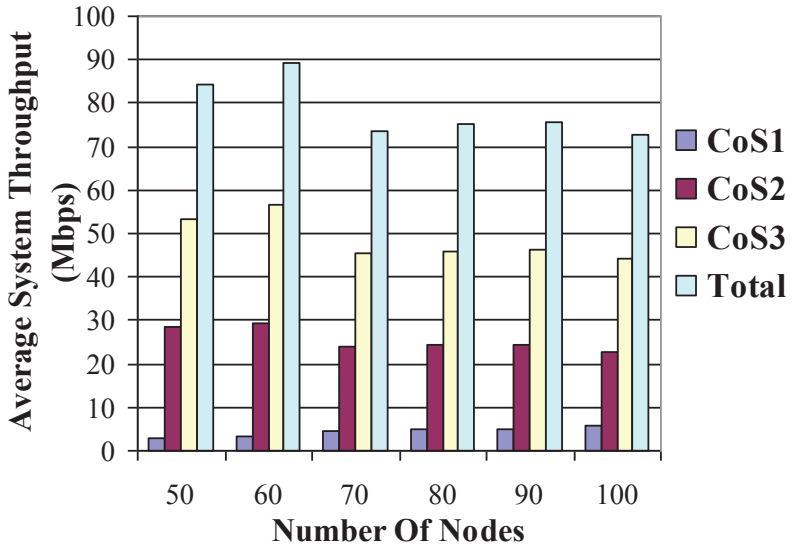

Figure 3.15: Impact of number of routers on the average throughput in gateway when system load is 100%

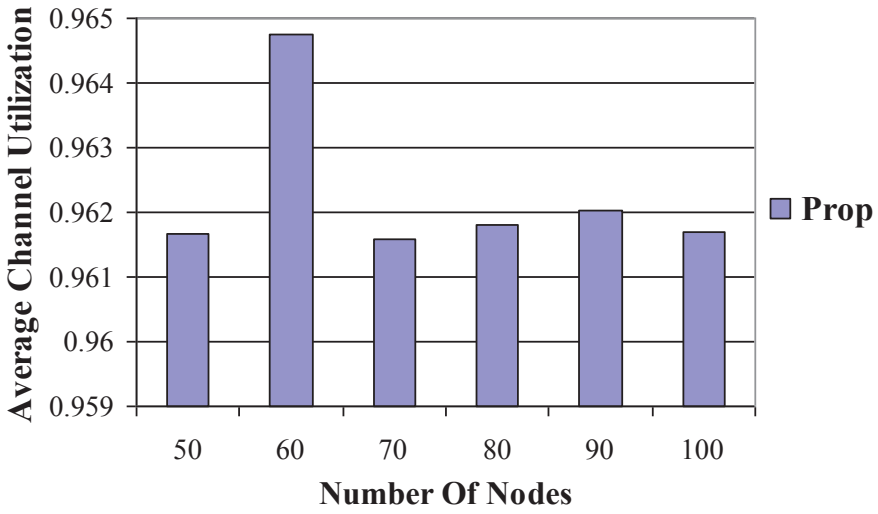

Figure 3.16: Impact of number of routers on the average channel utilization when system load is 100%

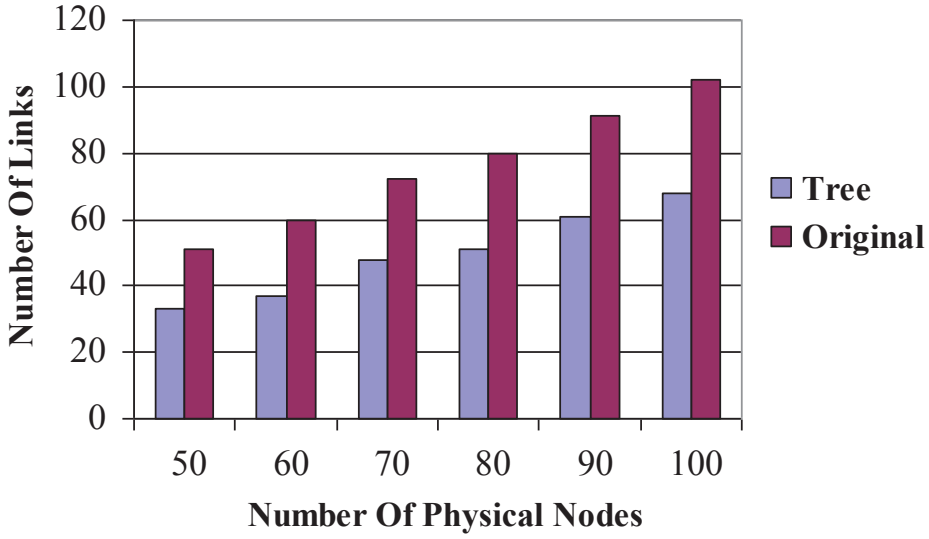

Figure 3.17: The number of links in the system

Fig. 3.16 depicts the average channel utilization of the system. Here, the average channel utilization of the system is defined as the ratio of the achieved system throughput to the total available capacity. A similar definition can be found in [183]. We can see that our proposed algorithm achieves a very high channel utilization.

Fig. 3.17 plots the number of links in the original system and in the generated tree topology as the number of routers increases. We can see that the number of links in our reduced tree topology is much smaller than the original topology. Since the number of links is reduced, the computation complexity of the algorithm is also reduced as mentioned before.

3.4 Summary

In this chapter, we proposed a joint routing, channel assignment and traffic scheduling algorithm for multiple-channel multiple-radio wireless mesh networks to maximize the gateway throughput while supporting the QoS differentiation. Transmission rate adaptation is used in our routing scheme to find a minimum delay path from each router to the gateway. We developed a solution in which the centralized weight aware link scheduling and channel assignment algorithm focuses on maximizing the gateway throughput while minimizing the interference. The distributed traffic scheduling algorithm improves the flexibility and robustness of the system. Simulation results show that our algorithm achieves a stable performance under different system conditions. The results also show that our proposed algorithm decreases the packet loss ratio and packet delay in each class-of-service under different system conditions. In next chapter, we will theoretically analyse the properties of random node failure in WMNs.

Chapter 4

Theoretical Analysis of the Properties of Random Node Failure in Wireless Networks

As discussed in Chapter 2, WMNs have been studied intensively over the past decade with focusing on traffic management functionalities such as channel-to-interface assignment, traffic routing and scheduling. These developed solutions always assumed continuous normal operation of all network components while failing to take into considering the failure-prone nature of wireless networks. In this chapter, we analyze the effects of node failure on the ability of network nodes to maintain their connectivity. More precisely, we present a tight upper bound on the node failure probabilities needed to maintain full network connectivity on the one hand. On the other hand, a lower bound, at which the system loses connectivity, is also derived. We show that these bounds are dependent only on the nodes' geometric distribution and density. We then verify these theoretical results against those obtained via experimentation. Our work is published in [32].

4.1 Theoretical Analysis

Due to the heterogeneity of the traffic loads and the fluctuation of the wireless link conditions, preserving the required performance of such MRMC wireless networks is still a challenging problem. Because of its destructive impact on the performance of wireless networks, the node failure problem has been explored extensively. Many of the existing research efforts aim at improving the robustness and survivability of MRMC wireless

networks by designing efficient routing and channel assignment algorithms. Wellons and Xue in [14] showed a routing formulation for MRMC wireless networks to handle the unexpected traffic demand changing (caused by jamming attack or link failure) by exploiting traffic demands which fell into a predicted region based on the knowledge of the historical traffic demand. Other robust routing algorithms and anti-collision protocols can be found in [16, 17, 18].

In addition to recovery schemes, several studies have been dedicated to the design of failure-resilient networks and to the problem of their asymptotic connectivity. In [3], the authors tested the resilience of networks with different topologies. Buldyrev *et al.* [2] analysed the cascade of failures in interdependent networks. In [251], the authors analysed the relation between the node's critical transmission power and asymptotic connectivity of wireless networks in a disk of unit area.

These studies did not consider an interesting but more fundamental question that is whether a cascade of node failures is related to the nodes' density and their geometric distributions. In this section, we theoretically analyse the connectivity of MRMC wireless networks based on a given node failure probability and nodes' geometric distributions. We present a tight upper bound on the node failure probabilities needed to maintain full network connectivity on the one hand and a lower bound at which the system loses connectivity on the other hand. Using these bounds, one can design more efficient wireless networks that consist of as small number of routers but are guaranteed to achieve their required reliability.

4.1.1 Model and Assumptions

Network Model. Similar to the models adopted in [252, 253], we consider a multi-hop wireless network with n nodes that can be represented by a geometric random graph $G(\mathcal{X}_n, f, \lambda_f)$. Here, $\mathcal{X}_n$=$\{X_1, \cdots, X_n\}$, denotes the set of the random location points of the nodes in the network on a two-dimensional area A. We also assume that the locations $X_1, X_2, \cdots, X_n$ are randomly distributed in A, according to f a random distribution which is used to distribute the nodes in the given area. Throughout this chapter we will derive our analysis for both two dimensional uniform and poisson distributions. Here, $\lambda_f = \frac{n}{A}$ defines the *network node density*, i.e., the average number of nodes within a unit area. Also, let p denote the node failure probability that is identical and independent for all nodes, such that a failed node disappears from the network permanently.

Similar to existing approaches, in our analysis, we fix λ_f as both n and A increase to

infinity, i.e., $n \to \infty$ and $A \to \infty$, and call this model the extended network model [252].

Interference model. Let P_t be the transmission power level used by all the nodes. Also, let the ambient noise power level be N_0 and let the network be configured such that the node density λ_f is set to λ_0. Assuming that the nodes' interference is represented through the physical interference model [254], then the maximum transmission range for any node in the network, d_{max}, is given by:

$$d_{max} = \left[\frac{P_t}{N_0 \delta_{min}}\right]^{\frac{1}{\alpha}} \tag{4.1}$$

A minimum signal-to-interference ratio (SIR) δ_{min} is necessary for successful receptions, and signal power decays with distance as $d^{\frac{1}{\alpha}}$. We will also assume that $\alpha > 2$, which is the common model outside a small neighbourhood of the transmitter [254]. The signal-to-interference-and-noise ratio (SINR) can also be employed.

4.1.2 The Critical Node Density

Clearly, there exists a node density threshold value, λ_0, at which all the nodes are active (i.e., with no node failures) and connected with the maximum transmission range and each node has at least one neighbor, such that there exists at least one communication path, through one or more hops, between any two nodes in the system. If the network node density, λ_f, is decreased below λ_0, then at least two nodes exist that do not share a communication path. We refer to this threshold value, λ_0, as *the critical node density* of the network. In other words, when the node density is equal to the critical node density, the whole system is operating with or covered by the minimum number of nodes. The first goal of this work is to calculate the critical node density for MRMC WMNs.

In such a configuration, as shown in Fig. 4.1, any three adjacent nodes, when communicating using their maximum transmission range, form an equilateral triangle, and in turn, any node, O, can communicate directly with a maximum of six neighbouring nodes. Hence, we can map the entire network on a hexagonal lattice with edge length set to the maximum transmission range of the nodes d_{max} [255].

Let O be a hypothetical middle point in the network, as depicted in Fig. 4.2, and divide its neighbourhood into six sections, one within each of the six directions. Then, the number of nodes that O can communicate using one hop in each direction is one (e.g., node A in the first direction and B in the second). Similarly, the number of nodes that O can communicate with using a maximum of two hops in one direction is

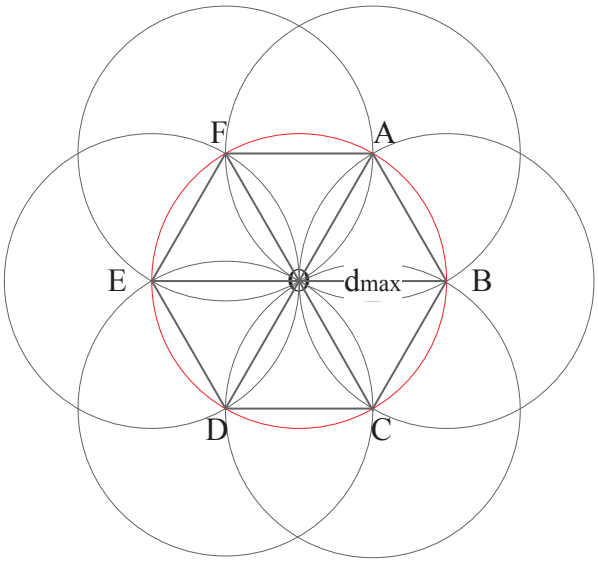

Figure 4.1: An illustration of a node connectivity at the critical node density λ_0

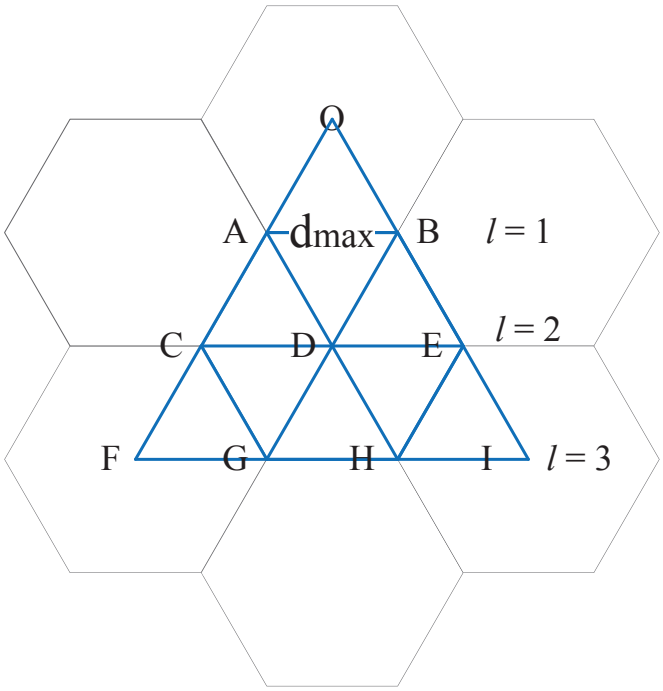

Figure 4.2: Illustration of the calculation of the critical node density

two. To generalize, the number of nodes that O can communicate using the shortest communication path with length at most l in a given direction is $\left[\frac{(l+3)l}{2} - l\right]$. In other words, the number of nodes that are within the area covered by the l-hops distance of O is $6 \times \left[\frac{(l+3)l}{2} - l\right]$ in addition to node O. The size of the area covered by l-hops from O equals to $\frac{3\sqrt{3}}{2} l^2 d_{max}^2$. We can now calculate the system critical node density, as follows:

$$\begin{aligned} \lambda_0 &= \lim_{l \to \infty} \frac{\left[\frac{(l+3)l}{2} - l\right] \times 6 + 1}{\frac{3\sqrt{3}}{2} l^2 d_{max}^2} \\ &= \lim_{l \to \infty} \frac{l^2 + l + \frac{1}{3}}{\frac{\sqrt{3}}{2} l^2 d_{max}^2} \qquad (4.2) \\ &= \frac{2}{\sqrt{3} \times d_{max}^2} \qquad (4.3) \end{aligned}$$

substituting with Eq. (4.1) for the value of d_{max}, we get

$$\lambda_0 = \frac{2}{\sqrt{3} \times \left[\frac{P_t}{N_0 \delta_{min}}\right]^{\frac{2}{\alpha}}} \qquad (4.4)$$

When the network node density λ_f is set to the critical node density λ_0, as shown in Fig. 4.1, we have a single node within each hexagon with edge length d_{max}. On the other hand, if λ_f is chosen to be larger than λ_0, then more than one node may occupy the same hexagon. In this case, there must be one or more paths between some two nodes located in any two hexagons.

4.1.3 Preliminary Results

Now, we can map the entire network on a hexagonal lattice with edge length set to the maximum transmission range of the nodes d_{max} [255]. If a number of random node failures occur, then there is a possibility that the nodes located inside the hexagon and on its boundary all fail. In this case, we say that this hexagon is *empty*. Let q_f be the probability that a given hexagon becomes empty given a node distribution function f over an area A, then we have

$$q_f = \sum_{k=1}^{\infty} P(N_{hex} = k) \times p^k \qquad (4.5)$$

, where $P(N_{hex} = k)$ is the probability that the number of nodes in a hexagon, N_{hex}, is equal to k and p is the given node failure probability. If we assume that the nodes are allocated in the network following a poisson distribution (i.e., $f \equiv poisson$ and $q_f \equiv q_p$) with node density λ_p; and given that the area of the hexagon is $\frac{3\sqrt{3}}{2} \times d_{max}^2$ and that the mean number of nodes in one hexagon is $\lambda_p \times \frac{3\sqrt{3}}{2} \times d_{max}^2$. Then q_p can be calculated as follows,

$$\begin{aligned} q_p &= \sum_{k=1}^{\infty} \frac{\left(\lambda_p \times \frac{3\sqrt{3}}{2} \times d_{max}^2\right)^k}{k!} e^{-\left(\lambda_p \times \frac{3\sqrt{3}}{2} \times d_{max}^2\right)} \times p^k \\ &= e^{-\left(\lambda_p \times \frac{3\sqrt{3}}{2} \times d_{max}^2\right)} \sum_{k=1}^{\infty} \frac{\left(\lambda_p \times \frac{3\sqrt{3}}{2} \times d_{max}^2 \times p\right)^k}{k!} \qquad (4.6) \\ &= e^{-\left(\lambda_p \times \frac{3\sqrt{3}}{2} \times d_{max}^2\right)(1-p)} \qquad (4.7) \end{aligned}$$

On the other hand, if we assume that the number of nodes n approaches infinity and that the node density is λ_u, following a uniform distribution (i.e., $f \equiv uniform$, $q_f \equiv q_u$), q_f can be easily shown to be,

$$q_u = p^{\lambda_u \times \frac{3\sqrt{3}}{2} \times d_{max}^2} \qquad (4.8)$$

4.1.4 Connectivity After Node Failures

In this section, we analyse the effects of the node failure probability and network density on the connectivity of the network.

First, we define a *giant connected component* of the network, or a *giant component* for short, as a set of surviving network nodes after a number of node failures satisfying following conditions: (i) every node in the set has a path to every other node; (ii) the set contains all surviving nodes.

Clearly, if all the nodes in a given hexagon fail, all the paths traversing this hexagon become broken. We call hexagon, empty. Hence, nodes of any two disjoint hexagons that can only communicate with each other by one of these broken paths become disconnected. As shown in Fig. 4.3, this scenario can occur, when, after one or more random node failures, the empty hexagons (shaded in grey in the figure) either form an area of contiguous hexagons or a closed loop that encompasses and isolates one or more

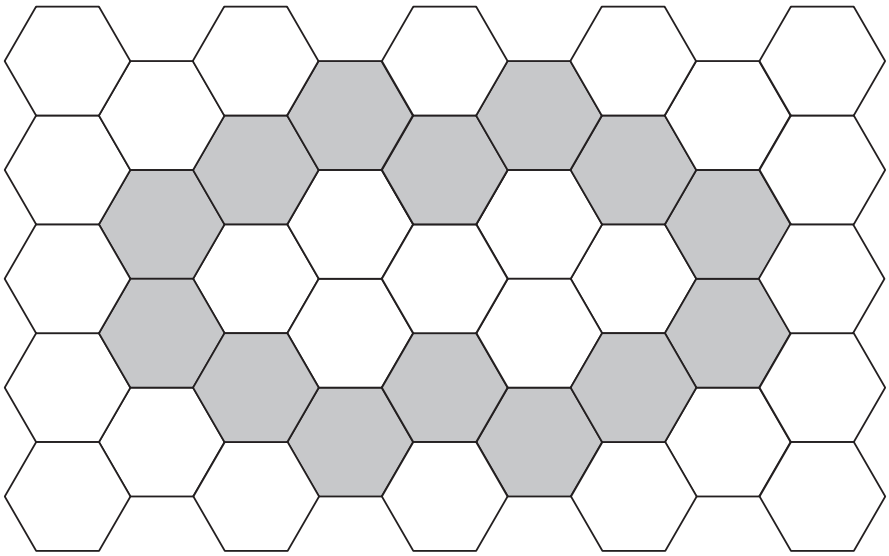

Figure 4.3: Illustration of the closed loop after the random node failure

hexagons with other operating nodes. In this case, and since the hexagon edge length is d_{max}, the surviving nodes located inside the closed loop of the empty hexagons become disconnected from the nodes outside the loop. In turn, the network becomes fragmented into two or more components that cannot communicate. No giant component exists in this case.

The following proposition demonstrates that network connectivity can be guaranteed if the node failure probability of the network routers exceeds a certain threshold, $p_0(f, \lambda_f)$, that depends only on the distribution of the nodes in the network and the node density λ_f.

Proposition 4.1. *Given, a wireless network represented by graph $G(\mathcal{X}_n, f, \lambda_f)$, if $\lambda_f > \lambda_0$, the surviving network always remains connected after one or more nodes fail if the node failure probability, p, is smaller than a threshold value, $p_0(f, \lambda_f)$, that depends only on f and λ_f.*

Proof. As described before, the network remains connected with a giant component despite the occurrence of one or more node failures as long as an additional node failure does not result in a closed loop of *empty* hexagons in the system. Then the probability that the network remains connected is equal to $1 - p_{Len}^{m+2}$, where $m = 1, 2, ..., \infty$ and p_{Len}^{m+2} denotes the probability that there is a closed loop with length $m + 2$ of empty hexagons.

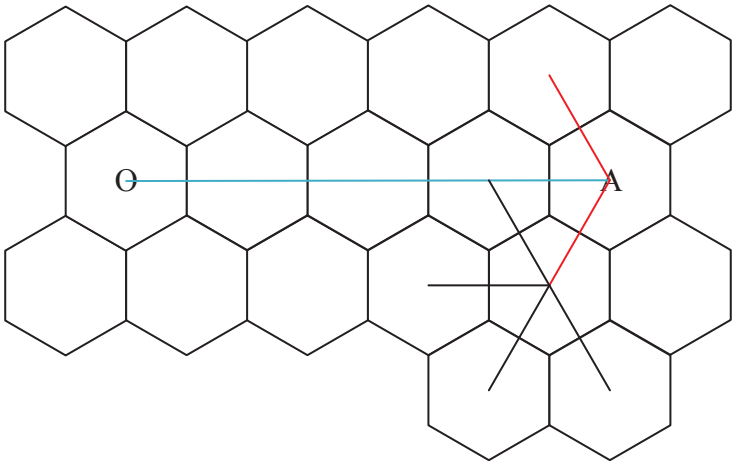

Figure 4.4: Calculation of the number of closed loops

Let the node failure probability in this case be denoted by p. Using the probability of an empty hexagon, q_f, calculated by Eq. (4.7) and (4.8), it can easily be seen that $p_{Len}^{m+2} < q_f^{\frac{m+2}{2}}$. In turn, we have $p_{Len}^{m+2} \leq \sum_{m=1}^{\infty} \mathcal{F}(m+2) q_f^{\frac{m+2}{2}}$, where $\mathcal{F}(m)$ is the number of closed loops whose lengths equal to m. As shown in Fig. 4.4, we assume that point A is the rightmost point of a closed loop whose length is m+2. The point A is at most $\mathcal{P}(m) = \lceil \frac{m+2}{2} \rceil$ away from the start point of the closed loop, which means the point A can locate on at most $\mathcal{P}(m)$ different positions. From Fig. 4.4, we can see that from the point A back to O there are at most two directions. And the two points, which can directly connect to point A, have at most four directions. All the other points have five options. So the number of closed loops with length of m+2 is at most $\mathcal{F}(m+2) = \mathcal{P}(m) \times 4^2 \times 5^{m-1}$. Then, we can calculate the probability of having an $m+2$ long closed loop by the given formula,

$$p_{Len}^{m+2} \leq \sum_{m=1}^{\infty} \mathcal{F}(m) q_f^{\frac{m+2}{2}} \tag{4.9}$$

$$= \sum_{m=1}^{\infty} \mathcal{P}(m) \times 4^2 \times 5^{m-1} q_f^{\frac{m+2}{2}} \tag{4.10}$$

$$= \tfrac{8}{5} q_f \sum_{m=1}^{\infty} \left(m 5^m q_f^{\frac{m}{2}} + 5^m q_f^{\frac{m}{2}} \right) \tag{4.11}$$

$$= \tfrac{8}{5} q_f \sum_{m=1}^{\infty} \left[m (5 q_f^{\frac{1}{2}})^m + (5 q_f^{\frac{1}{2}})^m \right] \tag{4.12}$$

$$= \tfrac{8}{5} q_f \left[5 q_f^{\frac{1}{2}} + \frac{2(5q_f^{\frac{1}{2}})^2 - (5q_f^{\frac{1}{2}})^3}{(1-5q_f^{\frac{1}{2}})^2} + \frac{5q_f^{\frac{1}{2}}}{1-5q_f^{\frac{1}{2}}} \right] < 1 \tag{4.13}$$

$$\Rightarrow \quad 40(q_f^{\frac{1}{2}})^4 - 16(q_f^{\frac{1}{2}})^3 + (5q_f^{\frac{1}{2}})^2 - 10(q_f^{\frac{1}{2}}) + 1 > 0 \tag{4.14}$$

$$\Rightarrow \quad \textit{we have } q_f < 0.1603 \tag{4.15}$$

When Eq. (4.15) is satisfied, p_{Len}^{m+2} is smaller than one and the probability of the network remaining connected is larger than zero. Because q_f, which is only determined by the given density and the node failure probability (i.e., $q_f \equiv F(\lambda_f, p)$), is *monotonically increasing* as p when λ_f is fixed (i.e., from Eq. (4.7) and (4.8)), we can conclude that when p is smaller than a threshold value $p_0(f, \lambda_f)$ (i.e., it can be calculated by Eq. (4.7), (4.8) and (4.15)) there always exists a surviving giant component in the system after random node failures occurred. Now the Proposition 4.1 is proved.

□

Next, we turn our attention to investigating the ability of the network to operate in the presence of a higher probability of node failure. The following proposition derives another failure probability threshold where no giant component can survive after one or more node failures.

Proposition 4.2. *Given, a wireless network represented by graph $G(\mathcal{X}_n, f, \lambda_f)$, if $\lambda_f > \lambda_0$, such that the probability that there is exactly one node left in each hexagon with edge $r = \frac{\sqrt{13}}{13} d_{max}$ is smaller than $\frac{1}{125}$, with high probability (i.e., it holds with probability $1 - O(n^{-c})$ for some $c > 0$ independent of n), there is no giant component left in the system after one or more node failures.*

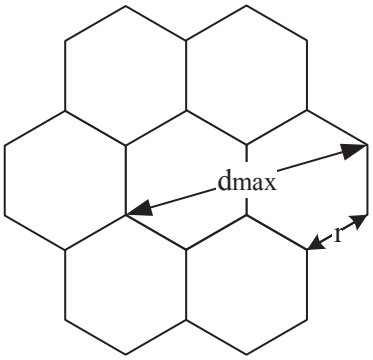

Figure 4.5: Calculate the hexagon edge

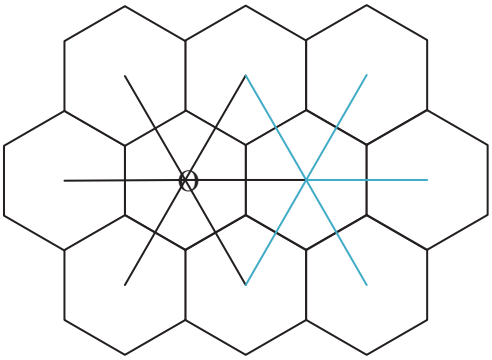

Figure 4.6: Illustration of the possible directions of connected links

Proof. In this case, we are mapping the system on another hexagonal lattice with the edge $r = \frac{\sqrt{13}}{13} d_{max}$, which is shown in Fig. 4.5. Based on this mapping, we assume that each hexagon not empty when there is at least one node located in it or there is a communication link going through it. First, we define p^1_{node} as the probability that there is one node left in a hexagon after node failures.

If there is a giant component surviving in the system, there must be an infinite number of connected hexagons in the system. So the probability of having a giant component p_{GC} is equal to the probability of having $3m$ long connected links p^{3m}_{Len}, where $m \to \infty$. Based on the definition of the hexagon edge, we also know that the longest communication link can go through two empty hexagons at most. So, there are at least $m+1$ hexagons that are surviving in the $3m$ long connected links. We have $p_{GC} = p^{3m}_{Len} \leq n(m) \times (p^1_{node})^{m+1}$, where $n(m)$ is the number of the possible $3m$ long connected links in the system. As shown in Fig. 4.6, because only the start point can have six directions and all the other points only have five options. We have $n(m) = 6 \times 5^{3m-1}$. Finally, we can calculate the

probability that there is a surviving giant component as follows,

$$\begin{aligned} p_{GC} &= p_{Len}^{3m} \leq n(m) \times (p_{node}^1)^{m+1} \\ &= 6 \times 5^{3m-1} \times (p_{node}^1)^{m+1} \\ &= \tfrac{6}{5} \times p_{node}^1 \times [125 \times (p_{node}^1)]^m \end{aligned} \tag{4.16}$$

From the above formula, we can see that if $p_{node}^1 < \frac{1}{125}$, the p_{GC} approaches to 0 when m approaches infinity, which means, with high probability, there is no giant component surviving in the system. Now, the Proposition 4.2 is proved.

□

The following corollary provides further details on the given poisson and uniform distributions.

Corollary 4.1. *There exists a threshold value $p_c(f, \lambda_f)$ that node failure probability p can not exceed. Otherwise, with high probability, there is no giant component left in the system after one or more node failures. For a poisson distribution and node density λ_p, p_c satisfies $(1-p_c)(1+e^{\lambda_p \times \frac{3\sqrt{3}}{2} \times r^2 \times p_c}) = \frac{e^{\lambda_p \times \frac{3\sqrt{3}}{2} \times r^2}}{125 \times \left(\lambda_p \times \frac{3\sqrt{3}}{2} \times r^2\right)}$. Similarly, for a uniform distribution with λ_u, we have $(1-p_c) \times p_c^{\lambda_u \times \frac{3\sqrt{3}}{2} \times r^2 - 1} = \frac{1}{125 \times \lambda_u \times \frac{3\sqrt{3}}{2} \times r^2}$.*

Proof. Following poisson distribution, we have

$$\begin{aligned} p_{node}^1 = & \sum_{k=1}^{\infty} P(N_{hex} = k) \times P(N_{hex}^{'} = 1 \mid N_{hex} = k) \\ = & \sum_{k=1}^{\infty} P(N_{hex} = k) \times k \times (1-p) \times p^{k-1} \\ = & \sum_{k=1}^{\infty} \frac{\left(\lambda \times \frac{3\sqrt{3}}{2} \times r^2\right)^k}{k!} e^{-\left(\lambda \times \frac{3\sqrt{3}}{2} \times r^2\right)} \times k \\ & \times (1-p) \times p^{k-1} \end{aligned} \tag{4.17}$$

If Eq. (4.17) is smaller than $\frac{1}{125}$, we have

$$
\begin{aligned}
p^1_{node} &= \sum_{k=1}^{\infty} \frac{\left(\lambda \times \frac{3\sqrt{3}}{2} \times r^2\right)^k}{k!} e^{-\left(\lambda \times \frac{3\sqrt{3}}{2} \times r^2\right)} \\
&\quad \times k \times (1-p) \times p^{k-1} < \tfrac{1}{125} \\
\Rightarrow \quad & (1-p)\left(\lambda \times \tfrac{3\sqrt{3}}{2} \times r^2\right) \times e^{-\left(\lambda \times \frac{3\sqrt{3}}{2} \times r^2\right)} \\
&\quad \times \sum_{k=1}^{\infty} \frac{\left(\lambda \times \frac{3\sqrt{3}}{2} \times r^2\right)^{k-1}}{(k-1)!} \times p^{k-1} < \tfrac{1}{125} \\
\Rightarrow \quad & (1-p)(1 + e^{\lambda \times \frac{3\sqrt{3}}{2} \times r^2 \times p}) < \frac{e^{\lambda \times \frac{3\sqrt{3}}{2} \times r^2}}{125 \times \left(\lambda \times \frac{3\sqrt{3}}{2} \times r^2\right)}
\end{aligned}
\tag{4.18}
$$

Also, based on the uniform distribution, we have

$$
\begin{aligned}
p^1_{node} &= \lambda \times \tfrac{3\sqrt{3}}{2} \times r^2 \times (1-p) \times p^{\lambda \times \frac{3\sqrt{3}}{2} \times r^2 - 1} < \tfrac{1}{125} \\
&\Rightarrow (1-p) \times p^{\lambda \times \frac{3\sqrt{3}}{2} \times r^2 - 1} < \frac{1}{125 \times \lambda \times \frac{3\sqrt{3}}{2} \times r^2}
\end{aligned}
\tag{4.19}
$$

If the node density λ_f is fixed, the right hands of both Eq. (4.18) and (4.19) are constant values and the left hand sides are *monotonically increasing* in p. So, there must exist a threshold value $p_c(f, \lambda_f)$ that node failure probability p can not exceed. Otherwise, with high probability, there is no giant component left in the system after one or more node failures.

The corollary is proved.

□

4.2 Experimental Verification

In this section, we verify the theoretical results obtained. Fig. 4.7 and Fig. 4.8 plot the values of $1 - q_f$ (q_f is obtained by Eq. (4.7) and (4.8), respectively), as a function of the node failure probability and node density when the node location is drawn from a uniform and a poisson distribution, respectively. Since the results are almost identical, we use only the uniform distribution in our simulation. We simulated the system in a 20×20 square unit area with the node density λ_f increasing from 1.0 to 6.0 in increments of 0.1 in each step. The node failure probability p_f increases from 0.01 to 1 in increments of 0.01 in each step. We repeated the simulation 100 times in each step. Fig. 4.9 depicts the probability of maintaining a giant connected component as the node failure probability increases, which is based on Proposition 4.1. In Fig. 4.10, we compare the theoretical results

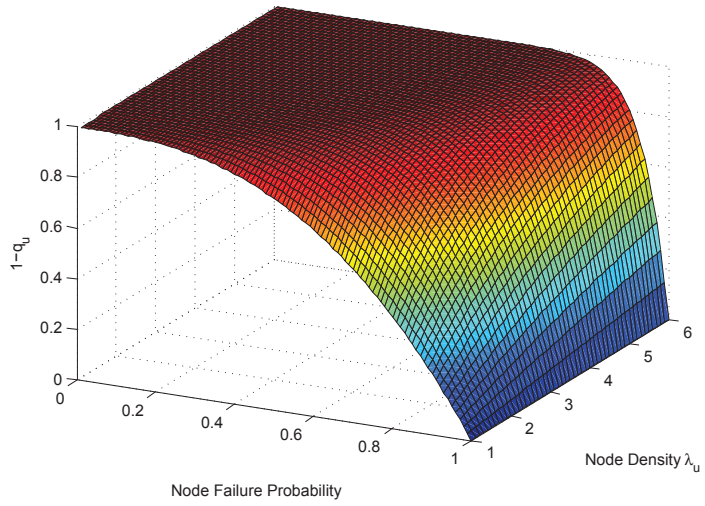

Figure 4.7: The value of $1 - q_u$ following an uniform distribution

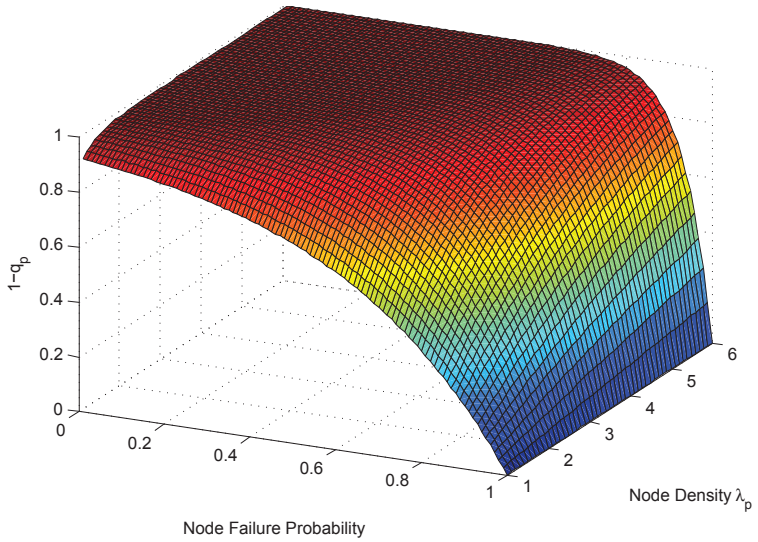

Figure 4.8: The value of $1 - q_p$ following a poisson distribution

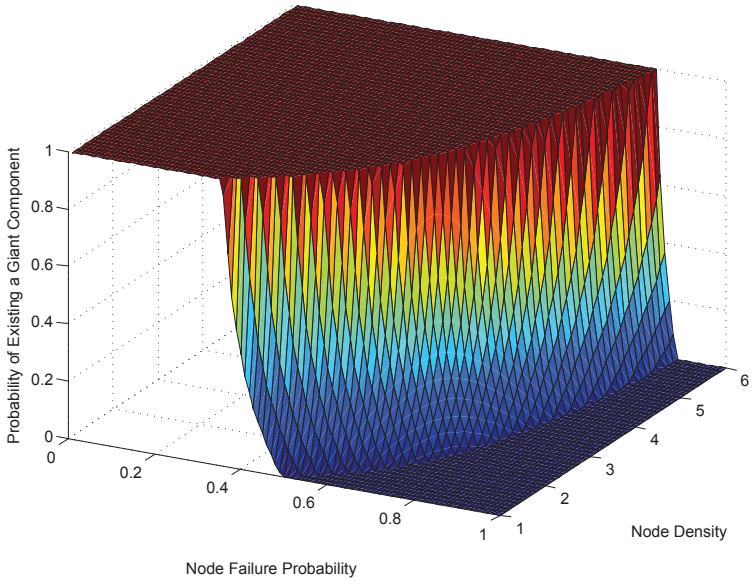

Figure 4.9: The probabilities of existing a survived giant component following uniform distribution

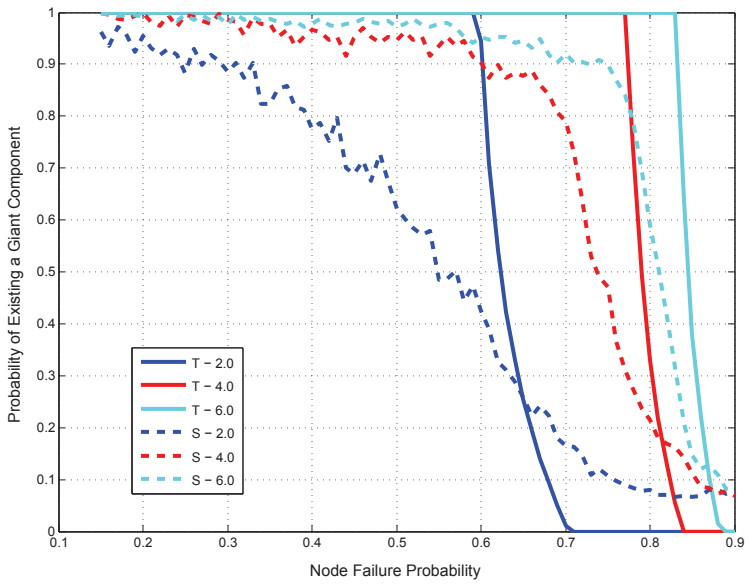

Figure 4.10: Comparison of Theoretical and Simulation results

against those results obtained from the simulation of a wireless system under different conditions (i.e., different node densities, different node failure probabilities). The figure shows a similar trend between the simulated (S-2.0, 4.0 and 6.0) and theoretical results (T-2.0, 4.0 and 6.0). Hence, it confirms that with high probability the network remains connected (indicated by the existence of a giant component) as long as the node failure probability remains smaller than a specific threshold that varies according to the node density. As the node failure probability increases beyond the threshold value, the system quickly loses its connectivity and collapses. However, while for the case of a $\lambda_f = 4.0$ and 6.0, the curves were almost identical with a small error gap. This gap increases as the density is reduced, and this can be attributed to the limited network size in the simulation.

The above phenomenon demonstrates an important role of individual node failure probabilities on network performance. It also plays a key role in understanding the connectivity behaviour of wireless networks and, in turn, in designing efficient failure recovery schemes.

4.3 Summary

In this chapter we studied the topology and resilience of MRMC WMNs in the presence of node failures. We first analysed the critical node density, which is the minimum node density that whole area can be covered by a MRMC WMN. Then we defined two parameters, node failure probability p and empty hexagon probability q_f to characterize the occurrence of random node failures and the changing of system connectivity, based on the given nodes' geometric distribution f. Then we derived the upper bounds on the node failure probabilities that could maintain full network connectivity. We also found a sufficient condition for the system losing connectivity. Also, we formulated the relation between these bounds and the nodes' geometric distributions and density. Finally we validated our theoretical results by simulations.

Chapter 5

The Random Node Failure Recovery Scheme for the Wireless Mesh Network

In Chapter 4, we theoretically analysed the connectivity of a wireless network after node failures. Based on both theoretical and simulation results shown in the previous chapter, we know that the network remains connected as long as the node failure probability is maintained below a certain threshold value. Therefore, in our design for an efficient node failure backup scheme, we aim to fully explore the capacity of the surviving network components in order to find new paths that do not overload the neighbours of the failed node which reduces the probability of generating congestion. First, we will describe the adopted system model chosen for the proposed scheme and state the necessary assumptions that will be used. The proposed work is published in [34].

5.1 Problem Formulation

Based on the theoretical analysis in previous chapter, we have known that the system can keep its functionality when the node failure probability is lower than a threshold value. So, when we design a backup scheme, we should fully explore the capacity of the survived giant component in the system. In this section, we will describe the system model and state the necessary assumptions that will be used in our design.

5.1.1 System Model

We consider a MRMC WMN consisting of multiple static wireless routers that form the wireless backbone network to relay the traffic from the source to the destination (e.g., from end-users to one or more gateways). Let V be the set of routers in the system, where each router $v_i \in V$ has a set of wireless radio interfaces presented by I_i. Each radio $r \in I_i$ can operate on a single channel selected from K orthogonal channels with identical maximum capacity [9, 10, 11, 174]. Clearly, the number of radios employed in each router, v_i, cannot exceed K, which means that the size of set I_i is typically smaller than K. Also, we assume that a router has at least two radios (one for uplink and another for downlink communication). Each router v_i in the system aggregates the data from all end-users associated with it. The local traffic load at v_i will be denoted as ld_i. Because we are focusing on maximising the throughput in the system, we are naturally concerned with the outgoing traffic from the routers to the destinations. So the load ld_i represents only the local outgoing traffic load. Also, we assume that ld_i follows a random distribution with a fixed long-term mean value [9, 30].

Two wireless routers can communicate with each other if they are within the communication range of each other with a common channel assigned to their radios. We assume that each node has identical interference range; the routers that use the same channel and are located in each other's interference range may interfere with each other. Router pairs using a different channel within each other's interference range can communicate simultaneously. Let d_{max} represent the maximum transmission range of all routers and $d(v_i, v_j)$ represents the physical distance between routers v_i and v_j. An edge $e(v_i, v_j) \in E$ exists if and only if $d(v_i, v_j) \leq d_{max}$, which means that router v_i can communicate with router v_j directly. The transmission rate, $r_{trans}(v_i, v_j)$, from router v_i to v_j is chosen by the parent router v_j based on the SINR of the received data from router v_i, which is introduced in IEEE 802.11 standards [246]. For simplicity, we assume that the transmission rate $r_{trans}(v_i, v_j)$ is based only on the distance $d(v_i, v_j)$ [8].

It is important to note that *our developed schemes are independent of the used interference model*. Hence, both the physical interference model [11] and the protocol interference model [30] can be employed in our algorithm.

Definitions of the variables used in the proposed work are summarized in Table 5.1.

Notation	Description
N	the number of routers in the system
K	the number of available channels in the system
ld_i	the local outgoing traffic load in router v_i
$e(v_i, v_j)$	the physic link between router v_i and v_j
C_i^r	the measured link capacity of radio r of router v_i
C_{req}	the request capacity of the backup flow
$C_i^{r'}$	the recalculated link capacity after local traffic distribution
$r_{trans}(v_i, v_j)$	the transmission rate from router v_i to v_j
$d(v_i, v_j)$	the distance between routers v_i and v_j
I_i	the set of radios in router v_i
L_i^r	the traffic load on radio r of router v_i
α_i^r	the measured channel occupancy ratio
l	the level parameter
τ_i^r	the transmission rate of radio r of router v_i
d_{max}	the maximum transmission range

Table 5.1: The definitions of variables used in this chapter

5.1.2 Proposed Re-routing Scheme

There are three types of re-routing approaches in MRMC WMNs: local re-routing, local-to-end re-routing, and end-to-end re-routing. Each of these strategies is illustrated in Fig. 5.1.(1), (2) and (3), respectively.

The local re-routing strategy, shown in Fig. 5.1.(1). A "maximum flow" model is used to find the (semi-)optimal placement of spare resources under a deterministic failure hypothesis, typically a single-node (link) failure model. A drawback of the local re-routing approach is that resource usage becomes inefficient after the failure recovery, because channel paths tend to be lengthened by local detouring. Generally, end-to-end re-routing is the best with respect to resource efficiency, local-to-end re-routing is the second, and local re-routing is the worst. The end-to-end re-routing strategy (Fig. 5.1.(3)), also called path restoration, has been studied intensively. Essentially, this strategy requires the intervention of the endpoints of each failed connection. There are two variations in this strategy, depending on whether the failure recovery paths are pre-computed before the failure occurrence, or determined after failures actually occur. There are several differences between these two methods. In the former, the pre-routed recovery paths should be separated with the corresponding original connection paths, while in the latter, the recovery paths can use the healthy components of their

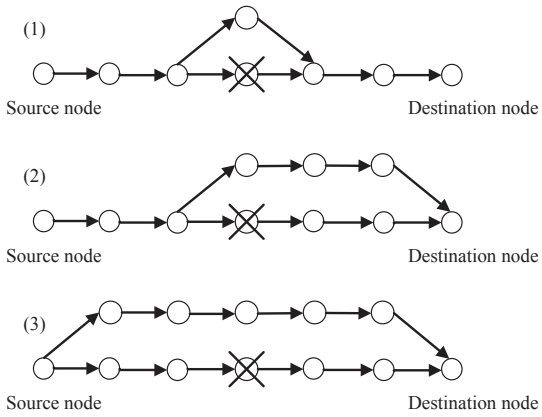

Figure 5.1: Illustration of the re-routing strategies

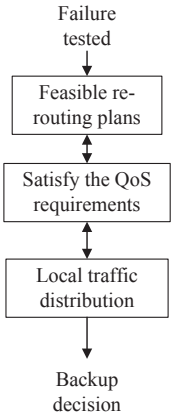

Figure 5.2: The backup process

original connection paths. However, because of fluctuating wireless link conditions, the former one cannot be adopted in MRMC WMNs. On the contrary, in the latter one, when failures occur each disabled connection will try to establish a new connection by "claiming" the shared spare resources, leading to the problem of resource contention. This recovery requires a large amount of message exchanges and generates a large delay. The local-to-end re-routing scheme (Fig. 5.1.(2)) can be considered as a tradeoff between the end-to-end re-routing and local re-routing. It has greater flexibility in routing the recovery paths, leading to higher potential resource efficiency than the local re-routing. Also, it has much less delay than the end-to-end re-routing. Because the local-to-end re-routing scheme generates an optimal recovery plan from the node which is located before the failed node to the destination. Therefore, even though resource contention may happen, the recovery paths still can be accepted successively by redistributing the traffic load in the system. So, in our backup scheme, we adopt the local-to-end re-routing scheme to find the detour path for recovering data flow affected by the node (link) failure. Also, in order to improve the acceptance rate of the recovered flows, we adopt the local re-routing to achieve local traffic load redistribution.

5.1.3 Overview of the Proposed Scheme

Our designed scheme is a distributed system that can be easily adopted by IEEE 802.11-based MRMC WMN. Every working node in the system monitors conditions of all its connected links to judge if neighbours are in poor working status. If it detects a neighbour

failure, the proposed scheme will be triggered. As shown in Fig. 5.2, the scheme works in three stages. In the first stage, the backup paths for the data streams which go through the failed node will be built based on a given re-routing scheme. Second, the scheme will test whether the generated re-routing plan can satisfy the QoS requirement of the backup stream. If the QoS requirements can be satisfied, the re-routing plan is accepted. Otherwise, the scheme needs to find a new re-routing plan and this process will stop when it reaches the maximum path length that calculated by the number of hops. Third, based on the accepted re-routing plan, local traffic distribution will be trigger. The original traffic flows will be re-distributed in the local area. If all three stages passed, the backup stream is accepted. Otherwise, the backup stream is dropped. We assume that while the backup scheme is running, all the messages are reliably transmitted by the given routing protocol.

5.1.4 Details of Proposed Backup Scheme

Fig. 5.3 describes the operation of the proposed backup scheme. The core function of the proposed scheme is local traffic load redistribution. Local traffic load redistribution is defined as a set of nodes' traffic changes (e.g., additional backup streams) which are necessary not only for a network to recover from a node(s) failure, but also for the potential backup paths in which there are usually multiple nodes which have high traffic loads. Existing re-routing algorithms [14, 182, 30] seek "optimal" solutions by considering tight QoS constraints on all links without considering the traffic load redistribution. Thus, traffic congestion may be generated in some nodes and the backup stream will be not accepted. In addition, the additional backup streams may affect the existing traffic stream in the node. By contrast, our proposed backup scheme redistributes the traffic load in a small area (i.e., three hops in our simulation) to reduce the probability of generating congestion. Also, local traffic load redistribution satisfies the QoS requirement of each data stream. As depicted in Fig. 5.2, the proposed scheme first utilizes the given routing and channel assignment algorithm to generate a set of feasible re-routing plans which enumerates feasible channel, link, and path changes to avoid the faulty node by considering the interference constraints, channel constraints and radio constraints. Then, in order to satisfy the QoS demands and improve the network throughput, the proposed scheme applies strict constraints (i.e., QoS requirement) within the set to redistribute traffic loads in a certain area.

Re-routing Plan Generation. Generating feasible plans is essential to search all

Algorithm 1: The proposed backup scheme

The backup scheme operating in the node i:

State 1: monitoring

1. **for** every neighbour j **do**
2. monitoring the neighbour state
3. **end for**

State 2: failure detection

4. **if** neighbour j is failed **then**
5. start the re-routing process to build the backup paths for the data streams go through neighbour j
6. **end if**

State 3: recovery processing

7. **if** node i is the source of the re-routing **then**
8. send a backup request with the level parameter l to its neighbour which is chosen by the given routing algorithm
9. **else if** node i is a regular working node and received backup request **then**
10. check the available transmission capacity C_i^r of the selected link
11. **if** $C_i^r >$requested backup stream C_{req} **then**
12. accept the backup stream and send the backup request to the next node on the path, if any
13. **else**
14. calculate new available capacity $C_i^{r'} = C_i^r + (R_i)^{-l} \times L_i^r$, L_i^r is current traffic load
15. **if** $C_i^{r'} < C_{req}$ **then**
16. refuse the backup request
17. **else if** $C_i^{r'} > C_{req}$ **and** satisfy the QoS requirement of the data stream
18. send backup request to its neighbour and $l = l + 1$
19. **if** received the accept message **then**
20. move portion of its current load to the neighbour and accept the backup request
21. **else**
22. refuse the backup request
23. **end if**
24. **end if**
25. **end if**
26. **end if**

Figure 5.3: The proposed backup scheme

legitimate changes in links configurations and their combinations to avoid the faulty area based on the given routing and channel assignment algorithm. Given multiple radios, channels, and nodes, the routing and channel assignment algorithm identifies feasible changes that help in avoiding a local node failure and maintaining the existing network connectivity as much as possible. However, in order to generate such plans, we have to address the following challenges:

Avoiding the faulty node. First, the re-routing scheme has to make sure that the faulty node needs to be avoided via reconfiguration. Specifically, to avoid the faulty node(s), the re-routing scheme will use a route-switch in which all data flows going through the faulty node can use detour paths instead of the faulty path. To this end, our proposed scheme considers three primitive link changes: 1) both end-radios of the detour link do not switch the given channel; 2) the channel associated with the source radio of the detour path switches to a new channel; 3) both end-radios of the detour link have to switch to a new channel simultaneously.

Maintaining network connectivity and throughput. While avoiding the use of the faulty node, re-routing needs to maintain the connectivity through the full utilization of radio resources. Because each radio can associate itself with multiple neighbouring nodes, a change in one link triggers other neighbouring links to change their settings. To arrange such propagation, the proposed backup scheme takes a two-step approach. First, the backup scheme generates feasible changes of each link using the primitive link changes mentioned above, and then combines a set of feasible changes that enable a network to maintain its own connectivity. Furthermore, for the channel assignment, the proposed scheme maximizes the utilization of network resources by making each radio of a node associate itself with a distinct channel to avoid the use of the same channel among radios in one node.

Controlling the scope of reconfiguration changes. the re-routing has to maintain network changes to be as locally as possible, but at the same time it needs to find a locally optimal solution by considering more network changes or the larger scope. To make this tradeoff, we assume that the routing scheme uses a local-to-end reconfiguration approach. The routing algorithm finds a backup path for each data flow from the node which is located before the faulty node(s) on the original path. The given channel assignment algorithm considers link changes within the first hops and generates feasible plans. If the channel assignment algorithm cannot find a local solution, it increases the number of hops so that the channel assignment algorithm may explore a broad range of link changes. Thus, the total number of reconfiguration changes is determined on the basis

of existing configurations around the backup path as well as the number of hops.

Satisfy the QoS requirement. Based on the detour paths obtained by the re-routing in the previous step, the backup scheme now needs to identify QoS-satisfying backup plans by checking if the QoS constraints are satisfied on the detour paths. Although each backup path ensures that the faulty node will be avoided and the system connectivity will be maintained, some plans might not satisfy the QoS constraints or even cause cascaded QoS failures on neighbouring nodes. In order to adopt as many backup paths as possible, the backup scheme has to solve the following challenges.

Link capacity estimation. For each backup path, the backup scheme has to check whether each link's configuration change satisfies its capacity (or bandwidth) requirement. Therefore, it is necessary to estimate link capacity. In MRMC WMNs, the achievable capacity (or throughput) of each link is mainly affected by two factors: the transmission capacity and the channel occupancy ratio (COR) [256] affected by activities of other links which share the same channel.

So, in order to estimate the link capacity, the backup scheme needs to accurately measure each link's transmission capacity and its available channel airtime. Even though numerous link capacity estimation techniques have been proposed, they focus on the average bandwidth of each node in a network or the end-to-end throughput of flows, which cannot be used to calculate the impact of individual link configuration changes. In contrast, the proposed scheme estimates the individual link's capacity based on the measured link-quality information: Signal-to-interference-plus-noise-ratio (SINR) and the COR of the channel measured by passively monitoring the transmissions of data flows, which is introduced in IEEE 802.11 standards [246]. Here, our scheme is assumed to keep link-quality information for other channels and uses the kept information to generate backup plans. If the achievable link bandwidth is not enough to adopt the backup data flow, the backup scheme triggers the local traffic load distribution to find a QoS-satisfiable plan.

Given measured link capacity and bandwidth requirements, the backup scheme has to check if the new backup path satisfies QoS requirements. Our scheme defines and uses the expected COR of each link to check the link's QoS satisfiability. After the re-routing plan generated, the node sends a local-to-end backup request message to one of its neighbours which is chosen by the re-routing scheme with a level parameter l, where l is the number of hops from the origin node to the neighbour. We assume that the required bandwidth of the backup flow is C_{req}. The link's COR is given by

$$\alpha_i^r = L_i^r / \tau_i^r \tag{5.1}$$

where τ_i^r is the transmission capacity on radio r of router v_i. α_i^r must not exceed 1.0 for a link to satisfy its bandwidth requirement. If multiple links share the capacity of one channel, the backup scheme calculates the aggregated COR of the channel, which is defined as

$$\beta_i^r = \sum_j (L_j^{r'} / \tau_j^{r'}), j = 1, 2, \cdots \tag{5.2}$$

where j represents the nodes interfered by node v_i and β_i^r is the aggregated COR of the set of the identical channel within and across the router v_i's interference range. Based on the calculated COR, the achievable link capacity can be calculated by

$$C_i^r = (1 - \beta_i^r) \times \tau_i^r \tag{5.3}$$

If the achievable capacity of the neighbour node C_i^r is enough for the requested backup stream, it accepts the backup stream. Otherwise, the local traffic redistribution will be triggered.

Local Traffic Load Distribution. As aforementioned in the previous section, if the required backup bandwidth $C_{req} < C_i^r$, the backup stream is accepted. the neighbour will check whether the capacity can satisfy the backup requirement after removing some traffic loads to its own neighbours. Then, a new capacity $C_i^{r'}$ will be calculated by

$$C_i^{r'} = C_i^r + (R_i)^{-l} \times L_i^r \tag{5.4}$$

where the L_i^r is the current traffic load of the link and R_i is the number of radios of the node. If $C_i^{r'}$ is larger than C_{req} and satisfies the QoS requirement of the backup stream, the neighbour will send a local backup message to its neighbour with new level parameter $l = l + 1$. If an accept message is received, the backup stream is accepted. Otherwise, the backup stream is dropped. In order to avoid network-wide ripple effects, we limited the number of levels to be 3. This process is illustrated in Fig. 5.4. After all the backup paths for the affected data flows have been built or refused, the backup process stops.

Fig. 5.5 depicts an example of local-to-end re-routing and local traffic redistribution. There are two original data flows existing in the given system. The first flow is from the source $S1$ to the destination $D1$; the second flow is from the source $S2$ to the destination $D2$. As shown in the figure, the Node2 loses its function. This node failure triggers the local-to-end re-routing scheme. A detour path from Node1 to the destination $D1$ will be found, which will go through Node5, 6, 7 and reach $D1$. Since the second flow also uses Node5, 6, 7 to transmit data, we assume that congestion will be generated in Node5,

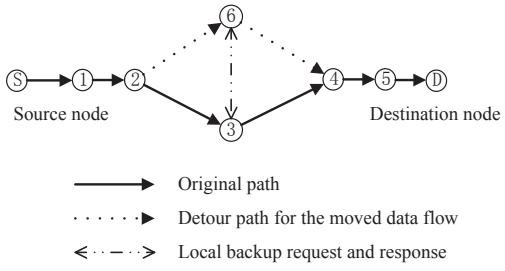

Figure 5.4: Illustration of the local traffic distribution

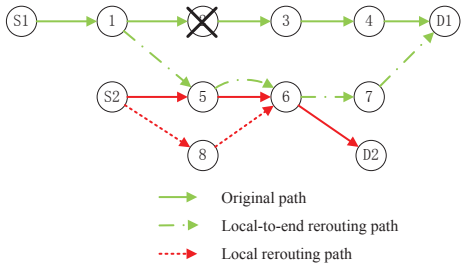

Figure 5.5: Illustration of the recovery process

which will then trigger the local traffic redistribution. Node5 will communicate with its own neighbour, Node8, to check whether Node8 can accept some of its traffic loads. If Node8 sends a positive feedback to Node5, which means Node8 can accept Node5's traffic load, Node5 will move some of its own traffic loads to Node8. Then, the second flow will use a new local detour path to go around Node5. When this recovery process is completed, both data flows are kept in the system.

5.2 Performance Evaluation

In this section, we conduct different simulation experiments to demonstrate the performance of our proposed scheme. We employ two performance metrics: the system throughput and the average backup path length.

5.2.1 Simulation Setup

Based on the protocol interference model introduced in [30], the transmission range and the interference range are set to 90 m and 180 m, respectively. Similar to [8], we assume that the transmission rates when two routers are within 30 m, 32 m, 37 m, 45 m, 60m,

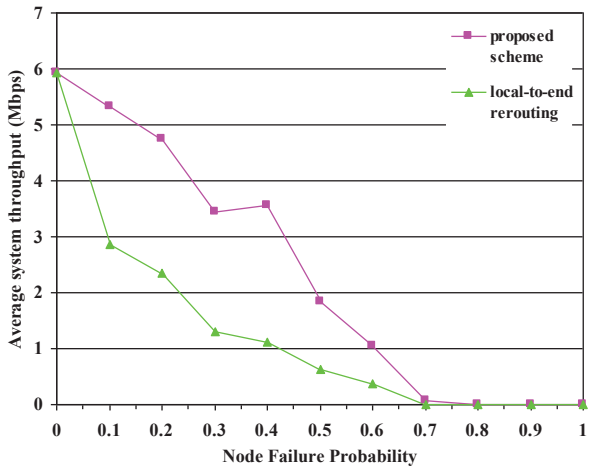

Figure 5.6: The system throughput of 50 nodes network

69 m, 77 m, 90 m are 54 Mbps, 48 Mbps, 36 Mbps, 24 Mbps, 18 Mbps, 12 Mbps, 9 Mbps, 6 Mbps, respectively. The number of available channels is 12, and the number of radios per router is randomly distributed in [2, 4] following the uniform distribution. Each router will randomly choose a destination. The inject data stream in each router is uniformly assigned in [100 Kbps, 200 Kbps] [30]. We simulated the scheme in two cases: 1) There are 50 routers in the system. The average distance between two routers is chosen to be 40 m. In this case, we have larger router density and interference is the main factor that affects the system performance. The node density in this case is around 5.0, so we can predict that the system will collapse when the node failure is higher than 0.7. 2) There are 200 routers uniformly distributed in a 1000 m$\times$1000 m area. In this case, the average distance between two routers is increased to 70 m. The node density is approximately 1.0. We can anticipate that the system will collapse when the node failure probability reaches the interval [0.2, 0.3]. The transmission capacity constraint will be the main factor that affects the system performance. We adopted the Dijsktra's routing algorithm [7] and the greedy channel assignment to generate the routing and channel assignment results in our simulation. Also, we assume that the data flow will be dropped if its backup path cannot be built.

5.2.2 Performance Analysis

Fig. 5.6 shows the system throughput of the system with 50 nodes in three different conditions. As we can see from this line graph, the throughput of the system decreases

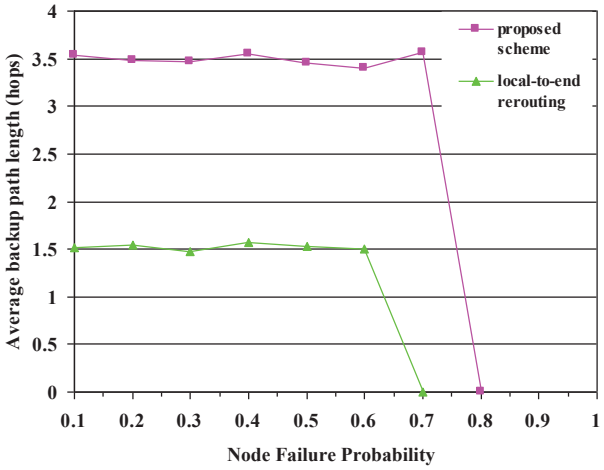

Figure 5.7: The average path length of 50 nodes network

dramatically following the increasing percentage of lost nodes. In contrast, the throughput descent of our backup stream is almost linear. The throughput of the original re-routing without the local traffic redistribution decreases approximately following a power law. Based on the simulation results, we can see that our scheme achieves twice the throughput of the original local-to-end backup scheme. Also, based on the results shown in both Fig. 4.9 and Fig. 4.10, we can see that the system collapsed when the node failure was higher than 0.7, which matches our hypothesis.

Fig. 5.7 describes the average path length of the system with 50 nodes. It can be seen from the graph that the average backup path length of the proposed scheme is longer than the original re-routing scheme without the local traffic redistribution. The reason for this phenomenon is that the longer path in the original backup scheme has a larger probability of being refused because of the resource constraints in the system. In our backup scheme, the intermediate node of the backup path may move a portion of its own traffic loads to its neighbours. This action redistributes the traffic load in the system which reduces the probability of congestion generated in the backup path.

Fig. 5.8 indicates the throughput of the system with 200 nodes. It can be clearly seen from the graph that our scheme has much better performance than the original backup scheme. We can also identify a fast throughput decay in this figure, which is similar to the complex network [3, 231, 232, 2]. The throughput of the original backup scheme approximately follows a power law function. The reason for this phenomenon is that following the loss of some nodes the whole system is separated into multiple small

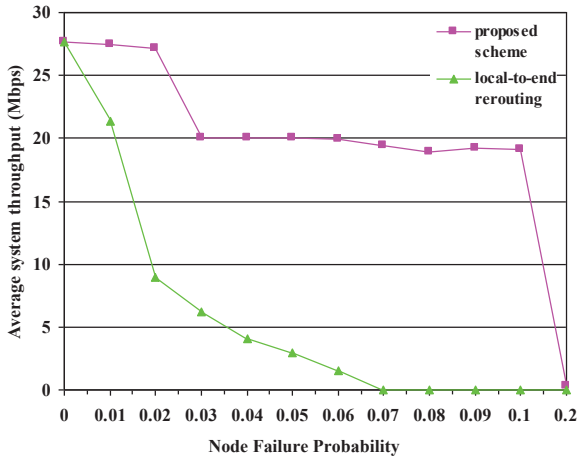

Figure 5.8: The system throughput of 200 nodes network

clusters and those clusters cannot communicate with each other. This phenomenon matches our prediction based on the theoretical and simulation results in section 4.1.3. According to the simulation result in Fig. 5.8, we can see that our proposed backup scheme has much higher system throughput than the original backup scheme. Since the average length between any two nodes in the system is much longer than the previous simulation, the average number of connected neighbours of each node is smaller than the previous test which means the connectivity of the system in this case is not as good as the previous one. There must be some nodes working as boundary nodes that connect multiple clusters of nodes together. As a result, when some of these kinds of nodes fail, the system throughput will be degraded dramatically. This is also the reason why the throughput of our scheme looks like a nonlinear step function.

Fig. 5.9 depicts the average backup path length of the system with 200 nodes. In this figure, we can see that the proposed scheme has much longer backup paths than the original scheme. In this simulation, the average distance between two connected nodes is much longer than it in the first case (the system with 50 nodes). In this case, the average transmission capacity of each working communication link is much smaller than it was in the first case. This causes a much larger probability of generating congestions in the backup paths, so the original scheme cannot find the available backup path for the data flows which are affected by the node(s) failure in this case. In contrast, our scheme redistributes the traffic load in a given area and reduces the probability of generating congestions in the backup path, so our proposed scheme gets longer average backup paths and achieves higher system throughput.

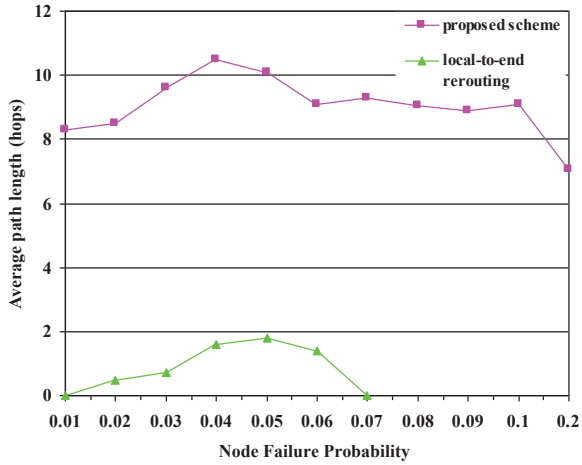

Figure 5.9: The average path length of 200 nodes network

5.3 Summary

In this chapter, we proposed a simple backup scheme algorithm for multiple-channel multiple-radio wireless mesh networks to maximize the network throughput after losing some of working nodes. Transmission rate adaptation is used in our backup scheme to satisfy the QoS requirement of each data flow to the destination. We developed a solution in which the local traffic load distribution scheme focuses on maximizing the system throughput while minimizing the probability of congestion generation. The results also showed that our proposed backup scheme has a much larger system throughput than the existing algorithm. From the simulation results, we can find that even though the wireless mesh network has similar properties with the complex networks, it has its distinct performance based on its unique properties such as multiple-channel multiple-radio and its robustness nature facing the node or link failure. In the future, we will do more researches about the failure recovery problem on the wireless mesh network to build a property mathematical model to represent the node failure performance in the wireless mesh networks.

Chapter 6

Theoretical Analysis and an Optimal Schedule to Prolong Battery life in Green Wireless Mesh Networks Nodes

Green energy is an environment friendly and a cost effective alternative to operate wireless mesh networks. Efficient rechargeable batteries are essential to the successful adoption of green wireless mesh networks. They overcome the energy supply fluctuation problem of various green energy sources by storing, and regulating the use of, the supplied energy used to receive and transmit data at each network router. This chapter develops a theoretical framework to analyze the behaviour of the residual energy of a wireless router's battery in two scenarios, namely, batteries with infinitely large and finite energy storage capacities. The residual energy is modelled using a general queuing model, which in contrast to existing approaches, makes no assumptions on the energy charging behavior or the router's traffic distributions. Rather, it employs the diffusion approximation modelling methodology while assuming general charging and traffic distributions. Closed formulations for the probability distribution functions of the residual capacity and the duration of the wake-up and operational periods of the wireless nodes for the two considered scenarios are then calculated. Obtained theoretical results demonstrate that the battery's energy depletion probability can be dramatically reduced by minimizing the variance in the energy consumption rate during data transmission. Based on these results, two novel energy efficient data transmission scheduling schemes are also

developed to maximize the router's operational period. The first scheme finds a theoretically optimal schedule that minimizes the variance in the node's energy consumption but assumes knowledge of future traffic needs and hence the expected energy consumption. The second relaxes this assumption and finds an efficient heuristics-based schedule. Simulation results demonstrate that the proposed schemes achieve significant increase in the battery lifetime while enhancing the total throughput and reducing packet losses. The proposed work has been submitted as [35].

6.1 Theoretical Analysis

Green WMNs that rely only on renewable energy sources (e.g., sunlight, hydrogen and wind) have been recently considered in [24, 25, 26, 27, 28] with focus on developing functionalities (e.g., routing and scheduling) that minimize the energy consumption. However, it is essential for these approaches to have a good estimate of the available energy in the routers' batteries and, in turn, their expected lifetimes. However, this is not a straightforward task since, unlike permanent electricity sources, the supply of green energy sources is irregular and fluctuates over time. For instance, a solar energy source provides varying energy levels across the time of the day and the season of the year and is affected by weather conditions and geography. As a result, the unreliable nature of the green energy source will affect the wireless node availability. Hence, it is necessary to analyse the wireless node's residual energy changing process and find out which parameter may affect the lifetime of the battery.

Consider a mesh router (node) in a MRMC wireless network that can communicate directly with a number of neighbouring nodes. The node is equipped with two or more radio interfaces and is powered by a battery which is recharged by a green energy source (e.g., solar or a wind power source or a small hydro-electric power generator). Similar to [239], we model the node using a system comprised of two dependent buffers; the first is used to store the received data. On the other hand, the second buffer models the battery that is used to store the harvested energy, as shown in Fig. 6.1. The node consumes energy to transmit received packets to its neighbouring nodes using its radio interfaces. The transmission rates are controlled by adjusting the node's transmission power. Similar to existing approaches [25] and to maintain the lucidity of our presentation, we do not consider other sources of energy consumption. These other sources are either negligible compared to the power needed to transmit data (e.g., energy consumed to receive data) or they can be considered as part of the transmission process (e.g., packet processing

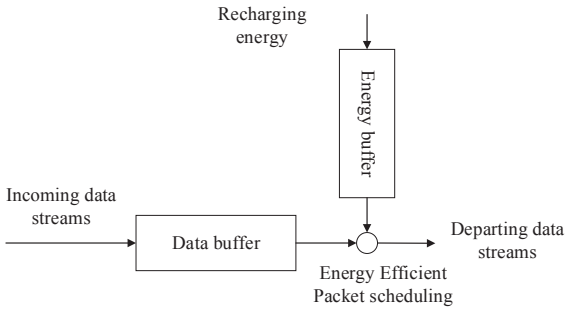

Figure 6.1: A Two-buffers model of the wireless node with a rechargeable battery

before transmission).

Clearly, if not planned carefully, energy consumption might exceed the battery's residual energy. This in turn will eventually deplete the battery's energy and shuts the node down. The over all result is a quick degradation in the performance of the entire MRMC wireless network. To circumvent this problem, we theoretically analyze the effects of the charging behaviour and the traffic departure parameters on the residual energy of the battery. Our objective is to prolong the battery lifetime by adjusting the energy consumed during the transmission process in reaction to the charging rate.

6.1.1 Theoretical Analysis of the Residual Energy

We model the inter-arrival times t_1, t_2,$\cdots$, between the recharging units arriving to the energy buffer using a generally distributed random variable with mean value $M_a = 1/\mu_a$ and variance σ_a^2. Here, M_a and μ_a represent the average inter-arrival time between charge units and their arrival rate, respectively. The battery is charged over time and the charge units are consumed by the node to transmit data stored in the data buffer shown in Fig. 6.1. In other words, the discharge process is tightly dependent on the arrival of the traffic to the node. In this work, and in contrast to existing approaches which mostly assume that the traffic arrival follows a poisson distribution [36], we make no such assumptions; rather, we model this random variable using a general distribution with only a known mean and variance. As shown in Fig. 6.1, the arriving traffic is stored in the data buffer and departs when it is served by the needed charges from the battery. This process as will be shown in the next section can be controlled by a scheduler that regulates the departure rate process. Consequently, we can regard the service times $\bar{t}_1$, $\bar{t}_2$, $\cdots$, for the charges inside the battery buffer as the times representing the waiting of the incoming

charge to be consumed due to transmission. In turn, this random variable will have a measurable mean, $M_b = 1/\mu_b$ and variance σ_b^2 that is fixed during a given period of time. In other words, M_b and μ_b represent average waiting time for the charge in the battery and its the discharge rate, respectively. The node repeatedly goes through two stages of operation, namely, a wake-up or a charging phase and an operational phase. The wake-up phase starts when the battery is completely depleted of its charge and continues until its residual capacity reaches a given threshold. Once the battery charge reaches this threshold, the operational phase starts. During this phase, the node can start receiving and transmitting packets while its battery is charging. This phase terminates and the node returns to the wake-up phase when the battery is depleted of its charge.

We model the battery's recharging and discharging behaviour using a single server queue, $G/G/1$, with a general distribution G for the arrival and the service time of the charge. The latter represents the time the charge stays in the queue until it is consumed by the transmission of packets. Define $E(t)$ as the residual energy in the battery, i.e., the queue length, at $t \geq 0$. We employ the diffusion approximation-based modelling approach [37] to describe $E(t)$. In other words, we model the length of the queue as the location of a moving particle suspended in a flowing fluid and moving randomly due to collisions with fluid particles. In turn, this movement is described using a continuous Markov process that has only continuous trajectories representing the path of this particle. The adoption of this approximation facilitates significantly the derivation of closed forms for the distribution of the residual energy and the depletion probabilities when general distributions are assumed. The following lemma provides a formal characterization of $E(t)$ using this model.

Lemma 6.1. *Let $\{E(t),\, t \geq 0\}$ be a stochastic process approximating the residual energy in the MRMC wireless network node battery at time t. For a large t and for all $E(t) > 0$, such that the battery is not depleted, $E(t)$ can be approximated as a continuous diffusion process such that the changes in $E(t)$, $dE(t) = E(t+\delta t) - E(t)$, are normally distributed with mean μ and variance σ^2, where*

$$\mu = \mu_a - \mu_b \tag{6.1}$$

$$\sigma^2 = \mu_a^3 \times \sigma_a^2 + \mu_b^3 \times \sigma_b^2 \tag{6.2}$$

Proof. Let $\alpha(t)$ be the amount of energy units that charged the battery from $t = 0$ and up to t. It can easily be shown that the probability that we have n or more new charges in the battery is equal to the probability that the arrival time of the n^{th} charge took

place on or before t, i.e.,

$$\Pr\{\alpha(t) \geq n\} = \Pr\{\tau_n \leq t\} \tag{6.3}$$

where $\tau_n = t_1 + t +_2 + \cdots + t_n$ is the time of the arrival of the n^{th} charge (it is equal to the sum of inter-arrival times up to n). As t increases significantly, τ_n becomes the sum of a very large number of identically distributed and independent (i.i.d.) random variables. Hence, applying the central limit theory, τ_n can be described using a normal (Gaussian) distribution with mean $n \times M_a$ and variance $n \times \sigma_a^2$. Consequently, with a simple change of variables, it can be shown that $\alpha(t)$ has also a normal distribution $N(M_a \times t, \sigma_a^2 \times M_a^3 \times t)$.

Using the same reasoning, let $\delta(t)$ be the charge amount leaving the queue up to t. Then, if the queue is never emptied, we have

$$\Pr\{\delta(t) \geq n\} = \Pr\{\bar{\tau}_n \leq t\} \tag{6.4}$$

where $\bar{\tau}_n = \bar{t}_1 + \bar{t}_2 + \cdots + \bar{t}_n$ is the time of departure of the n^{th} charge and is equal to the sum of service times $\bar{t}_i$. Consequently, with a simple change of variables, it can be shown that $\delta(t)$ has also a normal distribution $N(M_b \times t, \sigma_b^2 \times M_b^3 \times t)$.

Then, we have E(t)=$\alpha(t) - \delta(t)$, that is a linear combination of two normal distributions. Hence, $E(t)$ follows a normal distribution $N((M_a - M_b) \times t, (\sigma_a^2 \times M_b^3 + \sigma_b^2 \times M_b^3) \times t)$. With the change of $E(t)$ obtained by removing t. Hence, $E(t)$ can be approximated as a standard Wiener process, i.e., a diffusion process, that is a time continuous stochastic process with independent Gaussian increments. □

Lemma 6.1 approximates the evolution of $E(t)$ as a diffusion process with a state space $(0, \infty)$. The lemma also states that this approximation is valid as long as the batter is not depleted with $E(t) > 0$. Let $f(e, t|e_0)$ be the conditional probability density function (PDF) for the battery residual energy process $E(t)$ with an initial capacity $E(0) = e_0$, such that for $e > 0$ we have:

$$f(e, t|e_0) = Pr(e \leq E(t) < e + de|E(0) = e_0) \tag{6.5}$$

A direct consequence of the above lemma is that since $E(t)$ is a diffusion process $f(e, t|e_0)$ must satisfy the following Fokker-Planck relation [37], i.e., for all $E(t) > 0$ we have

$$\frac{\partial f(e, t|e_0)}{\partial t} = -\mu \frac{\partial f(e, t|e_0)}{\partial e} + \frac{\sigma^2}{2} \frac{\partial^2 f(e, t|e_0)}{\partial e^2} \tag{6.6}$$

This partial differential equation describes the time evolution of $f(e,t|e_0)$ due to its mean and variance. The solution of Eq. (6.6) provides us with the probability distribution of $E(T)$, i.e., the expected distribution of residual energy of the battery. The general solution for (6.6) is:

$$f(e,t|e_0) = \frac{1}{\sigma\sqrt{2\pi t}} \exp\Big(- \frac{(e - e_0 - \mu t)^2}{2\sigma^2 t}\Big) \tag{6.7}$$

This equation provides a good approximation, only as long the battery has a sufficient charging rate that it is never depleted and $E(t)$ never reaches zero as t tends to infinity. Otherwise, the solution will lead to a negative value for $E(t)$. In the following sections, we overcome this limitation in the adopted model in two different scenarios, namely, when the battery has an infinitely large capacity and when the battery capacity is limited to storing N charge units at most.

6.1.2 A G/G/1/∞ Model for the Infinite Capacity Battery

We first consider the case where the a rechargeable battery has an infinitely large capacity. In other words, the battery is large enough to store any incoming charge during a given period. With advances in battery manufacturing technologies, this scenario will be a typical one in the near future [257]; in this case, we model the battery buffer using a G/G/1/∞ queue. We divide the operational life cycle of a node into two phases; the first is the wake-up, or recharge, phase which starts with an initially empty battery that charges gradually. During this phase, the node cannot receive or transmit packets due to its low battery. This phase continues until the battery is charged up to a certain threshold e_0 that can be adjusted by the access point manufacturer or the network operator. Intuitively, a larger e_0 will result in a longer wake-up phase but will also prolong the length of the operational phase. We will formally derive these relations between e_0 and the length of the two phases in the next sections. The second phase, the active or operational phase, starts once the battery's residual energy reaches e_0 where the node starts receiving and transmitting packets. This phase is terminated when the battery is depleted. At this point in time, the node returns back to the wake-up phase.

6.1.2.1 Duration of the wake-up phase

At the beginning of the wake-up phase the node's battery is empty with $E(0) = 0$. The wireless node, hence, cannot receive or transmit any data and we set $\mu_b = \sigma_b = 0$.

Consequently, we can substitute these values in (6.1) and (6.2), to calculate the mean, μ_w and variance σ_w^2 of the battery's residual capacity during this phase,

$$\mu_w = \mu_a \tag{6.8}$$

$$\sigma_w^2 = \mu_a^3 \times \sigma_a^2 \tag{6.9}$$

Also, let $f_w(e,t|0)$ and $F_w(e,t|0)$ be the PDF and the cumulative distribution probability (CDF),respectively, of the battery's residual capacity during the wake-up period. More precisely, $f_w(e,t|0)=Pr\{e \leq E(t) < e+de|E(0)=0, E(\tau) < e_0, \forall 0 < \tau < t\}$ and $F_w(e,t|0)=Pr\{E(t) \leq e|E(0) < 0, E(\tau) < e_0 \forall 0 < \tau < t\}$. The latter CDF reflects the probability that the residual capacity is still below e at time t, such that $F_w(e,t|0) = \int_0^e f_w(e,t|0)de$.

During this phase, $E(t)$ can still be described using a diffusion process and $f_w(e,t|0)$ obeys the Fokker-Planck equation:

$$\frac{\partial f_w(e,t|0)}{\partial t} = -\mu_w \frac{\partial f_w(e,t|0)}{\partial e} + \frac{\sigma_w^2}{2} \frac{\partial^2 f_w(e,t|0)}{\partial e^2} \tag{6.10}$$

for $0 < e < e_0$. In order to force the process to stop once the threshold is reached, i.e., $E(t) = e_0$, we add an absorbing barrier for the diffusion particle that absorbs the particle once it is hit. This is achieved mathematically by setting the probability distribution to zero at that point[258]. Hence, the initial condition at $t = 0$ and the boundary condition at e_0, respectively, can now be formally stated as:

$$f_w(e,0|0) = \delta(e), \tag{6.11}$$

$$f_w(e_0,t|0) = 0, \quad \forall t > 0 \tag{6.12}$$

where $\delta(e)$ is the Dirac delta function[1]. The solution of (6.10)-(6.12) is given by the following lemma.

Lemma 6.2. *Let $\{E(t), t \geq 0\}$ be a stochastic process approximating the residual energy of the wireless node with an unlimited capacity battery during the wake-up phase as it is charged with mean $1/\mu_a$ and variance σ_a^2 from an initial depletion state to a desired*

[1] $\delta(e) = \infty$, for $e = 0$ and $\delta(e) = 0$, for $e \neq 0$.

wake-up threshold e_0. Then, $E(t)$, can be characterized by its PDF and CDF as follows

$$f_w(e,t|0) = \frac{1}{\sigma_w\sqrt{2\pi t}}\Big[\exp\Big(-\frac{(e-\mu_w t)^2}{2\sigma_w^2 t}\Big) - \exp\Big(\frac{2\mu_w e_0}{\sigma_w^2} - \frac{(e-2e_0-\mu_w t)^2}{2\sigma_w^2 t}\Big)\Big] \tag{6.13}$$

$$F_w(e,t|0) = \Phi\Big(\frac{e-\mu_w t}{\sigma_w\sqrt{t}}\Big) - \exp\Big(\frac{2\mu_w e_0}{\sigma_w^2}\Big)\Phi\Big(\frac{e-2e_0-\mu_w t}{\sigma_w\sqrt{t}}\Big) \tag{6.14}$$

where $\Phi(e)$, the standard normal integral, is given by:

$$\Phi(x) = \frac{1}{\sqrt{2\pi}}\int_{-\infty}^{x}\exp(-y^2/2)dy \tag{6.15}$$

Proof. Following Cox et. al.[258], the solution to (6.10)-(6.12) can be obtained by the method of images. In this method, the absorption barrier at $E(t) = e_0$ is modelled as a mirror. The image of the origin in that mirror is treated as another source for the particle, i.e., another diffusion process that starts at $E(0) = 2e_0$ Hence, the solution becomes

$$f_w(e,t|0) = f(e,t|0) + Af(e,t|2e_0) \tag{6.16}$$

where $f(.)$ is the solution of the unconstrained diffusion process as described in Eq. (6.5) and A is a constant. It can be shown that setting $A = -\exp(2\mu_w e_0/\sigma_w^2)$ satisfies Eq. (6.10)-Eq. (6.12). Hence, we obtain f_w, which is integrated to calculate F_w. □

The above lemma indicates that f_w is the result of two diffusion processes. The first, described by the first term, is that of a free moving diffusion process in the space $(-\infty, \infty)$ that started from $e = 0$ and the second term corrects the behavior of the first process by subtracting the effects of another diffusion process placed at $e = 2e_0$ that is scaled by a factor $-\exp(\frac{2e_0\mu_a}{\sigma_a^2})$. This imitates a mirror placed at $e = e_0$ that reflects the location of the origin [258].

Having obtained the distribution of the residual capacity $f_w(e,t|0)$, we turn our attention to the time it takes the battery to reach the threshold e_0. We note that the duration of the wake-up period is also a random variable T_w since it will depend on the charging process. It can be formally defined by the relation:

$$T_w = \min\{t|E(t) = e_0, \quad t > 0, \text{ s.t. } E(0) = 0\} \tag{6.17}$$

Let $G_w(t)$ be the CDF of T_w, we can relate T_w and $E(t)$ through their CDFs by noting that the event of reaching the threshold charge e_0 before t is complementary to the event that $E(t)$ is still below e_0 at t, i.e.,

$$\begin{aligned} G_w(t) &= Pr\{T_w \leq t\} = 1 - Pr\{E(t) \leq e_0\} \\ &= 1 - F_w(e_0, t|0) \\ &= 1 - \int_0^{e_0} f_w(e, t|0)de \end{aligned} \tag{6.18}$$

substituting (6.14) into (6.18) we obtain:

$$G_w(t) = 1 - \Phi\Big(\frac{e_0 - \mu_w t}{\sigma_w \sqrt{t}}\Big) + \exp\Big(\frac{2\mu_w e_0}{\sigma_w^2}\Big)\Phi\Big(-\frac{e_0 + \mu_w t}{\sigma_w \sqrt{t}}\Big) \tag{6.19}$$

We can now calculate $g_w(t)=\frac{dG_w(t)}{dt}$ the PDF of T_w and obtain the following lemma.

Lemma 6.3. *The wake-up time, T_w, for the wireless node, during the period at which the battery is charged with mean $1/\mu_a$ and variance σ_a^2 from an initial depletion state to a desired wake-up threshold e_0 has a distribution $g_w(t)$ with mean $\mathcal{E}(T_w)= \frac{e_0}{\mu_a}$ and variance $\mathcal{V}(T_w) = \frac{e_0\sigma_a^2}{2}$, such that*

$$g_w(t) = \frac{e_0}{\sigma_a\sqrt{2\pi t^3 \mu_a^3}} \exp\Big(-\frac{\mu_a^3(e_0 - \mu_a t)^2}{2\sigma_a^2 t}\Big) \tag{6.20}$$

Proof. To obtain g_w, we substitute Eq. (6.19) in $g_w(t)=\frac{dG_w(t)}{dt}$, and we obtain (6.20). The MGF. of T_w is then calculated as:

$$g_w^*(s) = \int_0^\infty e^{-st} g_w(t)dt \tag{6.21}$$

We then differentiate w.r.t s to obtain the mean $\mathcal{E}(T_w)= \frac{e_0}{\mu_w}$ and variance $\mathcal{V}(T_w) = \frac{e_0\sigma_w^2}{2\mu_w^3}$. □

The above lemma shows that the mean and variance of the duration of the wake-up phase increase linearly with the selected threshold e_0. Also, we see that as expected, decreasing the mean of the inter-arrival time $1/\mu_a$ of the charge units shortens the wake-up period.

6.1.2.2 Residual energy during the operational phase

Next, we analyze the second operational phase of the wireless node. This phase starts once we have $E(0)$=e_0 and continues until the battery is depleted. Again, we model the residual capacity in the battery, $E(t)$ during this period as a diffusion process that starts from time $t = 0$. We associate with $E(t)$, its PDF $f_p(e, t|e_0)$ and CDF $F_p(e, t|e_0)$ such that $f_p(e, t|e_0) = Pr\{e \leq E(t) < e + de|E(0) = e_0, E(\tau) > 0, \forall 0 < \tau < t\}$ and $F_p(e, t|e_0) = Pr\{E(t) \leq e|E(0) < e_0, E(\tau) > 0, \forall 0 < \tau < t\}$.

To ensure that the process stops when the battery is depleted, we adjust the Fokker-Planck relation Eq. (6.6) to allow $E(t)$=0, by adding an absorbing barrier at the origin of the diffusion process. The new diffusion equation becomes:

$$\frac{\partial f_p(e,t|e_0)}{\partial t} = -\mu_p \frac{\partial f_p(e,t|e_0)}{\partial e} + \frac{\sigma_p^2}{2} \frac{\partial^2 f_p(e,t|e_0)}{\partial e^2} \tag{6.22}$$

where μ_p and σ_p^2 are obtained by Eq. (6.1) and Eq. (6.2) from Lemma 6.1. with the initial and boundary conditions, respectively,

$$f_p(e, 0|e_0) = \delta(e - e_0) \tag{6.23}$$

$$f_p(0, t|e_0) = 0, t > 0 \tag{6.24}$$

Similar to Lemma 6.2, the following lemma characterizes the behaviour of $E(t)$ during the operational phase.

Lemma 6.4. *Let $\{E(t), t \geq 0\}$ be a stochastic process approximating the residual energy of the wireless node with the unlimited capacity battery during the operational phase. Then, $E(t)$ can be characterized by its PDF*

$$f_p(e,t|e_0) = \frac{1}{\sigma_p\sqrt{2\pi t}} \Bigg[\exp\Big(-\frac{(e - e_0 - \mu_p t)^2}{2\sigma_p^2 t}\Big) - \exp\Big(-\frac{2e_0\mu_p}{\sigma_p^2}\Big) \exp\Big(\frac{(e + e_0 - \mu_p t)^2}{2\sigma_p^2 t}\Big)\Bigg] \tag{6.25}$$

Proof. Similar to the proof of Lemma 6.2 and following Cox et. al.[258], the solution to (6.22)-(6.24) can be obtained by the method of images. In this method, the absorption barrier at $E(t) = 0$ is modelled as a mirror. The image of e_0 in that mirror is treated as another source for the particle, i.e., another diffusion process that starts at $E(0) = -e_0$ Hence, the solution becomes:

$$f_p(e, t|e_0) = f(e, t|e_0) + Af(e, t| - e_0) \tag{6.26}$$

where $f(.)$ is the solution of the unconstrained diffusion process as described in Eq. (6.5) and A is a constant. It can be shown that setting $A = -\exp(2\mu_p e_0/\sigma_p^2)$ satisfies Eq. (6.22)-(6.24). Hence, we obtain f_p. □

From the above lemma, the PDF of $E(t)$ is described by two terms. The first is that of a diffusion process of a unit strength that started from e_0 and moves in the unlimited space $(-\infty, \infty)$. The second part corrects this behavior by subtracting the probability loss due to the absorbing barrier by introducing another diffusion process at $e = -e_0$.

We note that, in contrast to wake up phase during which $E(t)$ was nondecreasing in time, the residual energy during the operational phase depends heavily on the relationship between μ_a and μ_b, summarized by the variable μ_p. Intuitively, if the arrival rate of the charges μ_a is larger than their consumption rate, μ_b, the probability of depleting the battery is very small. Otherwise, the battery will almost certainly deplete. We analyze this behavior in the following section.

6.1.2.3 Duration of the operational phase

The duration of the active phase for the wireless node signifies the length of the period starting from a residual capacity e_0 and transmitting data until the battery is depleted. The analogy for this period for the diffusion process is to estimate the time at which the diffusion process hits the absorbing barrier at the origin $e = 0$ given initial condition $E(0) = e_0$.

Formally, we define another random variable T_p to model the first time the battery is depleted, i.e.,

$$T_p = \min\{t | E(t) = 0, \text{ s.t. } E(0) = e_0, t > 0\} \tag{6.27}$$

We also associate with T_p its PDF $g_p(t)$ and CDF $G_p(t)$. Similar to the valuations of the wake-up time duration, we have the following lemma.

Lemma 6.5. *Consider a wireless node with an unlimited capacity battery that is charged with mean $1/\mu_a$ and variance σ_a^2 that operated with an initial capacity $E(0) = e_0$ until depletion. If the discharge rate follows a general distribution with mean $1/\mu_b$ and variance σ_b^2, then the node's operational time, T_p, has a distribution $g_p(t)$*

$$g_p(t) = \frac{e_0}{\sigma_p\sqrt{2\pi t^3}} \exp\Big(- \frac{(e_0 + \mu_p t)^2}{2\sigma_p^2 t}\Big) \tag{6.28}$$

and

$$\mathcal{E}(T_p) = \frac{-e_0 \exp\left(\frac{2e_0\mu_p}{\sigma_p^2}\right)}{\mu_p} \tag{6.29}$$

where μ_p and σ_p^2 are obtained in (6.1) *and* (6.2)*, respectively.*

Proof. We note that $G_p(t)= Pr\{T_p \leq t\}=1 - Pr\{E(t) \geq 0\}=1 - \int_0^\infty f_p(e,t|e_0)de$. Consequently, we have $g_p(t)= -\frac{d}{dt}\int_0^\infty f_p(e,t|e_0)dt$.

$$g_p(t) = \frac{\partial}{\partial t}\int_0^\infty f_p(e,t|E_0)de = \int_0^\infty \frac{\partial f_p(e,t|e_0)}{\partial t}de \tag{6.30}$$

Substitute Eq. (6.6)) in the above equation, we can calculate $g_p(t)$,[258],

$$\begin{aligned}
g_p(t) = & \frac{e_0}{\sigma_a\sqrt{2\pi t^3\mu_a^3}}\exp\Big(-\frac{\mu_a^3(e_0-\mu_a t)^2}{2\sigma_a^2 t}\Big) \qquad (6.31)\\
= & \lim_{e\to 0}\left(\frac{\sigma^2}{2}\frac{\partial f_p(e,t|e_0)}{\partial e} - \mu_p f_p(e,t|e_0)\right)\\
= & \frac{1}{\sigma_p\sqrt{2\pi t}}\lim_{e\to 0}\{\frac{\sigma_p^2}{2}\exp\Big(\frac{\mu_p}{\sigma_p^2}(e-e_0) - \frac{\mu_p^2}{2\sigma_p^2}t\Big)\\
& \times[\exp\Big(-\frac{(e-e_0)^2}{2\sigma_p^2 t}\Big)\Big(\frac{\mu_p}{\sigma_p^2} - \frac{e-e_0}{\sigma_p^2 t}\Big)\\
& -\exp\Big(-\frac{(e+e_0)^2}{2\sigma_p^2 t}\Big)\Big(\frac{\mu_p}{\sigma_p^2} - \frac{e+e_0}{\sigma_p^2 t}\Big)]\\
& -\mu_p f_p(e,t|e_0)\}\\
= & \frac{1}{\sigma_p\sqrt{2\pi t}}\{\frac{\sigma_p^2}{2}\exp\Big(-\frac{(e_0+\mu_p t)^2}{2\sigma_p^2 t}\Big)\Big[\exp\Big(-\frac{e_0^2}{2\sigma^2 t}\Big)\\
& \times\Big(\frac{\mu_p}{\sigma_p^2} + \frac{e_0}{\sigma_p^2 t}\Big) - \exp\Big(-\frac{e_0^2}{2\sigma_p^2 t}\Big)\Big(\frac{\mu_p}{\sigma_p^2} - \frac{e_0}{\sigma_p^2 t}\Big)\Big]\}\\
= & \frac{e_0}{\sigma_p\sqrt{2\pi t^3}}\exp\Big(-\frac{(e_0+\mu_p t)^2}{2\sigma_p^2 t}\Big) \qquad (6.32)
\end{aligned}$$

Hence proving the lemma. □

6.1.2.4 Depletion probability

We can now investigate the probability that the battery will be fully depleted. Since g_p is defined over $(0,\infty)$, the moment generating function (MGF), $g_p^*(s)$, of $g_p(t)$ can be

defined as its Laplace transform:

$$g_p^*(s) = \int_0^\infty \exp(-st) g_p(t) dt \tag{6.33}$$

and we have,

$$g_p^*(s) = \exp\Big(- \frac{e_0}{\sigma_p^2}(\mu_p + \sqrt{\mu_p^2 + 2\sigma_p^2 s})\Big) \tag{6.34}$$

when $s \to 0$, $g_p^*(s)$ gives the steady state probability p_0 of depleting the battery or in other words reaching the absorbing barrier. Hence,

$$\begin{aligned} p_0 &= \lim_{s\to 0} g_p^*(s) \\ &= \begin{cases} 1 & \mu_p \leq 0 \\ \exp\Big(- \frac{2e_0\mu_p}{\sigma_p^2}\Big), & \mu_p > 0 \end{cases} \end{aligned} \tag{6.35}$$

substituting with (6.1) and (6.2) in (6.35) yields the following corollary.

Corollary 6.1. *Consider a wireless node with an unlimited capacity battery that is charged with mean $1/\mu_a$ and variance σ_a^2 that operated an initial capacity $E(0) = e_0$ until depletion. If the discharge rate follows a general distribution with mean $1/\mu_b$ and variance σ_b^2, then the battery will be depleted with probability 1 if $\mu_a \leq \mu_b$. Whenever, $\mu_a > \mu_b$ the battery can still deplete with probability p_0 such that*

$$p_0 = \exp\Big(- \frac{2e_0(\mu_a - \mu_b)}{\mu_a^3\sigma_a^2 + \mu_b^3\sigma_b^2}\Big). \tag{6.36}$$

The above results indicate that the node will almost certainly stop transmitting and go to the wake-up phase whenever the mean charge arrival rate is less than or equal to the needed discharge rate due to packet transmissions; this is an obvious and expected result. On the other hand, depletion may still occur if the charge rate is higher than the discharge rate. In this case, the depletion probability decreases exponentially as μ_p and e_0 increase. Conversely, an increase in the the variance of the charge arrival and needed discharge rate to transmit packets will increase this probability at an exponential order. Whenever the recharge process and the mean value of the departure process are exogenous parameters, the only parameter that can be adjusted to reduce p_0 is the variance σ_b^2 of the departure process. This result will constitute the basic premise for our developed traffic scheduling scheme.

6.1.2.5 Distribution of the wake and active cycles

If the charge rate μ_a is smaller than the discharge rate μ_b Corollary 6.1 indicates that the battery will almost certainly be depleted and initiate another wake-up phase. We analyze the frequency of this repeated cycle of returning to the wake-up phase. Let $K(t)$ be a random variable that represents the number of times the wireless node have gone through the wake-up and active phases, where $K(t)$ is a nondecreasing function of time. Since $K(t)$ follows the behaviour of $E(t)$, it can also be approximated as a diffusion process. Denote by $f_{wp}(k,t|0)$ and $F_{wp}(k,t|0)$ the PDF and CDF functions of $K(t)$, i.e., $f_{wp}(k,t|0) = Pr\{k \leq K(t) < k+dt|K(0)=0\}$ and $F_{wp}(k,t|0) = Pr\{K(t) \leq k|K(0)=0\}$. Also, let μ_{wp} and σ^2_{wp} represent the mean and variance of $K(t)$, then $f_{wp}(k,t|0)$ satisfies the Fokker-Planck equation for $k(t) > 0$,

$$\frac{\partial f_{wp}(k,t|0)}{\partial t} = -\mu_{wp}\frac{\partial f_{wp}(k,t|0)}{\partial k} + \frac{\sigma^2_{wp}}{2}\frac{\partial^2 f_{wp}(k,t|0)}{\partial k^2} \tag{6.37}$$

with the initial and boundary conditions, respectively,

$$f_{wp}(k,0|0) = \delta(k) \tag{6.38}$$

$$f_{wp}(0,t|0) = 0, \quad t > 0 \tag{6.39}$$

The following lemma provides further details on the effect of the variance σ_b^2 of the departure process.

Lemma 6.6. *When the battery charge rate μ_a is smaller than the discharge rate μ_b consumed during transmissions, the number of wake-up and transmission cycles for a wireless node before time t can be characterised with a PDF $f_{wp}(k,t|0)$ such that:*

$$f_{wp}(k,t|0) = \frac{1}{\sigma_{wp}\sqrt{2\pi t}}\left[\exp\Big(-\frac{(k-\mu_{wp}t)^2}{2\sigma_w^2 t}\Big) - \exp\Big(\frac{2\mu_{wp}}{\sigma^2_{wp}} - \frac{(k-\mu_{wp}t)^2}{2\sigma^2_{wp}t}\Big)\right] \tag{6.40}$$

where

$$\mu_{wp} = -\frac{\mu_a(\mu_a-\mu_b)}{\mu_b e_0} \tag{6.41}$$

$$\sigma^2_{wp} = \frac{\mu_b^2\mu_a^3(\sigma_a^2+\sigma_b^2) + \sigma_a^2\mu_a^4(\mu_a-\mu_b)}{e_0^2\mu_b^2} \tag{6.42}$$

Proof. To first obtain μ_{wp} and σ^2_{wp}, we introduce another random variable T_{wp} to denote the inter-arrival time between two consecutive increments of $K(t)$. In other words, T_{wp}

represents the duration between two consecutive battery depletion events. Then we have, $\mu_{wp} = \frac{1}{\mathcal{E}(T_{wp})}$ and σ^2_{wp}=$\mathcal{V}(T_{wp}) \times \mathcal{E}(T_{wp})$.

We also note that the length of T_{wp} is equal to the sum of duration of wake-up phase T_w and duration of active phase T_p, i.e., $T_{wp} = T_w + T_p$. Since T_{wp} is the sum of two random variables, the PDF of T_{wp}, $g_{wp}(t)$, is obtained be convoluting the two PDFs of T_w and T_p i.e.,

$$g_{wp}(t) = g_w(t) \otimes g_p(t) \tag{6.43}$$

were $\otimes$ is the convolution operator. Then, the MGF of $g_T(t)$ can be calculated as follow,

$$g^*_T(s) = g^*_w(s) \cdot g^*_p(s) \tag{6.44}$$

When $\mu_p < 1$, i.e., $\mu_a < \mu_b$, we use the result of Lemma 6.3 to substitute for $g^*_w(s) = \exp\left(\frac{e_0(\mu_w - \sqrt{\mu_w^2 + 2s\sigma_w^2})}{\mu_w^2}\right)$ and into the above equation, we have

$$\mathcal{E}(T_{wp}) = -\frac{d}{ds} g^*_{wp}(s) \mid_{s=0} = -\frac{e_0 \mu_b}{\mu_a(\mu_a - \mu_b)} \tag{6.45}$$

and

$$\begin{aligned} \mathcal{V}(T_{wp}) &= \frac{d^2}{ds^2} g^*_{wp}(s) \mid_{s=0} - E^2(T_{wp}) \\ &= -\frac{e_0[\mu_b^3(\sigma_a^2 + \sigma_b^2) + 3\sigma_a^2 \mu_a \mu_b(\mu_a - \mu_b)]}{(\mu_a - \mu_b)^3} \end{aligned} \tag{6.46}$$

To find the solution for (6.37)-(6.38) we again use the method of images. In this method, the absorption barrier at $K(t) = 0$ is modelled as a mirror with another diffusion process Hence, the solution becomes

$$f_{wp}(k, t|0) = f(k, t|0) - Af(k, t|0) \tag{6.47}$$

where $f(.)$ is the solution of the unconstrained diffusion process as described in Eq. (6.5) and A is a constant. It can be shown that setting $A = -\exp(2\mu_{wp} e/\sigma^2_{wp})$ satisfies Eq. (6.10)-(6.12). Hence, we obtain f_{wp}, □

6.1.3 G/G/1/N Model for the Battery Energy

In this section, we analyze the scenario where the wireless node has a finite capacity that can store up to N charge units. In this case, the battery's buffer is modelled as an G/G/1/N queue. Clearly, the previously obtained results for the wake-up phase still

applies for the limited capacity battery as long as the threshold $e_0 < N$. We then turn our attention to analyzing the duration of the operational phase.

Again, we model the residual energy by a diffusion process $E(t)$ with an initial capacity $E(0) = e_0$. The diffusion process defined by the Fokker-Planck equation is adapted to represent two constraints. Similar to the previous results, the first constraint ensures that the operational phase terminates once the battery is depleted. This constraint is enforced by adding an absorbing barrier at $e = 0$. The second constraint is related to the limited capacity N and ensures that any additional charges that arrive to the battery after it is fully charged with N charges are not stored. This constraint is achieved by adding a reflecting barrier for the diffusion particle[258]. Furthermore, once the battery is fully charged, the process waits a random amount of time that is dependent on the discharge rate and then discharges one or more energy units to serve incoming traffic. This behaviour is realized by adding a reflecting barrier at $e = N$ with a random return to $N - 1$. The literature describing diffusion processes (e.g., [259, 234, 260]) shows that deriving a closed form for their PDFs is cumbersome. Hence, we limit our attention to deriving the first passage time to the $e = 0$ boundary, or in other words, the time it takes the battery to be depleted. First, we assume that when the battery is fully charged, it instantaneously discharges a random amount of energy, then we show how to relax this assumption.

6.1.3.1 Duration of the operational phase with random discharging at $e = N$

Let $f_p(e, t|e_0, N)$ be the PDF of $E(t)$ such that it satisfies the following the diffusion equation [261]:

$$\frac{\partial f_p(e,t|e_0,N)}{\partial t} = -\mu_p \frac{\partial f_p(e,t|e_0,N)}{\partial e} + \frac{\sigma_p^2}{2}\frac{\partial^2 f_p(e,t|e_0,N)}{\partial e^2} \tag{6.48}$$

for $0 < e < N$ and where μ_p and σ_p are obtained by (6.1) and (6.2) from Lemma 6.1. with the initial and boundary conditions, respectively

$$f_p(e,0|e_0,N) = \delta(e - e_0) \tag{6.49}$$

$$f_p(0,t|e_0,N) = 0, t > 0 \tag{6.50}$$

$$\mu_p \frac{\partial f_p(e,t|e_0,N)}{\partial e} - \frac{\sigma_p^2}{2}\frac{\partial^2 f_p(e,t|e_0,N)}{\partial e^2}|_{e=N} = 0 \tag{6.51}$$

noting that the last condition describes the existence of a reflecting barrier at $e = N$ [258] such that the residual energy change process reaches the reflect point $e = N$, it jumps back to a random point $e < N$ immediately.

Similar to the infinite capacity case, let, $g_p(t)$ and $G_p(t)$ be the PDF and CDF, respectively of T_p, the first time the battery is depleted. The following lemma

Lemma 6.7. *Consider a wireless node with a battery with capacity N that is charged with mean $1/\mu_a$ and variance σ_a^2 that started with an initial capacity $E(0) = e_0$ and operated until depletion and assume that the battery discharges a random amount of energy, immediately after it reaches the full capacity. If the discharge rate follows a general distribution with mean $1/\mu_b$ and variance σ_b^2, then the node's operational time, T_p, has a distribution $g_p(t)$ with a mean $\mathcal{E}(T_p)$ where*

$$\mathcal{E}(T_p) = \begin{cases} -\frac{e_0}{\mu_p} + \frac{\sigma_p^2 exp(\frac{2\mu_p N}{\sigma_p^2})}{2\mu^2}[1 - \exp\left(\frac{-2\mu_p e_0}{\sigma_p^2}\right)], & for \quad \mu_p \neq 0 \\ \frac{e_0(2N-e_0)}{\sigma_p^2}, & for \quad \mu_p = 0 \end{cases} \tag{6.52}$$

where μ_p and σ_p^2 are obtained in (6.1) *and* (6.2)*, respectively.*

Proof. To prove the lemma, first we note that according to Lemma 6.1 f_p satisfies the following equation[258]:

$$\frac{\sigma_p^2}{2}\frac{\partial^2 f_p(e,t|e_0,N)}{\partial e_0^2} + \mu_p \frac{\partial f_p(e,t|e_0,N)}{\partial e_0} = \frac{\partial f_p(e,t|e_0,N)}{\partial t} \tag{6.53}$$

which is similar to the Fokker Planck relation, but is referred to as the backward equation.

Let $g_p(t)$ denotes the MGF of the first passage time that the process reaches the absorbing barrier at $e = 0$. As before, $g_p(t) = -\frac{\partial}{\partial t}\int_0^N f_p(e,t|e_0,N)de$. Then, taking Laplace transforms of Eq. (6.53), we have

$$\frac{\sigma_p^2}{2}\frac{d^2 g_p^*(s)}{de_0^2} + \mu \frac{dg_p^*(.)}{de_0} = sg^*(s) \tag{6.54}$$

The boundary conditions given an absorbing barrier at $e = 0$ and a reflecting barrier at $e = N$ can be represented, respectively, by

$$\begin{cases} g^*(s) & = 1 \\ \frac{dg^*(s)}{de_0} & = 0 \end{cases} \tag{6.55}$$

Since the $g^*(s)$ denotes the MGF of the first passage time, we have,

$$g^*(s) = 1 + \sum_{n=0}^{\infty}(-s)^n m_n(e_0)/n! \tag{6.56}$$

where m_i is the i^{th} raw moment of T_p. Substituting above equation in Eq. (6.54) and equating coefficients of power of s, we obtain for $n = 1, 2, \ldots$,

$$\frac{\sigma_p^2}{2}\frac{d^2 m_n}{de_0^2} + \mu\frac{dm_n}{de_0} = -nm_{n-1} \tag{6.57}$$

Similarly, the boundary conditions can be converted to $m_n(0) = 0$ and $\frac{dm_n}{de_0}\ |_{e_0=N} = 0$. Now, for $\mu_p \neq 0$, let $m_1(e_0)$ denote the general solution for the homogeneous differential equation,

$$\frac{\sigma_p^2}{2}\frac{d^2 m_1}{de_0^2} + \mu\frac{dm_1}{de_0} = 0 \tag{6.58}$$

Hence, we have,

$$m_1(e_0) = A + B\exp(-\frac{2\mu_p e_0}{\sigma_p^2}) - \frac{e_0}{\mu_p} \tag{6.59}$$

where A and B are constants. Applying the boundary condition $\frac{dm_n}{de_0}\ |_{e_0=N} = 0$ to Eq. (6.59), we have

$$B = -\frac{\sigma_p^2}{2\mu_p^2}\exp(\frac{2\mu_p N}{\sigma_p^2}) \tag{6.60}$$

Substituting Eq. (6.60) in Eq. (6.59) and the boundary condition $m_n(0) = 0$ lead to

$$A = \frac{\sigma_p^2}{2\mu_p^2}\exp(\frac{2\mu_p N}{\sigma_p^2}) \tag{6.61}$$

From Eq. (6.59), Eq. (6.60) and Eq. (6.61), we obtain the mean time of the first passage time $\mathcal{E}(T_p)$ for $\mu \neq 0$ as follow,

$$\mathcal{E}(T_p) = -\frac{e_0}{\mu_p} + \frac{\sigma_p^2\exp(\frac{2\mu_p N}{\sigma_p^2})}{2\mu_p^2}[1 - \exp(\frac{-2\mu_p e_0}{\sigma_p^2})] \tag{6.62}$$

When $\mu_p = 0$, we have,

$$m_1(e_0) = -\frac{1}{\sigma_p^2}e_0^2 + Ce_0 + D \tag{6.63}$$

where C and D are constants. Applying the boundary conditions to above equation yields $C = \frac{2N}{\sigma_p^2}$ and $D = 0$. Hence, we obtain $\mathcal{E}(T)$, for $\mu_p = 0$, as follow,

$$\mathcal{E}(T) = \frac{e_0(2N - e_0)}{\sigma_p^2} \tag{6.64}$$

We combine Eq. (6.62) and Eq. (6.64) together and have

$$\mathcal{E}(T_p) = \begin{cases} -\frac{e_0}{\mu_p} + \frac{\sigma_p^2 \exp(\frac{2\mu_p N}{\sigma^2})}{2\mu_p^2}[1 - \exp(\frac{-2\mu_p e_0}{\sigma_p^2})], & for\, \mu_p \neq 0 \\ \frac{e_0(2N-e_0)}{\sigma_p^2}, & for\, \mu_p = 0 \end{cases} \tag{6.65}$$

□

6.1.3.2 Duration of the operational phase with exponential residual time waiting

In the above lemma, we have considered an instantaneous reflecting barrier as the boundary condition at $e = N$. In this case, when the residual energy changing process reaches the reflect point $e = N$, it jumps back immediately to a random point $e < N$. But this seems to be an underestimation of the actual process where the system remains in the state $e = N$ until servicing the currently incoming packet with additional charges. We follow Kimura *et al.* [262] and consider, for the special case of exponential service rate, the last arriving charge $e = N$ waits long enough for the currently serviced charge to finish in the queue. In this case, the waiting time of the charge is equal to the stationary residual life of the currently serviced traffic packet, that is equal to $\frac{\mathcal{E}[(\text{service time})^2]}{2\mathcal{E}[\text{service time}]} = \frac{\mu_b^2\sigma_b^2+1}{2\mu_b}$. Kimura *et al.* [262] showed that the inclusion of this type of reflecting barriers is equivalent to changing the location of the reflecting barrier from $e = N$ to $e = N + \Gamma$, in order to compensate for the delay before the return back to a point $e < N$ where

$$\Gamma = \frac{\mu_b^2\sigma_b^2 + 1}{4} \tag{6.66}$$

Lemma 6.8. *Consider a wireless node with a battery with capacity N that is charged with mean $1/\mu_a$ and variance σ_a^2 that started with an initial capacity $E(0) = e_0$ and operated until depletion and assume that the battery discharges a random amount of energy, immediately after it reaches the full capacity. If the discharge rate follows an exponential distribution with mean $1/\mu_b$ and variance σ_b^2, then the node's operational time, $\tilde{T}_p$, has a distribution $g_p(t)$ with a mean $\mathcal{E}(\tilde{T}_p)$ where*

$$\mathcal{E}(\tilde{T}_p) = \begin{cases} -\frac{e_0+\Gamma}{\mu_p} + \frac{\sigma_p^2\left[\exp\left(\frac{2\mu_p\Gamma}{\sigma_p^2}\right) - \exp(\frac{2\mu_p e_0}{\sigma_p^2})\right]}{2\mu_p^2 \exp(-\frac{2\mu_p N}{\sigma_p^2})}, & for\, \mu_p \neq 0 \\ \frac{(e_0+\Gamma)(2N-e_0+\Gamma)}{\sigma_p^2}, & for\, \mu_p = 0 \end{cases} \tag{6.67}$$

where μ_p and σ_p^2 are obtained by (6.1) *and* (6.2) *from Lemma 6.1.*

Proof. The proof of the lemma is similar to the pervious one but with the modified boundary conditions that resulted from moving the barrier from N to $N + \Gamma$. The new boundary conditions become:

$$\begin{cases} m_n(0) & = 0 \\ \frac{dm_n}{de_0} \mid_{e_0=\tilde{N}} & = 0 \end{cases} \tag{6.68}$$

Now, applying the second boundary condition to Eq. (6.59), we have

$$B' = -\frac{\sigma_p^2}{2\mu_p^2} \exp[\frac{2b(\tilde{N})}{\sigma_p^2}] \tag{6.69}$$

Substituting the above equation into Eq. (6.59) and based on the boundary condition $m_n(0) = 0$, we have

$$A' = \frac{\sigma_p^2}{2\mu_p^2} \exp[\frac{2b(\tilde{N})}{\sigma_p^2}] \tag{6.70}$$

Then, $\mathcal{E}(\tilde{T}_p)$ for $\mu_p \neq 0$ is given by

$$\mathcal{E}(\tilde{T}_p) = -\frac{e_0 + \Gamma}{\mu_p} + \frac{\sigma_p^2 \exp(\frac{2\mu_p N}{\sigma_p^2})}{2\mu_p^2}[\exp(\frac{2\mu_p \Gamma}{\sigma_p^2}) - exp(\frac{2\mu_p e_0}{\sigma_p^2})] \tag{6.71}$$

When $\mu_p = 0$, based on Eq. (6.63) and the modified boundary conditions, we have $C' = \frac{2(N+\Gamma)}{\sigma_p^2}$ and $D' = 0$. Hence, for $\mu_p = 0$, $\mathcal{E}(\tilde{T}_p)$ is given by

$$\mathcal{E}(\tilde{T}_p) = \frac{(e_0 + \Gamma)(2N - e_0 + \Gamma)}{\sigma_p^2} \tag{6.72}$$

Now, the mean time of the first passage time $\mathcal{E}(\tilde{T}_p)$ with modified boundary is given by,

$$E(\tilde{T}_p) = \begin{cases} -\frac{e_0+\Gamma}{\mu_p} + \frac{\sigma_p^2[exp(\frac{2\mu_p \Gamma}{\sigma_p^2}) - exp(\frac{2\mu_p e_0}{\sigma_p^2})]}{2\mu_p^2 \exp(-\frac{2\mu_p N}{\sigma_p^2})}, & for\, \mu \neq 0 \\ \frac{(e_0+\Gamma)(2N-e_0+\Gamma)}{\sigma_p^2}, & for\, \mu_p = 0 \end{cases} \tag{6.73}$$

□

Similar to the results obtained for the case of the infinite battery, whenever the recharge process and the mean value of the departure process are exogenous parameters, the only parameter that can be adjusted to increase the mean of $\tilde{T}_p$ is the variance σ_b^2 of the departure process.

6.2 Proposed Energy Efficient Packet Scheduling

Theoretical results obtained in the pervious section characterized the dependency of the battery depletion probability and the duration of the operational phase on the mean and variance of the charge and discharge distributions and the threshold e_0. Clearly, μ_a and σ_a^2 are exogenous parameters and depend on the nature of the energy source and the environment. On the other hand, although the recharge threshold can be adjusted by the network provider or the battery manufacture, it is usually adjusted during deployment and my not be calibrated frequently. Finally, the mean of the discharge process for the wireless node's battery is closely tied to the mean of the traffic transmission. However, decreasing this mean will result in a poor quality of the serviced traffic. Hence, we focus our attention on controlling the variance of energy discharge process. As demonstrated by the results of the previous section and as will be shown in the performance evaluation section, decreasing σ_b^2 will result in an exponential decrease in the depletion probability and a similar increase in the duration of the operational phase. More precisely, this section proposes two novel packet scheduling schemes to manage both data and energy buffers in order to minimize the energy discharge variance. The objective of the proposed schemes is to prolong the battery lifetime while achieving the specified quality of service (QoS) requirements for each data flow served by the wireless node.

6.2.1 Optimal Energy Efficient Offline Scheduling

We first develop an offline scheduling scheme that assumes full knowledge about the incoming traffic and hence the needed energy to transmit this traffic. In this scheme, we obtain an optimal scheduling policy that dictates the amount of energy to be consumed for a number of time slots where information regarding expected traffic transmission demand, and hence, the estimation of the needed departure energy is known in advance. Similar to the assumptions adopted in [242, 239, 241, 263, 27], we assume that starting from any point in time t, the time in the system is well slotted into equal periods that start at times $t, t+1, t+2, \cdots$. We denote by $B(t), B(t+1), B(t+2), \cdots$ the required energy units for transmitting data as the packets arrive to the node at times $t, t+1, t+2, \cdots$. Moreover, for simplicity, we assume that all arriving packets share a common transmission deadline of t_{max} time slots, i.e., if a packet arrives at t it must be transmitted before $t + t_{max}$, such that μ_b is the expected discharge rate in the battery to serve $B(t), \cdots, B(t + t_{max} - 1)$. The main premise of the proposed scheduling technique is to redistribute the energy $B(t)$, at each time point t to be used over the t_{max} time slots

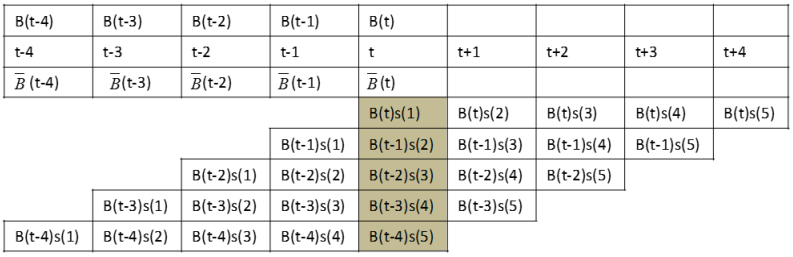

Figure 6.2: Illustration of calculation of $\bar{B}(t)$

$t, t+1, \cdots, t_{max}-1$, rather than on the time slot that starts at t. The objective of this redistribution is to reduce the variance in the discharge rate while keeping the mean μ_b unchanged. This in turn will maintain the required service guarantees for the transmitted traffic.

Define a discrete scheduling function $S(t_s, t) \in [0, 1]$ as the fraction of, $B(t_s)$, the charges originally planned for transmission at time t_s but reassigned to the time slot $[t, t+1)$, $t_s \leq t < t_s + t_{max} - 1$. Hence, the total energy assigned to slot $[t, t+1)$ according to the new schedule becomes that of the sum of all energy that arrives during previous $t_{max} - 1$ time slots and assigned to the slot $[t, t+1)$, which is shown in Fig. 6.2. The new amount of charges used to send data at time t, $\bar{B}(t)$, can be calculated as follows

$$\bar{B}(t) = \sum_{t_s=t-t_{max}+1}^{t} B(t_s) S(t_s, t) \tag{6.74}$$

The above equation shows that $\bar{B}(t)$ is a linear combination of input $B(t)$. If we define the scheduling function $S(t_s, t)$ to be only dependent on the difference $t - t_s$, and not on the absolute time t, then, the output $\bar{B}(t)$ becomes a sum of weighted shifted impulses $S(t)\delta[t - t_s]$ of its input. This system is a linear-time-invariant (LTI) one [264]. For such systems, shifting the input on the time axis leads to an equivalent shifting of the output along the time axis, with no other changes. Based on the superposition property of a linear system, the response of the system to the input $B(t)$ in Eq. (6.74) is simply the weighted linear combination of these basic responses and we can characterize it by its impulse response. Let $\mathbf{b}(t)'=[B(t), \cdots, B(t + t_{max} - 1)]'$ where $'$ is the vector transpose operator and $\mathbf{s} = [s_1, s_2, \cdots, s_{t_{max}}]$, the time invariant schedule, then the

impulse response of the new time invariant system becomes:

$$\begin{aligned}
\bar{B}(t) &= \mathbf{b}(t) * \mathbf{s} \\
&= \begin{bmatrix} s_1 & s_2 & \cdots & s_{t_{max}} \end{bmatrix} \begin{bmatrix} B(t) \\ B(t-1) \\ \vdots \\ B(t-t_{max}+1) \end{bmatrix} \\
&= \mathbf{s}'\mathbf{B}(t) \qquad (6.75)
\end{aligned}$$

We again stress that $\bar{B}(t)$ is the total energy assigned to the time slot $[t, t+1)$. The variance in the energy depasturing from the battery is given by

$$\begin{aligned}
\sigma_b^2 &= \mathcal{E}\left[(\bar{B}(t) - \mu_b)^2\right] \qquad (6.76) \\
&= \mathcal{E}\left[\bar{B}(t)^2\right] - \mu_b^2 \\
&= \mathcal{E}\left[\mathbf{s}'\mathbf{b}(t)\mathbf{s}'\mathbf{b}(t)\right] - \mu_b^2 \\
&= \mathcal{E}\left[\mathbf{s}'\mathbf{b}(t)\mathbf{b}(t)'\mathbf{s}\right] - \mu_b^2 \\
&= \mathbf{s}'\mathbf{R}\mathbf{s} - \mu_b^2 \qquad (6.77)
\end{aligned}$$

Where $\mathbf{R} = \mathcal{E}[\mathbf{b}(t)\mathbf{b}(t)']$ is the lag t_{max} autocorrelation matrix of originally estimated departure energy process. If we assume μ_b is exogenous, then our objective is to minimize $\mathbf{s}'\mathbf{R}\mathbf{s}$. In this case, we can use *Lagrange multiplier method* to solve this optimization problem. The Lagrange gain is given by

$$L(\mathbf{s}, \lambda) = \mathbf{s}'\mathbf{R}\mathbf{s} + \lambda(\mathbf{s} \cdot \mathbf{u} - 1) \qquad (6.78)$$

Where $\mathbf{u}$ is a unitary vector with t_{max} components and $\mathbf{s} \cdot \mathbf{u} = 1$ is the *delay constraint*, since the package must be sent during the time interval $[t_s, t_s + t_{max})$. The gradient of L is $2\mathbf{R}\mathbf{s} + \lambda\mathbf{u}'$ with a solution of

$$\mathbf{s}^\star = -\frac{\lambda^\star \mathbf{R}^{-1}\mathbf{u}'}{2} \qquad (6.79)$$

We then use the constraint to find the value of Λ and substitute its value in the above equation to get the optimal value:

$$\mathbf{s}^* = \frac{\mathbf{R}^{-1}\mathbf{u}'}{\mathbf{u}\mathbf{R}^{-1}\mathbf{u}'} \qquad (6.80)$$

The above solution shows the impact of the autocorrelation of $B(t)$ on the scheduling. This autocorrelation can be measured according to the history of departure energy process. Whenever the incoming traffic is *self-similar* [265, 266], the autocorrelation matrix

becomes independent of the lag t_{max}. In this case, one can find a fixed energy redistribution vector $\mathbf{s}^*$ using traffic estimates observed at a single time epoch. On the other hand, if the traffic is asymptotically self-similar, then the same feature is reserved for large t_{max}. In this case, t_{max} can be increased gradually to obtain a better estimate of $\mathbf{s}^*$.

Once we obtain $\mathbf{s}^*$, we can calculate the new optimal energy $\bar{B^*}(t)$=$\mathbf{s}^{*\prime}\mathbf{B}(t)$. At each time period $[t, t+1)$, the battery queue discharges $\bar{B^*}(t)$ at a rate μ_b and with the new minimum variance σ_B^{2*}=$\mathbf{s}^{*\prime}\mathbf{R}\mathbf{s} - \mu_b^2$. The discharged energy units are then used to transmit the traffic stored in the data buffer. This leads to the required optimal battery life and duration of the node operational phase for a given schedule length.

Next, we develop another online scheme that makes no assumptions about the knowledge of the incoming traffic or its deadline constraints.

6.2.2 Online QoS Aware Scheduling

We consider the traffic flows with packets stored in the buffer at time t and develop a per packet schedule during the period $[t, t+\Delta t]$. Here, Δt is the online scheduling period and is chosen by the provider. First, for each packet in the buffer to be transmitted, the proposed scheme calculates a priority value according to its QoS requirements. In this chapter, we focus on the *delay* as the main QoS requirement, but additional parameters can be easily incorporated. At each period $[t, t+\Delta t]$, we have a number of flows stored in the buffer for transmission. Let ζ_i be the observed average throughput of stream i. Also, let b_{ij} be the amount of energy needed to transmit the packet j at t. Then, we can calculate a transmission priority value ρ_{ij} for each packet j belonging to a traffic flow i serviced during the scheduling period such that

$$\begin{aligned}
\rho_{ij} &= \alpha^m \frac{t_{max}^{ij} - t}{t_{max}^{ij}} + (1-\alpha)^m \Big[\frac{P_{max}}{P_i}(1 - 2^{-\beta}) \\
&\quad +2^{-\beta}\Big(\frac{\sum_j b_{ij}(t)}{\sum_i \sum_j b_{ij}(t)} - \frac{\zeta_i}{\sum_i \zeta_i}\Big)\Big] \qquad (6.81) \\
\alpha &= \frac{E(t)}{N} \\
\beta &= \begin{cases} 1, & \alpha = 1 \\ \frac{E(t)}{N-E(t)} = \frac{\alpha}{1-\alpha}, & \alpha \neq 1 \end{cases}
\end{aligned}$$

As before, $E(t)$ is the residual energy in the battery at t and N is the maximum capacity of the battery. The parameters α and β are two weight parameters that reflect the criticality of the battery's depletion status. The parameter $m \in (0, 1]$ is a control parameter that can be adjusted dynamically to control the behaviour of the scheduler according to the provider's objectives with respect to reducing the experienced delay and servicing more flows with smaller transmission power requirements.

The priority ρ_{ij} has two main components; The term evaluates the criticality of the packet delay. A packet which is closer to its deadline delay t^{ij}_{max} receives a higher priority.

The second term in calculating ρ_{ij} reflects the effects of the energy needed for transmitting the packet on the depletion of the battery. This is realized by the weighted sums of the ratio of the needed transmission power for flow i, P_i to maximum power P_{max} of the wireless node and the data transmission requirements for i relative to other flows. Note here, that we model the power values P_i and P_{max} as the amount of energy charges needed and can be used by the node for transmission at a time, respectively.

We note that we use the dynamic weight parameter α to adjust the weight for each component according to the current status of the battery. When the battery's residual energy is small, the energy component has larger weight. The system pays more attention to saving power. The system favors the transmission of packets with lower transmission power requirements in order to prolong the battery life time.

Now, we assume that all incoming data in the buffer will be stored in a decreasing order according to ρ_{ij}. We use a vector $\mathbf{P}(t)$ to represent the energy needed for transmitting the ordered packets in buffer at time t. We let $\mathbf{t}_{max}(t)$ be the delay vector for all the packets such that the elements in $\mathbf{t}_{max}(t)$ corresponds to the packets in $\mathbf{P}(t)$. Then, we define a new *one-dimensional periodical scheduling vector* $\theta(t)$ and elements in $\theta(t)$ can only be 0 or 1, to reflect whether the corresponding packet in the vector $\mathbf{P}(t)$ will be transmitted or remain in the buffer during $[t, t + 1)$.

Our objective now is to find the vector $\theta(t)$ that minimizes the difference between the regulated energy consumption during a period Δt, $\mu_p \Delta t$, and the actual transmission energy used $\theta(t)'\mathbf{P}$ during that period, i.e, minimizing $\mu_p \Delta t$- $\theta(t)'\mathbf{P}$. This schedule must ensure that the requested QoS is not violated for each packet. Hence, it must satisfy that the the remaining time before the deadline $t^{ij}_{max} - t$, for every packet that will not be transmitted $(1 - \theta_{ij})$, is larger than two scheduling periods. This constraint accounts for the probability of not transmitting the packet during this scheduling period and having to wait until the end of the next scheduling period, each with length Δt. In other words, the scheduling vector $\theta(t)$ must satisfy the relation: $(1 - \theta_{ij})(t^{ij}_{max} - t) \geq 2\Delta t$. The

Algorithm: The Online packet scheduling Scheme

1. Update the mean value of the energy departure process, μ_b, based on previous observations.
2. Calculate ρ_{ij} for all packets j of all flows i.
3. Order all elements in the buffer according to ρ_{ij} in a decreasing order.
4. Calculate $\mathbf{P}(t)$ and $\mathbf{t}_{max}$ for the ordered packets and set all the elements in $\theta(t)$ to 0.
5. **while** $(\theta'(t)\mathbf{P}(t) \leq \mu_b \times \Delta t)$ and the buffer has more packets **do**
6. Get the next packet j for flow i from the buffer.
7. **if**$(t_{max}^{ij} - t) < 2\Delta t$
8. **then** $\theta_{ij}(t) = 1$
9. **end if**
10. **end while**
11. **while** $(\theta'(t)\mathbf{P}(t) \leq \mu_b \times \Delta t)$ and buffer has more packets **do**
12. Get a new packet j for flow i from the buffer such that $\theta ij(t) \neq 1$ and mark as visited.
13. Set $\theta_{ij}(t) = 1$
14. **end while**

Figure 6.3: The proposed online scheme

following heuristics-based algorithm provide a pseudo code for the developed scheme.

6.3 Performance Evaluation

6.3.1 Verification of Theoretical Results

We first verify the obtained theoretical results, we use MATLAB to simulate a single-input single-output G/G/1/N buffer. We adopt parameters $\mu_a = 2.3$, $\sigma_a^2 = 1.21$, $\mu_b = 2.33$ and $N = 5$ which are the same parameters used in [234], and change σ_b^2 from 5.44 to 0.5. We set the simulation time to 1500 time units. We repeat the simulation 200 times for each plotted point. Fig. 6.4 shows that $\mathcal{E}(T_p)$ decreases exponentially with the linear increase of σ_b^2 for the two theoretical values against the simulated buffer. It

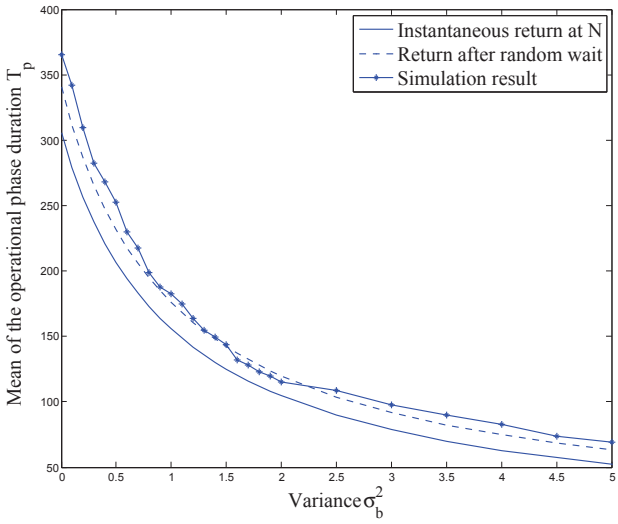

Figure 6.4: Comparison of simulation and theoretical results

also shows that the diffusion process with the random return, obtained by Lemma 6.8 is almost identical to the simulation results and has a much smaller error difference to the obtained simulation results as compared to the diffusion process with the immediate return. The small error can be attributed to the limited simulation period and limited number of simulation times.

6.3.2 Effects of σ_p^2

Next, we demonstrate the significant effects that σ_p^2 has on the behaviour of the battery's residual energy. We first plot the probability of depletion for the case of the infinite energy buffer (Eq. (6.36)). As shown in Fig. 6.5, p_0 increases exponentially as we increase σ_p^2 linearly.

For the case of the finite buffer, as shown in Fig. 6.6, the average residual energy during the operational phase drops exponentially as σ_p^2 increases.

6.3.3 Simulation Setup

To evaluate the performance of the proposed scheduler, we consider a wireless network and focus on a single node connected with n destination nodes. These nodes can be represented by a geometric random graph $G(\mathcal{X}_n, f)$. Here, $\mathcal{X}_n=\{X_1, \cdots, X_n\}$, denotes the set of the random location points of the nodes on a two-dimensional area A. We

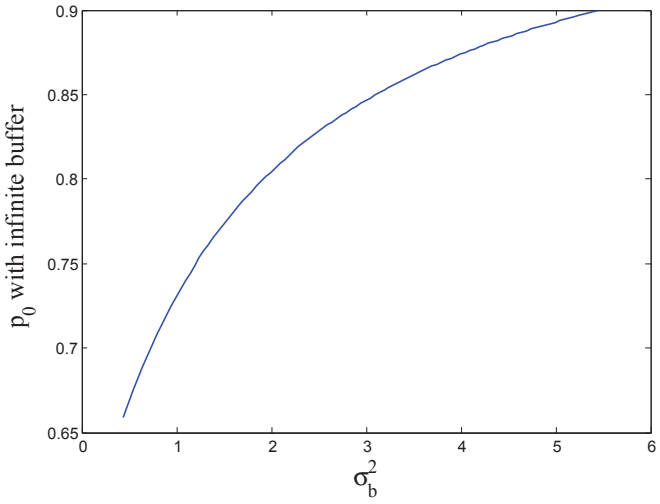

Figure 6.5: A plot of p_0 with an infinite buffer and $e_0 = 5$, $\mu_a = 2.3$, $\sigma_a^2 = 1.21$, $\mu_b = 2.33$

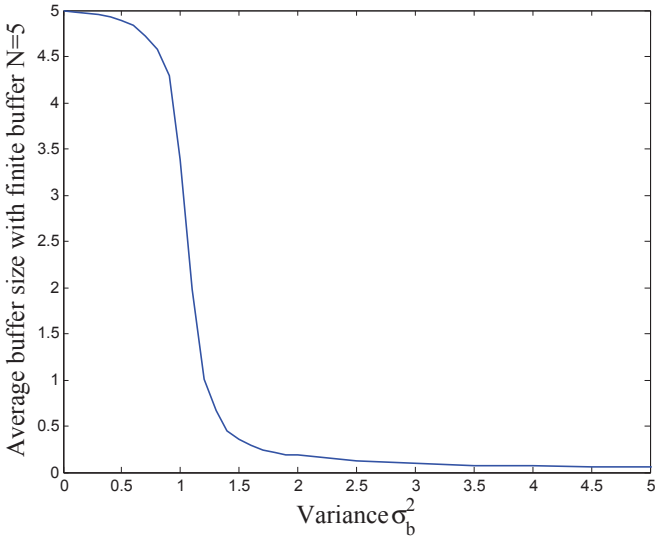

Figure 6.6: Average battery residual energy with $N = 5$, $\mu_a = 2.3$, $\sigma_a^2 = 1.21$, $\mu_b = 2.33$

also assume that the locations $X_1, X_2, \cdots, X_n$ are randomly distributed in A, according to f a random distribution which is used to distribute the nodes in the given area. The simulations are conducted to analyze the energy buffer and evaluate the performance of the proposed scheduling schemes, based on a discrete time event-driven simulator coded in C++.

Let P_t be the transmission power used by the nodes. Also, let the ambient noise power level be N_0. Assuming that the nodes' interference is represented through the physical interference model, then the required transmission power from source to any destination node in the network based on the distance l, is given by:

$$P_t = l^{\alpha} N_0 \delta_{min} \tag{6.82}$$

A minimum signal-to-interference ratio (SIR) δ_{min} is necessary for successful receptions, and signal power decays with distance as $l^{\frac{1}{\alpha}}$. We also assume that $\alpha > 2$, which is a common model outside the small neighbourhood of the transmitter.

We adopt the DiffServ service management discipline [7] and employ three classes of services (CoS): CoS1, CoS2 and CoS3. CoS1 to represent low-loss, delay-sensitive expedited forwarding (EF) services, which typically provide for CBR VoIP data. CoS2 data represents Assured Forwarding (AF) services. It is suitable for non-delay sensitive, bandwidth guaranteed VBR video/data. Finally, CoS3 represents Best Effort (BE) services, which requires no bandwidth commitment from the system and is suitable for WWW data. The data rate of CBR CoS1 data is 64Kbps with 120bytes packet based on the G.711 codec [248]. We use an ON-OFF source to generate traffic for each of CoS2 and CoS3. The two sources have identical parameters. For each source, the ON and OFF (silent) intervals are drawn according to a Pareto distribution, which has been widely used to model self-similar traffic in the Internet [36]. The Pareto distribution is a heavy-tailed distribution characterized by a shape parameter and a location parameter. This distribution has a finite mean and infinite variance when the shape parameter is chosen in the interval $[1, 11]$. We set the shape parameter for the ON and OFF intervals to 1.4 and 1.2, respectively [11]. We also set the buffer size of each routers to 5Mbytes. The buffer is shared by all the CoSs queues. One node will be randomly selected as the intermediate node. All the other nodes will send data through this selected intermediate node to their destinations. Because the battery size cannot be infinite in reality, in our simulation, we only consider the energy buffer with finite size. The battery size of the selected node is set to be $1J$. The required data rate for each node is randomly picked up from $[50Mbps, 200Mbps]$. Also, the data flows oriented from each node consist of all

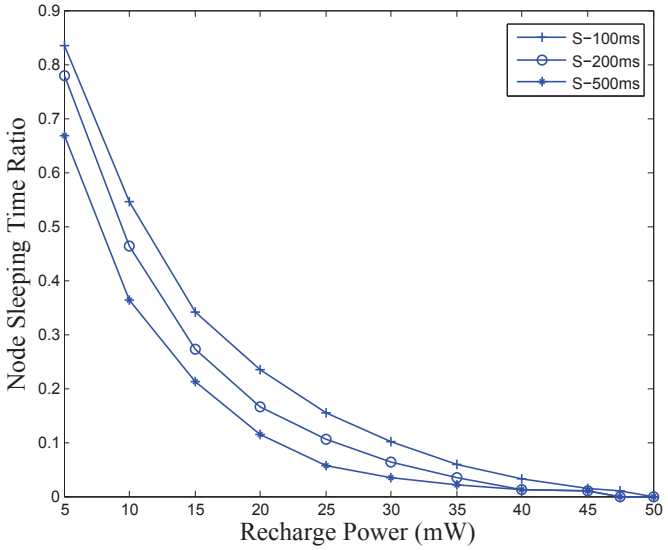

Figure 6.7: The node sleeping time ratio with different lengths of **s**

three CoSs. We assume that CoS3 traffic load is twice as that of CoS2 traffic. Based on these assumptions, the aggregate data stream from each node can follow the long-term mean value with short-term traffic bursts. We employ the node ratio between the node sleeping time to the experiment duration, the packet drop ratio and the node throughput as our main performance parameters.

6.3.4 Simulation Results

6.3.4.1 Effects of the size of s∗:

Next, we analyze the effect of the length of the vector **s** on the performance of the offline scheme. We evaluated the scheme's performance while setting the lag t_{max} and hence the vector length to take the values 10, 20 and 50. Figs 6.7, 6.8 and Fig. 6.9 plot the obtained sleeping time ratio, the average throughput and the average packet drop ratio, respectively. As shown in the figures, the increase in the length of the scheduling enhances the performance of the scheme. This is more noticeable when the battery recharge rate is small. The reason for this phenomenon is that with larger **s**, the proposed scheme can calculate a more accurate autocorrelation of the time series representing the needed energy for transmission. In turn, the obtained energy scheduling vector comes closer to optimally minimizing the variance of the departure energy. On the other hand, the recharge rate increases, the probability of battery depletion becomes small and hence the

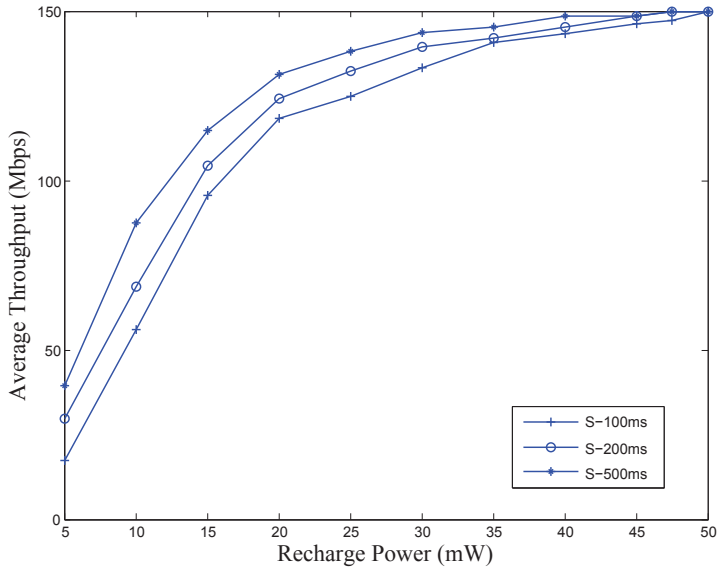

Figure 6.8: Illustration of average throughput with different size of **S**

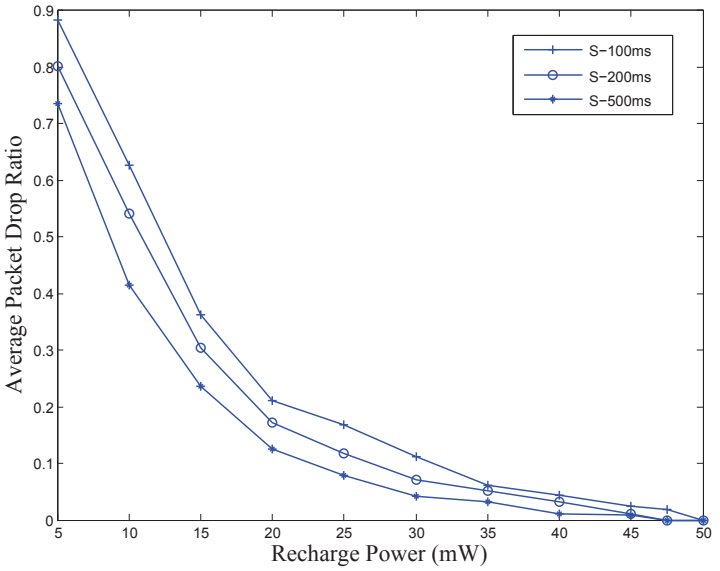

Figure 6.9: The comparison of average packet drop ratio with different size of **S**

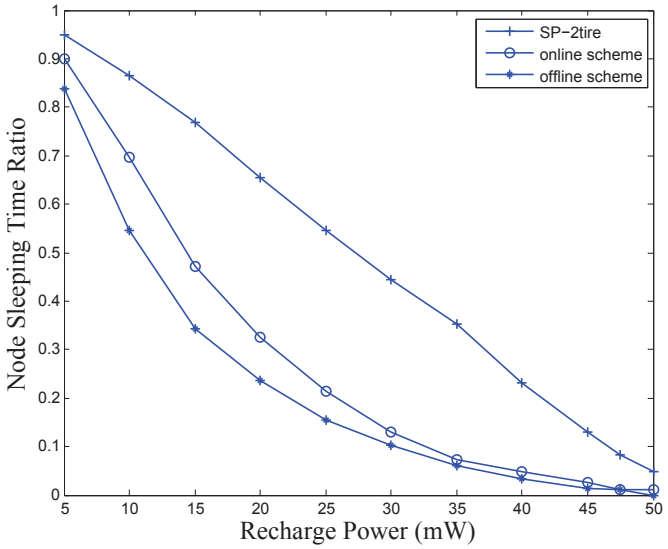

Figure 6.10: The comparison of node sleeping time ratio

need for the minimization of the variance becomes less critical.

6.3.4.2 Comparison between the two proposed schemes

Next, we compare the performance of the proposed schemes against the 2-tire Strict Priority (SP-2tire) scheme. In the latter scheme, the incoming traffic is managed by a weighted random early Detection (WRED) scheme [267] and then sent based on the strict priority [7]. For the online scheduling scheme, we set the size of energy scheduling vector $\mathbf{s}$ to be 10 time slots and the length of each time slot to $10ms$.

From Fig. 6.10, we can see that the proposed scheduling scheme achieves a much better performance compared to the SP 2-tire scheme. Because the SP-2tire scheme sends data only based on the priority of the data. Even if the residual energy is low, the SP 2-tire scheme still sends data with high priority no matter how large the transmission power required by the data packet is. This results in a significant reduction in the battery lifetime. On the other hand, the proposed scheme overcomes this limitation by favoring flows with smaller transmission requirements, where the usage of the priority ρ_{ij} adapts the choices of the packets to be transmitted based on the residual capacity. The system favors the transmission of packets with lower transmission energy requirements in order to save energy until the battery is recharged. Since the offline scheme has the knowledge of the departure process. We can see that the offline scheme achieved the best performance. Because the size of $\mathbf{S}$ is limited. The accuracy of the calculated

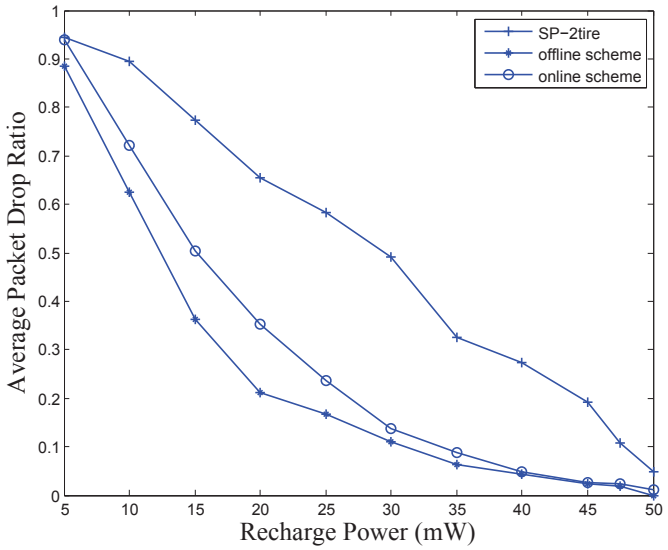

Figure 6.11: Illustration of average packet drop ratio

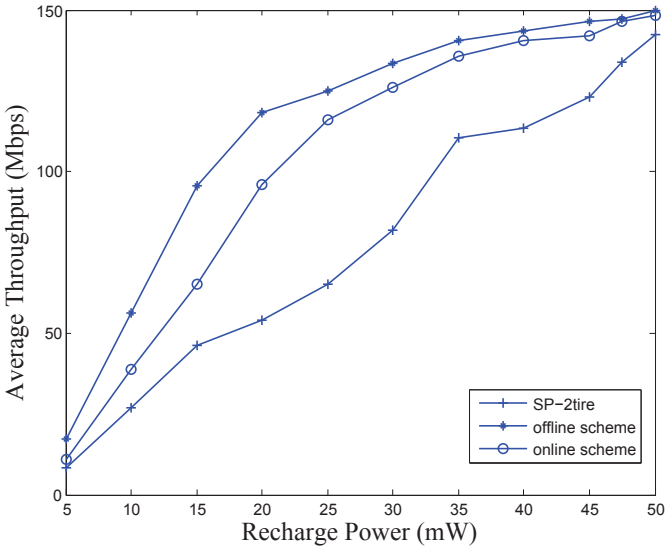

Figure 6.12: Illustration of average throughput

autocorrelation is reduced. Fig. 6.11 and Fig. 6.12 illustrate the average packet drop ratio and average throughput respectively. We can see that online scheme achieved much better performance than the SP-2tire scheme.

6.4 Conclusion

This chapter addressed the problem of battery depletion for green wireless mesh networks. A theoretical framework to analyze the behaviour of the residual energy of a wireless router's battery given two scenarios was first developed; the first scenario assumed that the battery has an infinitely large capacity such that it can store all incoming charges. In the second, we considered a finite capacity battery. We modeled the battery's residual energy using a general queuing model with no assumptions on the distribution of the charging and discharging process. Diffusion approximation based modelling was employed to derive closed formulations for the relationship between the variance of the discharge rate due to transmission and the duration of the battery lifetime. Based on the theoretical results, an offline and an online QoS aware energy efficient scheduling scheme was developed to prolong the battery's lifetime while satisfying the required QoS of the serviced flows. Simulation results demonstrated the significant reduction in the node sleep time ratio while increasing the node throughput.

Chapter 7

Conclusions and Planned Work

In this chapter, we briefly summarize our work and explain our planned work. We believe that our work shown in this dissertation is helpful to the network management and deployment.

7.1 The Dissertation Conclusions

Since most traffic converges to gateways, the links connected to a gateway always have heavier loads. When not enough transmission resources (i.e., channels and time slots) are dedicated to these critical links, congestion is created and bottlenecks are formed. On the other hand, congestion is also created in links far away from the gateway when too many resources are dedicated to links closed to the gateway. Hence, balancing the allocated resources in the system is an important issue that must be carefully considered. So we proposed a joint routing, channel assignment and traffic scheduling algorithm for multiple channel multiple-radio wireless mesh networks to maximize the gateway throughput while supporting the QoS differentiation. Transmission rate adaptation is used in our routing scheme to find a minimum delay path from each router to the gateway. We developed a solution in which the centralized weight aware link scheduling and channel assignment algorithm focuses on maximizing the gateway throughput while minimizing the interference. The distributed traffic scheduling algorithm improves the flexibility and robustness of the system. Simulation results show that our algorithm achieves a stable performance under different system conditions. The results also show that our proposed algorithm decreases the packet loss ratio and packet delay in each class-of-service under different system conditions.

Then, we studied the topology and resilience of MRMC WMNs in the presence of node failures. We first analysed the critical node density, which is the minimum node density that whole area can be covered by a MRMC WMN. Then we defined two parameters, node failure probability p and empty hexagon probability q_f to characterize the occurrence of random node failures and the changing of system connectivity, based on the given nodes' geometric distribution f. Then we derived the upper bounds on the node failure probabilities that could maintain full network connectivity. We also found a lower bound for the system losing connectivity. Also, we formulated the relation between these bounds and the nodes' geometric distributions and density. We also validated our theoretical results by simulations.

Depend on the theoretical results about the survivability of wireless mesh network, we then proposed a simple backup scheme to maximize the network throughput after losing some of working nodes. Transmission rate adaptation is used in our backup scheme to satisfy the QoS requirement of each data flow to the destination. We developed a solution in which the local traffic load distribution scheme focuses on maximizing the system throughput while minimizing the probability of congestion generation. The results also showed that our proposed backup scheme has a much larger system throughput than the existing algorithm.

As energy saving and environmental protection become global demands and inevitable trends, wireless researchers and engineers need to shift their focus to energy-efficiency-oriented design, that is, green communication. We designed an optimal energy efficient packet scheduling scheme for MRMC WMNs. We tried to maximize the battery life of the wireless node in order to sustain the network performance. Firstly, we theoretically analysed the residual energy changing process in the battery with an infinite and finite capacity cases, respectively. Two different G/G/1/∞ and G/G/1/N queueing models are adopted. Based on the analysis results, we found that the node battery life time can be maximized by minimizing the variance of the energy departure process. Then, we proposed both offline and online QoS aware energy efficient scheduling scheme to achieve the energy efficiency while achieving the required QoS. Our simulation results show that the node battery life time performance can be significantly improved by proposed scheduling scheme.

My future plans include exploring new areas for research in wireless networks, and extending my research in capacity enhancement, network reliability, and green communications. I intend to balance the mix of research problems between the ones that are futuristic in nature and those that are worthy of immediate applications in the industry.

I am excited at the prospect of contributing my knowledge and learning new.

Bibliography

[1] W. Si, S. Selvakennedy, and A. Y. Zomaya. An overview of channel assignment methods for multi-radio multi-channel wireless mesh networks. *Journal of Parallel and Distributed Computing (JPDC), Elsevier*, 70:505 – 524, 2010.

[2] Sergey V. Buldyrev, Roni Parshani, Gerald Paul, H. Eugene Stanley, and Shlomo Havlin. Catastrophic cascade of failures in interdependent networks. *NATURE*, 464:1025 – 1028, APRIL 2010.

[3] Reka Albert, Hawoong Jeong, and Albert-Laszlo Barabasi. Error and attack tolerance of complex networks. *NATURE*, 406:378 – 382, JULY 2000.

[4] Parth H. Pathak and Rudra Dutta. A survey of network design problems and joint design approaches in wireless mesh networks. *IEEE COMMUNICATIONS SURVEYS & TUTORIALS*, 13(3):396 – 428, THIRD QUARTER 2011.

[5] Ian F. Akyildiz, Xudong Wang, and Weilin Wang. Wireless mesh networks: a survey. *Computer Networks*, 47(4):445 – 487, MARCH 2005.

[6] Ashish Raniwala and Tzi Cker Chiueh. Architecture and algorithms for an ieee 802.11-based multi-channel wireless mesh network. *Proceedings IEEE 24th Annual Joint Conference of the IEEE Computer and Communications Societies, INFOCOM*, 3:2223 – 2234, 2005.

[7] William Stallings. *Data and Computer Communications*. Prentice Hall, 8th edition, 2006.

[8] Mansoor Alicherry, Randeep Bhatia, and Li Erran Li. Joint channel assignment and routing for throughput optimization in multiradio wireless mesh networks. *IEEE JOURNAL ON SELECTED AREAS IN COMMUNICATIONS*, 24(11):1960 – 1971, NOVEMBER 2006.

[9] Rongsheng Huang, Sunmyeng Kim, Chi Zhang, and Yuguang Fang. Exploiting the capacity of multichannel multiradio wireless mesh networks. *IEEE TRANSACTIONS ON VEHICULAR TECHNOLOGY*, 58(9):5037 –5047, NOVEMBER 2009.

[10] A. Hamed Mohsenian-Rad and Vincent W. S. Wong. Joint logical topology design, interface assignment, channel allocation, and routing for multi-channel wireless mesh networks. *IEEE TRANSACTIONS ON WIRELESS COMMUNICATIONS*, 6(12):4432 – 4440, DECEMBER 2007.

[11] Nessrine Chakchouk and Bechir Hamdaoui. Traffic and interference aware scheduling for multiradio multichannel wireless mesh networks. *IEEE TRANSACTIONS ON VEHICULAR TECHNOLOGY*, 60(2):555 – 565, FEBRUARY 2011.

[12] Anand Prabhu Subramanian, Himanshu Gupta, Samir R. Das, and Jing Cao. Minimum interference channel assignment in multiradio wireless mesh networks. *IEEE TRANSACTIONS ON MOBILE COMPUTING*, 7(12):1459 – 1473, DECEMBER 2008.

[13] Peng Sun. Dynamic resource allocation algorithms for long term evolution (lte) wireless broadband networks. Master thesis, Lakehead University, Thunder Bay, Ontario, Canada, SEPTEMBER 2010.

[14] Jonathan Wellons and Yuan Xue. Towards robust and efficient routing in multi-radio, multi-channel wireless mesh networks. *Proceedings IEEE INFOCOM*, pages 91 – 95, Shanghai, APRIL 2011.

[15] Song Han, Xiuming Zhu, Aloysius K. Mok, Deji Chen, and Mark Nixon. Reliable and real-time communication in industrial wireless mesh networks. *17th IEEE Real-Time and Embedded Technology and Applications Symposium*, pages 3 – 12, Chicago, IL, APRIL, 2011.

[16] Dong Xiang. Deadlock-free adaptive routing in meshes with fault-tolerance ability based on channel overlapping. *IEEE TRANSACTIONS ON DEPENDABLE AND SECURE COMPUTING*, 8(1), JANUARY-FEBRUARY 2011.

[17] Yue Cao, Zhili Sun, Ning Wang, Haitham Cruickshank, and Naveed Ahmad. A reliable and efficient geographic routing scheme for delay/disruption tolerant net-

works. *IEEE WIRELESS COMMUNICATIONS LETTERS*, 2(6), DECEMBER 2013.

[18] Lijuan Zhang, Wei Xiang, and Xiaohu Tang. An adaptive anti-collision protocol for large-scale rfid tag identification. *IEEE WIRELESS COMMUNICATIONS LETTERS*, to appear, DOI:10.1109/LWC.2014.2359461, 2014.

[19] Ian Dobson, Benjamin A. Carreras, and David E. Newman. A loading-dependent model of probabilistic cascading failure. *Probability in the Engineering and Informational Sciences*, 19(01):15 – 32, JANUARY 2005.

[20] Djohara Benyamina, Abdelhakim Hafid, and Michel Gendreau. Wireless mesh networks design - A survey. *IEEE Communications Surveys and Tutorials*, 14(2):299–310, 2012.

[21] Anfeng Liu, Zhongming Zheng, Chao Zhang, Zhigang Chen, and Xuemin (Sherman) Shen. Secure and energy-efficient disjoint multipath routing for wsns. *IEEE TRANSACTIONS ON VEHICULAR TECHNOLOGY*, 61(7):3255–3265, SEPTEMBER 2012.

[22] Deqiang Chen, Martin Haenggi, and J. Nicholas Laneman. Distributed spectrum-efficient routing algorithms in wireless networks. *IEEE TRANSACTIONS ON WIRELESS COMMUNICATIONS*, 7(12):5297–5305, DECEMBER 2008.

[23] Wenchi Cheng, Xi Zhang, and Hailin Zhang. Joint spectrum and power efficiencies optimization for statistical qos provisionings over siso/mimo wireless networks. *IEEE Journal on Selected Areas in Communications*, 31(5):903–915, MAY 2013.

[24] Sarra Mamechaoui, Sidi Mohammed Senouci, Fedoua Didi, and Guy Pujolle. Energy efficient management for wireless mesh networks with green routers. *MONET*, 20(5):567–582, 2015.

[25] Changqing Luo, Shengyong Guo, Song Guo, Laurence T. Yang, Geyong Min, and Xia Xie. Green communication in energy renewable wireless mesh networks: Routing, rate control, and power allocation. *IEEE Transactions on Parallel and Distributed Systems*, 25(12):3211–3220, 2014.

[26] G.H. Badawy, A.A. Sayegh, and T.D. Todd. Energy provisioning in solar-powered wireless mesh networks. *IEEE Transactions on Vehicular Technology*, 59(8):3859–3871, 2010.

[27] Xiaojing Chen, Wei Ni, Xin Wang, and Yichuang Sun. Provisioning quality-of-service to energy harvesting wireless communications. *IEEE Communications Magazine*, 53(4):102–109, APRIL 2015.

[28] Meng Li, H. Nishiyama, N. Kato, Y. Owada, and K. Hamaguchi. On the energy-efficient of throughput-based scheme using renewable energy for wireless mesh networks in disaster area. *Emerging Topics in Computing, IEEE Transactions on*, 3(3):420–431, Sept 2015.

[29] Tehuang Liu, Wanjiun Liao, and Jeng-Farn Lee. Distributed contention-aware call admission control for ieee 802.11 multi-radio multi-rate multi-channel wireless mesh networks. *Mobile Networks and Applications*, 14(2):134–142, 2009.

[30] Ronghui Hou, King-Shan Lui, Fred Baker, and Jiandong Li. Hop-by-hop routing in wireless mesh networks with bandwidth guarantees. *IEEE TRANSACTIONS ON MOBILE COMPUTING*, 11(2):264 – 277, FEBRUARY 2012.

[31] Peng Sun and Nancy Samaan. A qos aware joint design for wireless mesh networks. *ACM/Springer Wireless Networks*, 20:961 – 973, 2014.

[32] Peng Sun and Nancy Samaan. Random node failures and wireless networks connectivity: Theoretical analysis. *IEEE Wireless Communications Letters*, 4(5):461 – 464, OCTOBER 2015.

[33] Osameh M. Al-Kofahi and Ahmed E. Kamal. Network coding-based protection of many-to-one flow networks. *IEEE Internatonal Conference on Mobile Adhoc and Sensor Systems*, pages 1 – 10, Pisa, OCTOBER 2007.

[34] Peng Sun and Nancy Samaan. Random node failures and wireless networks connectivity: a novel recovery scheme. *IEEE Canadian Conference on Electrical and Computer Engineering (CCECE) 2016, Vancouver, Canada*, MAY 2016.

[35] Peng Sun and Nancy Samaan. Theoretical analysis and an optimal schedule to prolong battery life in green wireless mesh networks nodes. *IEEE Transactions on Networking*, No. TNET-2016-00121, 2016.

[36] Vern Paxson and Sally Floyd. Wide-area traffic: The failure of poisson modeling. *ACM/IEEE TRANSACTIONS ON NETWORKING*, 3(3):226–244, JUNE 1995.

[37] Leonard Kleinrock. *Queueing Systems Volume II: Computer Applications, Chapter 2, pp. 62-87*. Wiley, 1976.

[38] Andrew Brzezinski, Gil Zussman, and Eytan Modiano. Distributed throughput maximization in wireless mesh networks via pre-partitioning. *IEEE/ACM TRANSACTIONS ON NETWORKING*, 16(6):1406–1419, DECEMBER 2008.

[39] Jose Barrameda and Nancy Samaan. Bounds for minimum interference in full multi-interface multi-channel wireless networks. *IEEE TRANSCATIONS ON WIRELESS COMMUNICATIONS*, 10(11):3956–3965, 2011.

[40] Mahesh K. Marina and Samir R. Das. A topology control approach for utilizing multiple channels in multi-radio wireless mesh networks. *The 2nd International Conference on Broadband Networks*, 1:381 – 390, 2005.

[41] Ashish Raniwaha, Kartik Gopalan, and Tzi cker Chiueh. Centralized channel assignment and routing algorithms for multi-channel wireless mesh networks. *ACM SIGMOBILE Mobile Computing and Communications Review*, 8(2):50 – 65, APRIL 2004.

[42] Andrew Brzezinski, Gil Zussman, and Eytan Modiano. Enabling distributed throughput maximization in wireless mesh networks: a partitioning approach. *ACM MobiCom '60*, pages 26 – 37, Los Angeles, CA, USA, 2006.

[43] Pradeep Kyasanur and Nitin H. Vaidya. Routing and link-layer protocols for multi-channel multi-interface ad hoc wireless networks. *ACM SIGMOBILE Mobile Computing and Communications Review*, 10(1):31 – 43, 2006.

[44] Jian Tang, Guoliang Xue, and Weiyi Zhang. Interference-aware topology control and qos routing in multi-channel wireless mesh networks. *ACM MobiHoc '05, Urbana-Champaign, Illinois, USA*, pages 68 – 77, MAY 2005.

[45] Murali Kodialam and Thyaga Nandagopal. Characterizing the capacity region in multi-radio multi-channel wireless mesh networks. *ACM MobiCom, Cologne, Germany*, pages 73 – 87, 2005.

[46] Stefano Avallone and Ian F. Akyildiz. A channel assignment algorithm for multi-radio wireless mesh networks. *Proceedings of 16th International Conference on Computer Communications and Networks (ICCCN)*, pages 1034 – 1039, Honolulu, HI, AUGUST 2007.

[47] Saumitra M. Das, Himabindu Pucha, Dimitrios Koutsonikolas, Y. Charlie Hu, and Dimitrios Peroulis. Dmesh: Incorporating practical directional antennas in multichannel wireless mesh networks. *IEEE JOURNAL ON SELECTED AREAS IN COMMUNICATIONS*, 24(11):2028 – 2039, NOVEMBER 2006.

[48] A. Hamed Mohsenian Rad and Vincent W.S. Wong. Joint optimal channel assignment and congestion control for multi-channel wireless mesh networks. *IEEE International Conference on Communications ICC '06*, pages 1984 – 1989, Istanbul, JUNE 2006.

[49] Krishna N. Ramachandran, Elizabeth M. Belding, Kevin C. Almeroth, and Milind M. Buddhikot. Interference-aware channel assignment in multi-radio wireless mesh networks. *Proceedings of 25th IEEE International Conference on Computer Communications*, pages 1 – 12, INFOCOM Barcelona, Spain, 2006.

[50] Anjum Naveed, Salil S. Kanhere, and Sanjay K. Jha. Topology control and channel assignment in multi-radio multi-channel wireless mesh networks. *IEEE Internatonal Conference on Mobile Adhoc and Sensor Systems (MASS'07)*, pages 1 – 9, Pisa, OCTOBER 2007.

[51] Kai Xing, Xiuzhen Cheng, Liran Ma, and Qilian Liang. Superimposed code based channel assignment in multi-radio multi-channel wireless mesh networks. *Proceedings of the 13th annual ACM international conference on Mobile computing and networking, ACM MobiCom'07*, pages 15 – 26, 2007.

[52] Anand Prabhu Subramanian, Himanshu Gupta, and Samir R. Das. Minimum interference channel assignment in multi-radio wireless mesh networks. *4th Annual IEEE Communications Society Conference on Sensor, Mesh and Ad Hoc Communications and Networks, SECON '07*, pages 481 – 490, JUNE 2007.

[53] Bong-Jun Ko, Vishal Misra, Jitendra Padhye, and Dan Rubenstein. Distributed channel assignment in multi-radio 802.11 mesh networks. *IEEE Wireless Communications and Networking Conference (WCNC)*, pages 3978 – 3983, Kowloon, MARCH 2007.

[54] Atul Adya, Paramvir Bahl, Jitendra Padhye, Alec Wolman, and Lidong Zhou. A multi-radio unification protocol for ieee 802.11 wireless networks. *First International Conference on Broadband Networks, BroadNets '04*, pages 344 – 354, OCTOBER 2004.

[55] Arunabha Sen, Sudheendra Murthy, Samrat Ganguly, and Sudeept Bhatnagar. An interference-aware channel assignment scheme for wireless mesh networks. *IEEE International Conference on Communications, ICC '07*, pages 3471 – 3476, Glasgow, JUNE 2007.

[56] A. Hamed Mohsenian Rad and Vincent W.S. Wong. Wsn16-4: Logical topology design and interface assignment for multi-channel wireless mesh networks. *IEEE Global Telecommunications Conference, GLOBECOM '06*, pages 1 – 6, San Francisco, CA, NOVEMBER 2006.

[57] A. Hamed Mohsenian Rad and Vincent W.S. Wong. Joint channel allocation, interface assignment and mac design for multi-channel wireless mesh networks. *26th IEEE International Conference on Computer Communications, INFOCOM '07*, pages 1469–1477, Anchorage, AK, MAY 2007.

[58] Ehsan Aryafar, Omer Gurewitz, and Edward W. Knightly. Distance-1 constrained channel assignment in single radio wireless mesh networks. *The 27th IEEE Conference on Computer Communications, INFOCOM '08*, pages 762 – 770, Phoenix, AZ, APRIL 2008.

[59] Ramanuja Vedantham, Sandeep Kakumanu, Sriram Lakshmanan, and Raghupathy Sivakumar. Component based channel assignment in single radio, multi-channel ad hoc networks. *Proceedings of the 12th annual international conference on Mobile computing and networking, ACM MobiCom '06*, pages 378 – 389, 2006.

[60] Hejiao Huang, Xiaolu Cao, Xiaohua Jia, and Xiaolong Wang. A bibd-based channal assignment algorithm for multi-radio wireless mesh networks. *International Conference on Machine Learning and Cybernetics*, pages 4419 – 4424, Dalian, China, AUGUST 2006.

[61] Jing Zhu and Sumit Roy. 802.11 mesh networks with two-radio access points. *IEEE International Conference on Communications, ICC'05*, 5:3609 – 3615, MAY 2005.

[62] Arindam K. Das, Hamed M. K. Alazemi, Rajiv Vijayakumar, and Sumit Roy. Optimization models for fixed channel assignment in wireless mesh networks with multiple radios. *Second Annual IEEE Communications Society Conference on Sensor and Ad Hoc Communications and Networks, SECON '05*, pages 463 – 474, SEPTEMBER 2005.

[63] Jungmin So and Nitin Vaidya. Multi-channel mac for ad hoc networks: handling multi-channel hidden terminals using a single transceiver. *Proceedings of the 5th ACM international symposium on Mobile ad hoc networking and computing, ACM MobiHoc '04*, pages 222 – 233, 2004.

[64] Paramvir Bahl, Ranveer Chandra, and John Dunagan. Ssch: slotted seeded channel hopping for capacity improvement in ieee 802.11 ad-hoc wireless networks. *Proceedings of the 10th annual international conference on Mobile computing and networking, ACM MobiCom '04*, pages 216 – 230, 2004.

[65] Ritesh Maheshwari, Himanshu Gupta, and Samir R. Das. Multichannel mac protocols for wireless networks. *3rd Annual IEEE Communications Society on Sensor and Ad Hoc Communications and Networks, SECON '06*, 2:393 – 401, SEPTEMBER 2004.

[66] Nachum Shacham and Peter J. B. King. Architectures and performance of multichannel multihop packet radio networks. *IEEE Journal on Selected Areas in Communications*, 5(6):1013 – 1025, JULY 1987.

[67] Jingpu Shi, Theodoros Salonidis, and Edward W. Knightly. Starvation mitigation through multi-channel coordination in csma multi-hop wireless networks. *Proceedings of the 7th ACM international symposium on Mobile ad hoc networking and computing, ACM MobiHoc '06*, pages 214 – 225, 2006.

[68] Michele Garetto, Theodoros Salonidis, and Edward W. Knightly. Modeling per-flow throughput and capturing starvation in csma multi-hop wireless networks. *IEEE/ACM TRANSACTIONS ON NETWORKING*, 16(4):864 – 877, AUGUST 2008.

[69] Minho Shin, Seungjoon Lee, and Yoo ah Kim. Distributed channel assignment for multi-radio wireless networks. *IEEE International Conference on Mobile Adhoc and Sensor Systems, MASS '06*, pages 417 – 426, Vancouver, BC, OCTOBER 2006.

[70] Eric Rozner, Yogita Mehta, Aditya Akella, and Lili Qiu. Traffic-aware channel assignment in enterprise wireless lans. *IEEE International Conference on Network Protocols, ICNP '07.*, pages 133 – 143, Beijing, China, OCTOBER 2007.

[71] Michelle X. Gong and Scott F. Midkiff. Distributed channel assignment protocols: a cross-layer approach [wireless ad hoc networks]. *IEEE Wireless Communications and Networking Conference*, 4:2195 – 2200, MARCH 2005.

[72] Kyu-Han Kim and Kang G. Shin. Self-healing multi-radio wireless mesh networks. *Proceedings of the 13th annual ACM international conference on Mobile computing and networking, ACM MobiCom '07*, pages 326 – 329, 2007.

[73] Dheeraj Agrawal, Arunesh Mishra, Kevin Springborn, Suman Banerjee, and Samrat Ganguly. Dynamic interference adaptation for wireless mesh networks. *2nd IEEE Workshop on Wireless Mesh Networks, WiMesh '06*, pages 33 – 37, Reston, VA, SEPTEMBER 2006.

[74] Pradeep Kyasanur and Nitin H. Vaidya. Routing and interface assignment in multi-channel multi-interface wireless networks. *IEEE Wireless Communications and Networking Conference*, 4:2051 – 2056, MARCH 2005.

[75] Arunesh Mishra, Eric Rozner, Suman Banerjee, and William Arbaugh. Exploiting partially overlapping channels in wireless networks: turning a peril into an advantage. *Proceedings of the 5th ACM SIGCOMM conference on Internet Measurement, IMC '05*, pages 311 – 316, 2005.

[76] Arunesh Mishra, Suman Banerjee, and William Arbaugh. Using partially overlapped channels in wireless meshes. *IEEE Workshop on Wireless Mesh Networks, WiMesh '05*, 2005.

[77] Zhenhua Feng and Yaling Yang. How much improvement can we get from partially overlapped channels? *IEEE Wireless Communications and Networking Conference, WCNC '08*, pages 2957 – 2962, Las Vegas, NV, APRIL 2008.

[78] Tao Chen, Honggang Zhang, Gian Mario Maggio, and Imrich Chlamtac. Topology management in cogmesh: A cluster-based cognitive radio mesh network. *IEEE International Conference on Communications, ICC '07*, pages 6516 – 6521, Glasgow, JUNE 2007.

[79] Pradeep Kyasanur, Xue Yang, and Nitin H. Vaidya. Mesh networking protocols to exploit physical layer capabilities. *IEEE Workshop on Wireless Mesh Networks, WiMesh '05*, 2005.

[80] Douglas S. J. De Couto, Daniel Aguayo, Benjamin A. Chambers, and Robert Morris. Performance of multihop wireless networks: shortest path is not enough. *ACM SIGCOMM Computer Communication Review*, 33(1):83 – 88, JANUARY 2003.

[81] Yaling Yang, Jun Wang, and Robin Kravets. Designing routing metrics for mesh networks. *IEEE Workshop on Wireless Mesh Networks, WiMesh '05*, 2005.

[82] Douglas S. J. De Couto, Daniel Aguayo, John Bicket, and Robert Morris. A high-throughput path metric for multi-hop wireless routing. *Springer Wireless Networks*, 11:419 – 434, 2005.

[83] Richard Draves, Jitendra Padhye, and Brian Zill. Routing in multi-radio, multi-hop wireless mesh networks. *Proceedings of the 10th annual international conference on Mobile computing and networking, ACM MobiCom '04*, pages 114 – 128, Philadelphia, PA, USA, 2004.

[84] Turgay Korkmaz and Wei Zhou. On finding optimal paths in multi-radio, multi-hop mesh networks using wcett metric. *Proceedings of the 2006 international conference on Wireless communications and mobile computing, ACM IWCMC '06*, pages 1375 – 1380, Vancouver, British Columbia, 2006.

[85] Yaling Yang, Jun Wang, and Robin Kravets. Interference-aware load balancing for multihop wireless networks. University of Illinois at Urbana-Champaign, Technical Report, [Available online]: `http://www.cs.uiuc.edu/research/techreports.php?report=UIUCDCS-R-2005-2526`, 2005.

[86] Weirong Jiang, Zhiming Zhang, and Xiaofeng Zhong. High throughput routing in large-scale multi-radio wireless mesh networks. *Wireless Communications and Networking Conference, WCNC '07*, pages 2598 – 3602, Kowloon, MARCH 2007.

[87] Anand P. Subramanian, Milind M. Buddhikot, and Scott Miller. Interference aware routing in multi-radio wireless mesh networks. *2nd IEEE Workshop on Wireless Mesh Networks, WiMesh '06*, pages 55 – 63, Reston, VA, SEPTEMBER 2006.

[88] Gentian Jakllari, Stephan Eidenbenz, Nicolas Hengartner, Srikanth V. Krishnamurthy, and Michalis Faloutsos. Link positions matter: A noncommutative routing metric for wireless mesh network. *IEEE The 27th Conference on Computer Communications, INFOCOM '08*, pages 744 – 752, Phoenix, AZ, APRIL 2008.

[89] Gentian Jakllari, Stephan Eidenbenz, Nicolas Hengartner, Srikanth V. Krishnamurthy, and Michalis Faloutsos. Revisiting minimum cost reliable routing in wireless mesh networks. *Proceedings of the 13th annual ACM international conference on Mobile computing and networking, ACM MobiCom '07*, pages 302 – 305, 2007.

[90] Sabyasachi Roy, Dimitrios Koutsonikolas, Saumitra Das, and Y. Charlie Hu. High-throughput multicast routing metrics in wireless mesh networks. *Proceedings of the 26th IEEE International Conference on Distributed Computing Systems, ICDCS 06*, page 48, 2006.

[91] Qunfeng Dong, Suman Banerjee, Micah Adler, and Archan Misra. Minimum energy reliable paths using unreliable wireless links. *Proceedings of the 6th ACM international symposium on Mobile ad hoc networking and computing, ACM MobiHoc '05*, pages 449 – 459, 2005.

[92] Suman Banerjee and Archan Misra. Minimum energy paths for reliable communication in multi-hop wireless networks. *Proceedings of the 3rd ACM international symposium on Mobile ad hoc networking & computing, ACM MobiHoc '02*, pages 146 – 156, 2002.

[93] C. Perkins, E. Royer, and S.R. Das. Ad hoc on demand distance vector (aodv) routing. [Available online]: `http://www.ietf.org/rfc/rfc3561.txt`.

[94] D. Johnson. Routing in ad hoc networks of mobile hosts. *Workshop on Mobile Computing Systems and Applications, Santa Cruz, CA, U.S.*, 1994.

[95] T. Clausen and P. Jacquet. Optimized link state routing protocol (olsr). [Available online]: `http://www.ietf.org/rfc/rfc3626.txt`.

[96] Babel – a loop-avoiding distance-vector routing protocol. [Available online]: `http://www.pps.univ-paris-diderot.fr/~jch/software/babel/`.

[97] B.a.t.m.a.n. - better approach to mobile ad-hoc networking. [Available online]: `http://www.open-mesh.org/projects/open-mesh/wiki`.

[98] M. Abolhasan, B. Hagelstein, and J. C.-P. Wang. Real-world performance of current proactive multi-hop mesh protocols. *IEEE Asia-Pacific Conference on Communications, APCC '09*, pages 44 – 47, Shanghai, China, OCTOBER 2009.

[99] Krishna N. Ramachandran, Milind M. Buddhikot, Girish Chandranmenon, Scott Miller, Elizabeth M. Belding-Royer, and Kevin C. Almeroth. On the design and implementation of infrastructure mesh networks. *1st IEEE Workshop on Wireless Mesh Networks, WiMesh '05*, 2005.

[100] Xuhui Hu, Myung J. Lee, and Tarek N. Saadawi. Progressive route calculation protocol for wireless mesh networks. *IEEE International Conference on Communications, ICC '07*, pages 4973 – 4978, Glasgow, JUNE 2007.

[101] A. Boukerche and A. Darehshoorzadeh. Opportunistic routing in wireless networks: Models, algorithms and classifications. *ACM Computing Surveys*, 47(2):22 – 36, 2014.

[102] Sanjit Biswas and Robert Morris. Exor: opportunistic multi-hop routing for wireless networks. *ACM SIGCOMM Computer Communication Review - Proceedings of the 2005 conference on Applications, technologies, architectures, and protocols for computer communications*, 35(4):133 – 144, OCTOBER 2005.

[103] Eric Rozner, Jayesh Seshadri, Yogita Mehta, and Lili Qiu. Simple opportunistic routing protocol for wireless mesh networks. *2nd IEEE Workshop on Wireless Mesh Networks, WiMesh '06*, pages 48 – 54, Reston, VA, SEPTEMBER 2006.

[104] Szymon Chachulski, Michael Jennings, Sachin Katti, and Dina Katabi. Trading structure for randomness in wireless opportunistic routing. *Proceedings of the 2007 conference on Applications, technologies, architectures, and protocols for computer communications, ACM SIGCOMM '07*, pages 169 – 180, 2007.

[105] Sudipta Sengupta, Shravan Rayanchu, and Suman Banerjee. An analysis of wireless network coding for unicast sessions: The case for coding-aware routing. *26th IEEE International Conference on Computer Communications, INFOCOM '07*, pages 1028 – 1036, Anchorage, AK, MAY 2007.

[106] Sachin Katti, Hariharan Rahul, Wenjun Hu, Dina Katabi, Muriel Médard, and Jon Crowcroft. Xors in the air: practical wireless network coding. *ACM SIGCOMM Computer Communication Review - Proceedings of the 2006 conference on Applications, technologies, architectures, and protocols for computer communications*, 36(4):243 – 254, OCTOBER 2006.

[107] Yuan Yuan, Hao Yang, Starsky H. Y. Wong, Songwu Lu, and William Arbaugh. Romer: Resilient opportunistic mesh routing for wireless mesh networks. *The 1st IEEE Workshop on Wireless Mesh Networks, WiMesh '05*, 2005.

[108] Nagesh S. Nandiraju, Deepti S. Nandiraju, and Dharma P. Agrawal. Multipath routing in wireless mesh networks. *IEEE International Conference on Mobile Adhoc and Sensor Systems, MASS '06*, pages 741 – 746, Vancouver, BC, OCTOBER 2006.

[109] Jack Tsai and Tim Moors. A review of multipath routing protocols: From wireless ad hoc to mesh networks. *Proceeding of ACoRN Early Career Researcher Workshop on Wireless Multihop Networking*, JULY 2006.

[110] Sung-Ju Lee and Mario Gerla. Aodv-br: backup routing in ad hoc networks. *Wireless Communications and Networking Conference, WCNC '00*, 3:1311 – 1316, Chicago, IL, 2000.

[111] Peter P. Pham and Sylvie Perreau. Performance analysis of reactive shortest path and multipath routing mechanism with load balance. *IEEE Societies Twenty-Second Annual Joint Conference of the IEEE Computer and Communications Societies, INFOCOM '03*, 1:251 – 259, 2003.

[112] Yashar Ganjali and Abtin Keshavanian. Load balancing in ad hoc networks: single-path routing vs. multi-path routing. *Twenty-third AnnualJoint Conference of the IEEE Computer and Communications Societies, INFOCOM '04*, 2:1120 – 1125, 2004.

[113] Sungoh Kwon and Ness B. Shroff. Paradox of shortest path routing for large multi-hop wireless networks. *26th IEEE International Conference on Computer Communications, INFOCOM '07*, pages 1001 – 1009, Anchorage, AK, MAY 2007.

[114] Lucian Popa, Afshin Rostamizadeh, Richard Karp, Christos Papadimitriou, and Ion Stoica. Balancing traffic load in wireless networks with curveball routing. *Proceedings of the 8th ACM international symposium on Mobile ad hoc networking and computing, ACM MobiHoc '07*, pages 170 – 179, 2007.

[115] Esa Hyytiä, Pasi Lassila, and Jorma Virtamo. Spatial node distribution of the random waypoint mobility model with applications. *IEEE TRANSACTIONS ON MOBILE COMPUTING*, 5(6):680 – 694, JUNE 2006.

[116] Fan Li and Yu Wang. Circular sailing routing for wireless networks. *The 27th IEEE Conference on Computer Communications, INFOCOM '08*, pages 1346 – 1354, Phoenix, AZ, APRIL 2008.

[117] Alessandro Mei and Julinda Stefa. Routing in outer space. *The 27th IEEE Conference on Computer Communications, INFOCOM '08*, pages 2234–2242, Phoenix, AZ, APRIL 2008.

[118] Stephane Durocher, Evangelos Kranakis, Danny Krizanc, and Lata Narayanan. Balancing traffic load using one-turn rectilinear routing. In *Proceedings of the 5th International Conference on Theory and Applications of Models of Computation*, TAMC'08, pages 467 – 478, 2008.

[119] Load balancing in dence wireless multihop networks. [Available online]: `http://https://www.netlab.tkk.fi/~esa/java/multihop/`.

[120] Fan Li and Yu Wang. Stretch factor of curveball routing in wireless network: Cost of load balancing. *IEEE International Conference on Communications, ICC '08*, pages 2650 – 2654, Beijing, China, MAY 2008.

[121] Jie Gao and Li Zhang. Trade-offs between stretch factor and load-balancing ratio in routing on growth-restricted graphs. *IEEE TRANSACTIONS ON PARALLEL AND DISTRIBUTED SYSTEMS*, 20(2):171 – 179, FEBRUARY 2009.

[122] M. Mauve, J. Widmer, and H. Hartenstein. A survey on position-based routing in mobile ad hoc networks. *IEEE Network*, 15(6):30 – 39, 2001.

[123] D. Chen and P. K. Varshney. A survey of void handling techniques for geographic routing in wireless networks. *IEEE Communications Surveys & Tutorials*, 9:50 – 67, 2007.

[124] H. Frey and I. Stojmenovic. On delivery guarantees of face and combined greedy-face routing in ad hoc and sensor networks. *ACM MobiCom*, pages 390 – 401, Los Angeles, CA, USA, 2006.

[125] Tehuang Liu and Wanjiun Liao. Interference-aware qos routing for multi-rate multi-radio multi-channel ieee 802.11 wireless mesh networks. *IEEE TRANSACTIONS ON WIRELESS COMMUNICATIONS*, 8(1):166 – 175, JANUARY 2009.

[126] Farshad Javadi and Abbas Jamalipour. A multi-path cognitive resource management mechanism for qos provisioning in wireless mesh networks. *Springer/ACM Wireless Networks*, 17:277 – 290, 2011.

[127] Azzedine Boukerche, Xiuzhen Cheng, and Joseph Linus. Energy-aware data-centric routing in microsensor networks. *Proceedings of the 6th ACM international workshop on Modeling analysis and simulation of wireless and mobile systems, MSWiM'03*, pages 42 – 49, San Diego, CA, September 2003.

[128] G.M Shaullah, Amoakoh Gyasi-Agyei, and Peter J Wolfs. A survey of energy-efficient and qos-aware routing protocols for wireless sensor networks. *Novel Algorithms and Techniques in Telecommunications, Automation and Industrial Electronics, Springer Science+Business Media B.V.*, pages 352 – 357, 2008.

[129] Sonia Waharte, Brent Ishibashi, Raouf Boutaba, and Djamal-Eddine Meddour. Design and performance evaluation of iar: Interference-aware routing metric for wireless mesh networks. *Springer Mobile Networks and Applications*, 14(5):649 – 660, 2009.

[130] A Boukerche, B Turgut, N Aydin, MZ Ahmad, L Boloni, and D Turgut. Routing protocols in ad hoc networks: A survey. *Computer Networks*, 55(13):3032 – 3080, 2011.

[131] Thomas Moscibroda and Roger Wattenhofer. Coloring unstructured radio networks. *Proceedings of the seventeenth annual ACM symposium on Parallelism in algorithms and architectures, SPAA'05, New York, NY, USA*, pages 39 – 48, 2005.

[132] Shashidhar Gandham, Milind Dawande, and Ravi Prakash. Link scheduling in wireless sensor networks: Distributed edge-coloring revisited. *Journal of Parallel and Distributed Computing*, 68(8):1122 – 1134, 2008.

[133] Subramanian Ramanathan and Errol L. Lloyd. Scheduling algorithms for multihop radio networks. *IEEE/ACM TRANSACTIONS ON NETWORKING*, 1(2):166 – 177, APRIL 1993.

[134] Jimmi Grönkvist and Anders Hansson. Comparison between graph-based and interference-based stdma scheduling. *Proceedings of the 2nd ACM international symposium on Mobile ad hoc networking & computing, MobiHoc '01*, pages 255 – 258, New York, NY, USA, 2001.

[135] Arash Behzad and Izhak Rubin. On the performance of graph-based scheduling algorithms for packet radio networks. *IEEE Global Telecommunications Conference, GLOBECOM '03*, 6:3432 – 3436, DECEMBER 2003.

[136] Thomas Moscibroda, Roger Wattenhofer, and Yves Weber. Protocol design beyond graph-based models. *Proceedings of the 5th ACM SIGCOMM Workshop on Hot Topics in Networks HotNets '06*, 2006.

[137] Jochen H. Schiller. *Mobile Communications*. ADDISON-WESLEY, An imprint of Pearson Eduction, second edition, 2003.

[138] Jimmi Grönkvist, Jan Nilsson, and Di Yuan. Throughput of optimal spatial reuse tdma for wireless ad-hoc networks. *IEEE 59th Vehicular Technology Conference, VTC '04-Spring*, 4:2156 – 2160, May 2004.

[139] Jimmi Grönkvist. Traffic controlled spatial reuse tdma in multi-hop radio networks. *The Ninth IEEE International Symposium on Personal, Indoor and Mobile Radio Communications*, 3:1203 – 1207, SEPTEMBER 1998.

[140] Kamal Jain, Jitendra Padhye, Venkat Padmanabhan, and Lili Qiu. Impact of interference on multi-hop wireless network performance. *Proceedings of the 9th annual international conference on Mobile computing and networking, MobiCom '03, New York, NY, USA*, pages 66 – 80, 2003.

[141] Gurashish Brar, Douglas M. Blough, and Paolo Santi. Computationally efficient scheduling with the physical interference model for throughput improvement in wireless mesh networks. *Proceedings of the 12th annual international conference on Mobile computing and networking, MobiCom '06*, pages 2 – 13, Los Angeles, CA, USA, 2006.

[142] Parth H. Pathak, Divya Gupta, and Rudra Dutta. Loner links aware routing and scheduling wireless mesh networks. *IEEE 2nd Advanced Networking and Telecommunications System Conference, ANTS '08*, pages 1 – 3, Mumbai, DECEMBER 2008.

[143] Patrik Björklund, Peter Värbrand, and Di Yuan. A column generation method for spatial tdma scheduling in ad hoc networks. *Ad Hoc Networks*, 2(4):405 – 418, OCTOBER 2004.

[144] Petar Djukic and Shahrokh Valaee. Link scheduling for minimum delay in spatial re-use tdma. *IEEE 26th IEEE International Conference on Computer Communications, INFOCOM '07*, pages 28 – 36, Anchorage, AK, MAY 2007.

[145] Petar Djukic and Shahrokh Valaee. Distributed link scheduling for tdma mesh networks. *IEEE International Conference on Communications, ICC '07*, pages 3823–3828, Anchorage, AK, JUNE 2007.

[146] Leandros Tassiulas and Anthony Ephremides. Stability properties of constrained queueing systems and scheduling policies for maximum throughput in multihop radio networks. *IEEE TRANSACTIONS ON AUTOMATIC CONTROL*, 37(12):1936 – 1948, DECEMBER 1992.

[147] Xiaojun Lin, Ness B. Shroff, and R. Srikant. A tutorial on cross-layer optimization in wireless networks. *IEEE Journal on Selected Areas in Communications*, 24(8):1452 – 1463, AUGUST 2006.

[148] Changhee Joo, Xiaojun Lin, and Ness B. Shroff. Understanding the capacity region of the greedy maximal scheduling algorithm in multi-hop wireless networks. *IEEE The 27th Conference on Computer Communications, INFOCOM '08*, pages 1103 – 1111, Phoenix, AZ, APRIL 2008.

[149] Xiaojun Lin and Ness B. Shroff. The impact of imperfect scheduling on cross-layer rate control in wireless networks. *Proceedings of IEEE 24th Annual Joint Conference of the IEEE Computer and Communications Societies, INFOCOM '05*, 3:1804 – 1814, Miami, FL, MARCH 2005.

[150] Prasanna Chaporkar, Koushik Kar, and Saswati Sarkar. Throughput guarantees through maximal scheduling in wireless networks. *Proceedings of 43d Annual Allerton Conference on Communication, Control and Computing*, pages 28 – 30, Monticello, Illinois, 2005.

[151] Gaurav Sharma, Ravi R. Mazumdar, and Ness R. Shroff. On the complexity of scheduling in wireless networks. *Proceedings of the 12th annual international conference on Mobile computing and networking, ACM MobiCom '06*, pages 227 – 238, Los Angeles, CA, 2006.

[152] Antonis Dimakis and Jean Walrand. Sufficient conditions for stability of longest-queue-first scheduling: Second-order properties using fluid limits. *Advances in Applied Probability*, 38:505 – 521, 2006.

[153] Xiaojun Lin and Ness B. Shroff. The impact of imperfect scheduling on cross-layer congestion control in wireless networks. *IEEE/ACM TRANSACTIONS ON NETWORKING*, 14(2):302 – 315, APRIL 2006.

[154] Abhinav Gupta, Xiaojun Lin, and R. Srikant. Low-complexity distributed scheduling algorithms for wireless networks. *IEEE 26th IEEE International Conference on Computer Communications, INFOCOM '07*, pages 1631 – 1639, Anchorage, AK, MAY 2007.

[155] Gaurav Sharma, Ness B. Shroff, and Ravi R. Mazumdar. Joint congestion control and distributed scheduling for throughput guarantees in wireless networks. *IEEE 26th IEEE International Conference on Computer Communications, INFOCOM '07*, pages 2072 – 2080, Anchorage, AK, MAY 2007.

[156] Xiaojun Lin and Shahzada Rasool. A distributed joint channel-assignment, scheduling and routing algorithm for multi-channel ad-hoc wireless networks. *IEEE 26th IEEE International Conference on Computer Communications, INFOCOM '07*, pages 1118 – 1126, Anchorage, AK, MAY 2007.

[157] Longbi Lin, Xiaojun Lin, and Ness B. Shroff. Low-complexity and distributed energy minimization in multi-hop wireless networks. *IEEE 26th IEEE International Conference on Computer Communications, INFOCOM '07*, pages 1685 – 1693, Anchorage, AK, MAY 2007.

[158] Rajiv Gandhi, Srinivasan Parthasarathy, and Arunesh Mishra. Minimizing broadcast latency and redundancy in ad hoc networks. *Proceedings of the 4th ACM international symposium on Mobile ad hoc networking & computing, ACM MobiHoc '03*, pages 222 – 232, 2003.

[159] Michael Elkin and Guy Kortsarz. Improved broadcast schedule for radio networks. *Symposium on Discrete Algorithms (SODA)*, pages 222 – 231, Vancouver, British Columbia, 2005.

[160] Leszek Gasieniec, David Peleg, and Qin Xin. Faster communication in known topology radio networks. *Proceedings of the twenty-fourth annual ACM symposium on Principles of distributed computing, PODC '05*, pages 129 – 137, 2005.

[161] Ferdinando Cicalese, Fredrik Manne, and Qin Xin. Faster centralized communication in radio networks. *Proceedings of the 17th International Conference on Algorithms and Computation, ISAAC '06*, pages 339 – 348, Kolkata, 2006.

[162] Dariusz R. Kowalski and Andrzej Pelc. Optimal deterministic broadcasting in known topology radio networks. *Distributed Computing*, 19(3):185 – 195, JANUARY 2007.

[163] Scott C.-H. Huang, Peng-Jun Wan, Xiaohua Jia, Hongwei Du, and Weiping Shang. Minimum-latency broadcast scheduling in wireless ad hoc networks. *IEEE 26th IEEE International Conference on Computer Communications, INFOCOM '07*, pages 733 – 739, Anchorage, AK, MAY 2007.

[164] Arup Acharya, Sachin Ganu, and Archan Misra. Dcma: A label switching mac for efficient packet forwarding in multihop wireless networks. *IEEE JOURNAL ON SELECTED AREAS IN COMMUNICATIONS*, 24(11):1995 – 2004, NOVEMBER 2006.

[165] Joo Ghee Lim, Chun Tung Chou, Alfandika Nyandoro, and Sanjay Jha. A cut-through mac for multiple interface, multiple channel wireless mesh networks. *IEEE Wireless Communications and Networking Conference, WCNC '07*, pages 2373 – 2378, Kowloon, MARCH 2007.

[166] Kimaya Mittal and Elizabeth M. Belding. Rtss/ctss: mitigation of exposed terminals in static 802.11-based mesh networks. *2nd IEEE Workshop on Wireless Mesh Networks, WiMesh '06*, pages 3 – 12, Reston, VA, SEPTEMBER 2006.

[167] Jitendra Padhye, Sharad Agarwal, Venkata N. Padmanabhan, Lili Qiu, Ananth Rao, and Brian Zill. Estimation of link interference in static multi-hop wireless networks. *Proceedings of the 5th ACM SIGCOMM conference on Internet Measurement, IMC '05*, pages 28 – 33, Berkeley, CA, 2005.

[168] Seung Min Hur, Shiwen Mao, Y. Thomas Hou, Kwanghee Nam, and Jeffrey H. Reed. A location-assisted mac protocol for multi-hop wireless networks. *IEEE*

Wireless Communications and Networking Conference, WCNC '07, pages 322 – 327, Kowloon, MARCH 2007.

[169] Bhaskaran Raman and Kameswari Chebrolu. Design and evaluation of a new mac protocol for long-distance 802.11 mesh networks. *Proceedings of the 11th annual international conference on Mobile computing and networking, ACM MobiCom '05*, pages 156 – 169, Cologne, Germany, 2005.

[170] Feiyi Huang, Yang Yang, and Xiaodong Zhang. Receiver sense multiple access protocol for wireless mesh access networks. *IEEE International Conference on Communications, ICC '07*, pages 3764 – 3769, Glasgow, JUNE 2007.

[171] Seongkwan Kim, Sung-Ju Lee, and Sunghyun Choi. The impact of ieee 802.11 mac strategies on multi-hop wireless mesh networks. *2nd IEEE Workshop on Wireless Mesh Networks, WiMesh '06*, pages 38 – 47, Reston, VA, SEPTEMBER 2006.

[172] Xue Yang and Nitin Vaidya. Spatial backoff contention resolution for wireless networks. *2nd IEEE Workshop on Wireless Mesh Networks, WiMesh '06*, pages 13 – 22, Reston, VA, SEPTEMBER 2006.

[173] Ashish Raniwala, Pradipta De, Srikant Sharma, Rupa Krishnan, and Tzi cker Chiueh. End-to-end flow fairness over ieee 802.11-based wireless mesh networks. *IEEE 26th International Conference on Computer Communications, INFOCOM '07*, pages 2361 – 2365, Anchorage, AK, MAY 2007.

[174] Hon Sun Chiu and Kwan L. Yeung. Maximizing multi-cast call acceptance rate in multi-channel multi-interface wireless mesh networks. *IEEE TRANSACTIONS ON WIRELESS COMMUNICATIONS*, 9(8):2622 – 2631, AUGUST 2010.

[175] Azzedine Boukerche. *Algorithms and protocols for wireless, mobile Ad Hoc networks*. John Wiley & Sons, 2008.

[176] HABF De Oliveira, A Boukerche, EF Nakamura, and AAF Loureiro. An efficient directed localization recursion protocol for wireless sensor networks. *IEEE TRANSACTIONS ON COMPUTERS*, 58(5):677 – 691, 2009.

[177] A Boukerche and S Rogers. Gps query optimization in mobile and wireless networks. *Proceedings of Sixth IEEE Symposium on Computers and Communications*, pages 198 – 203, Hammamet, July 2001.

[178] A Boukerche, RWN Pazzi, and RB Araujo. Hpeq a hierarchical periodic, event-driven and query-based wireless sensor network protocol. *The IEEE Conference on Local Computer Networks, LCN'05*, pages 560 – 567, Sydney, NSW, November 2005.

[179] Yiwen Wu, Joseph Hui, and Hongxia Sun. Fast restoring gigabit wireless networks using a directional mesh architecture. *Computer Communications*, 26(17):1957 – 1964, 2003.

[180] Shifang Dai, Xinming Zhang, Jin Wang, and Jianping Wang. An efficient coding scheme designed for n+k protection in wireless mesh networks. *IEEE COMMUNICATIONS LETTERS*, 16(8):1266 – 1269, AUGUST 2012.

[181] Chenglin Li, Hongkai Xiong, Junni Zou, and Chang Wen Chen. Distributed robust optimization for scalable video multirate multicast over wireless networks. *IEEE TRANSACTIONS ON CIRCUITS AND SYSTEMS FOR VIDEO TECHNOLOGY*, 22(6):943 – 957, JUNE 2012.

[182] Shanshan Jiang and Yuan Xue. Providing survivability against jamming attack for multi-radio multi-channel wireless mesh networks. *Journal of Network and Computer Applications*, 34:443–454, 2011.

[183] Kyu-Han Kim and Kang G. Shin. Self-reconfigurable wireless mesh networks. *IEEE/ACM TRANSACTIONS ON NETWORKING*, 19(2):393 – 404, APRIL 2011.

[184] Vicky Sharma, Koushik Kar, K. K. Ramakrishnan, and Shivkumar Kalyanaraman. A transport protocol to exploit multipath diversity in wireless networks. *IEEE/ACM TRANSACTIONS ON NETWORKING*, 20(4):1024 – 1039, AUGUST 2012.

[185] C. Perkins and P. Bhagwat. Highly dynamic destination-sequenced distance-vector routing (dsdv) for mobile computers. *ACM SIGCOMM '94 Conference on Communications Architectures, Protocols and Applications*, pages 234 – 244, London, UK, 1994.

[186] V.D. Park and M.S. Corson. A highly adaptive distributed routing algorithm for mobile wireless networks. *IEEE INFOCOM*, 3:1405 – 1413, Kobe, 1997.

[187] Z.J. Haas and M.R. Pearlman. The performance of query control schemes for the zone routing protocol. *IEEE/ACM Transactions on Networking*, 9(4):427 – 438, AUGUST 2001.

[188] Long Le. Multipath routing design for wireless mesh networks. *IEEE Global Telecommunications Conference (GLOBECOM)*, pages 1 – 6, Houston, TX, USA, 2011.

[189] Farshad Javadi, Kumudu S. Munasinghe, and Abbas Jamalipour. Rapid and reliable routing mesh protocol (rrrmp). *IEEE International Conference on Communications (ICC)*, pages 1 – 5, Cape Town, 2010.

[190] K. Valarmathi and N. Malmurugan. Multi path routing protocol for improving reliability in ieee 802.16 wireless mesh networks. *3rd International Conference on Trendz in Information Sciences and Computing (TISC)*, pages 116 – 121, Chennai, 2011.

[191] Yu Li. A reputation system for wireless mesh network using multi-path routing protocol. *IEEE 30th International Performance Computing and Communications Conference (IPCCC)*, pages 1 – 6, Orlando, FL, 2011.

[192] Rubin Zheng, Yongmei Li, Li Sa, and Xiaoxi Guo. A hybrid multi-path routing for wireless mesh network backbone. *4th International Conference on Wireless Communications, Networking and Mobile Computing (WiCOM)*, pages 1 – 4, Dalian, China, OCTOBER 2008.

[193] R.Gunasundari, S.Shanmugavel, and K.Bakyalakshmi. Fault tolerant hawaii protocol for ip services in wireless networks. *22nd International Conference on Advanced Information Networking and Applications - Workshops*, pages 457 – 462, Okinawa, 2008.

[194] J. Li, J. Jannotti, D. De Couto, D. Karger, and R. Morris. A scalable location service for geographic ad-hoc routing. *Proceedings of the 6th ACM International Conference on Mobile Computing and Networking (MobiCom '00)*, pages 120–130, Boston, Massachusetts, USA, AUGUST 2000.

[195] Roie Melamed, Idit Keidar, and Yoav Barel. Octopus: A fault-tolerant and efficient ad-hoc routing protocol. *ACM/Springer Wireless Networks*, 14:777 – 793, 2008.

[196] Flaminia Luccio Giuseppe Anastasi, Alberto Bartoli. Fault-tolerant support for reliable multicast in mobile wireless systems: Design and evaluation. *ACM/Springer Wireless Networks*, 10:259 – 269, 2004.

[197] Qin Xin and Yan Zhang. Optimal fault-tolerant broadcasting in wireless mesh networks. *International Conference on High Performance Switching and Routing (HSPR)*, pages 151 – 157, Shanghai, China, 2008.

[198] Fan Wei, Liumei Zhang, Tianshi Liu, Md.Emadadul Haque, Xiaodong Lu, and Kinji Mori. Autonomous fault tolerance technology of emergency community in wireless sensor network. *IEEE Eleventh International Symposium on Autonomous Decentralized Systems (ISADS)*, pages 1 – 6, Mexico City, Mexico, MARCH 2013.

[199] Jiajia Liu, Xiaohong Jiang, Hiroki Nishiyama, and Nei Kato. Reliability assessment for wireless mesh networks under probabilistic region failure model. *IEEE TRANSACTIONS ON VEHICULAR TECHNOLOGY*, 60(5):2253 – 5564, JUNE 2011.

[200] Sangsu Jung, Malaz Kserawi, Dujeong Lee, and June-Koo Kevin Rhee. Distributed potential field based routing and autonomous load balancing for wireless mesh networks. *IEEE COMMUNICATIONS LETTERS*, 13(6):429 – 431, JUNE 2009.

[201] Wei Wang, Donghyun Kim, Min Kyung An, Wei Gao, Xianyue Li, Zhao Zhang, and Weili Wu. On construction of quality fault-tolerant virtual backbone in wireless networks. *IEEE/ACM TRANSACTIONS ON NETWORKING*, 21(5):1499 – 1510, OCTOBER 2013.

[202] Sarasvathi Va and N.Ch.S.N.Iyengar. Centralized rank based channel assignment for multi-radio multi-channel wireless mesh networks. *Procedia Technology*, 4:182 – 186, 2012.

[203] I. Koutsopoulos and L. Tassiulas. Joint optimal access point selection and channel assignment in wireless networks. *IEEE/ACM TRANSACTIONS ON NETWORKING*, 15(3):521–532, OCTOBER 2007.

[204] Mohammadreza Balouchestani, Kaamran Raahemifar, and Sridhar Krishnan. Increasing the reliability of wireless sensor network with a new testing approach based on compressed sensing theory. *Eighth International Conference on Wireless and Optical Communications Networks (WOCN)*, pages 1 – 4, Paris, MAY 2011.

[205] Xi Deng and Yuanyuan Yang. An efficient mac multicast protocol for reliable wireless communications with network coding. *IEEE Global Telecommunications Conference (GLOBECOM)*, pages 1 – 6, Houston, TX, USA, DECEMBER 2011.

[206] Xiang-Yang Li, Peng-Jun Wan, Yu Wang, and Chih-Wei Yi. Fault tolerant deployment and topology control in wireless networks. *Proceedings of the 4th ACM international symposium on Mobile ad hoc networking & computing (MobiHoc '03), New York, NY, USA*, pages 117 – 128, 2003.

[207] Svilen Ivanov and Edgar Nett. Using localization for fault-tolerant radio coverage in wireless mesh networks. *IEEE 26th International Parallel and Distributed Processing Symposium Workshops & PhD Forum (IPDPSW)*, pages 1496 – 1505, Shanghai, MAY 2012.

[208] Svilen Ivanov and Edgar Nett. Localization-based radio model calibration for fault-tolerant wireless mesh networks. *IEEE TRANSACTIONS ON INDUSTRIAL INFORMATICS*, 9(1):246 – 253, FEBRUARY 2013.

[209] Svilen Ivanov, Edgar Nett, and Ralf Schumann. Fault-tolerant base station planning of wireless mesh networks in dynamic industrial environments. *IEEE Conference on Emerging Technologies and Factory Automation (ETFA)*, pages 1 – 8, Bilbao, SEPTEMBER 2010.

[210] Richard Alena, Ray Gilstrap, Jarren Baldwin, Thom Stone, and Pete Wilson. Fault tolerance in zigbee wireless sensor networks. *IEEE Aerospace Conference*, pages 1 – 15, Big Sky, MT, MARCH 2011.

[211] Yong Chen and S.H. Son. A fault tolerant topology control in wireless sensor networks. *The 3rd ACS/IEEE International Conference on Computer Systems and Applications, Cairo*, 2005.

[212] Ning Li and Jennifer C. Hou. Flss: A fault-tolerant topology control algorithm for wireless networks. *Proceedings of the 10th annual international conference on Mobile computing and networking (MobiCom '04)*, pages 275 – 286, Philadelphia, PA, USA, 2004.

[213] Paolo Santi. Topology control in wireless ad hoc and sensor networks. *ACM Computing Surveys (CSUR)*, 37(2):164 – 194, JUNE 2005.

[214] M. Bahramgiri, M.T. Hajiaghayi, and V.S. Mirrokni. Fault tolerant and 3-dimensional distributed topology control algorithms in wireless multi-hop networks. *ACM/Springer Wireless Networks*, 8:179 – 188, 2006.

[215] Indranil Saha, Lokesh Kumar Sambasivan, Subhas Kumar Ghosh, and Ranjeet Kumar Patro. Distributed fault-tolerant topology control in wireless multi-hop networks. *ACM/Springer Wireless Networks*, 16:1511 – 1524, 2010.

[216] Ziyi Zhang, Qiang Ma, and Xin Wang. Exploiting use of a new performance metric for construction of robust and efficient wireless backbone network. *18th International Workshop on Quality of Service (IWQoS)*, pages 1 – 9, Beijing, China, JUNE 2010.

[217] Ziyi Zhang, Xin Wang, and Qin Xin. A new performance metric for construction of robust and efficient wireless backbone network. *IEEE TRANSACTIONS ON COMPUTERS*, 61(10):1495 – 1506, OCTOBER 2012.

[218] Stephen Boyd, Arpita Ghosh, Balaji Prabhakar, and Devavrat Shah. Gossip algorithms: Design, analysis and applications. *Proceedings IEEE Infocom, Miami*, 3:1653 – 1664, MARCH 2005.

[219] Stephen Boyd, Arpita Ghosh, Balaji Prabhakar, and Devavrat Shah. Randomized gossip algorithms. *IEEE TRANSACTIONS ON INFORMATION THEORY*, 52(6):2508 – 2530, JUNE 2006.

[220] Bernd Thallner, Heinrich Moser, and Ulrich Schmid. Topology control for fault-tolerant communication in wireless ad hoc networks. *ACM/Springer Wireless Networks*, 16:387 – 404, 2010.

[221] A Boukerche, A Martirosyan, and R Pazzi. An inter-cluster communication based energy aware and fault tolerant protocol for wireless sensor networks. *Mobile Networks and Applications*, 13(6):614 – 626, 2008.

[222] Noriki Uchida, Kazuo Takahata, Yoshitaka Shibata, and Norio Shiratori. Never die network extended with cognitive wireless network for disaster information system. *International Conference on Complex, Intelligent, and Software Intensive Systems*, pages 24 – 31, Seoul, JUNE 2011.

[223] Taiming Feng and Lu Ruan. Design of a survivable hybrid wireless-optical broadband-access network. *IEEE/OSA Journal of Optical Communications and Networking*, 3(5):458 – 464, MAY 2011.

[224] Aqeel Ahmad Qureshi, Muhammad Ramzan, and S.M.H Zaidi. Fault aware routing algorithm to enhance network resiliency & achieve load balancing in hybrid wireless optical broadband access network. *High-Capacity Optical Networks and Enabling Technologies (HONET)*, pages 252 – 257, Cairo, DECEMBER 2010.

[225] Parag Kulkarni, Sedat Gormus, Zhong Fan, and Benjamin Motz. A mesh-radio-based solution for smart metering networks. *IEEE Communications Magazine*, 50(7):86 – 95, JULY 2012.

[226] Parag Kulkarni, Sedat Gormus, Zhong Fan, and Filipe Ramos. Ami mesh networks - a practical solution and its performance evaluation. *IEEE TRANSACTIONS ON SMART GRID*, 3(3):1469 – 1481, SEPTEMBER 2012.

[227] Raquel Barco, Pedro Lazaro, and Pablo Munoz. A unified framework for self-healing in wireless networks. *IEEE Communications Magazine*, 50(12):134 – 142, DECEMBER 2012.

[228] Xuefeng Liu, Jiannong Cao, and Shaojie Tang. Fault tolerant complex event detection in wsns: A case study in structural health monitoring. *Proceedings of IEEE INFOCOM*, pages 1384 – 1392, Turin, APRIL 2013.

[229] Osianoh Glenn Aliu, Ali Imran, Muhammad Ali Imran, and Barry Evans. A survey of self organisation in future cellular networks. *IEEE COMMUNICATIONS SURVEYS and TUTORIALS*, 15(1):336 – 361, FIRST QUARTER 2013.

[230] Herve Kerivin and A. Ridha Mahjoub. Design of survivable networks: A survey. *NETWORKS, Wiley Periodicals Inc.*, 46(1):1 – 21, AUGUST 2005.

[231] V. Latora and M. Marchiori. Efficient behavior of small-world networks. *Physical Review Letters*, 87(19):198701, OCTOBER 2001.

[232] P. Crucitti, V. Latora, and M. Marchiori. Model for cascading failures in complex networks. *Physical Review Letters*, 69(4):045104, APRIL 2004.

[233] Chris Barrett, Richard Beckman, Karthik Channakeshava, Fei Huang, V.S. Anil Kumar Achla Marathe, Madhav V. Marathe, and Guanhong Pei. Cascading failures

in multiple infrastructures: From transportation to communication network. *5th International Conference on Critical Infrastructure (CRIS)*, pages 1 – 8, Beijing, China, 2010.

[234] Lin X. Cai, Yongkang Liu, Tom H. Luan, Xuemin (Sherman) Shen, Jon W. Mark, and H. Vincent Poor. Sustainability analysis and resource management for wireless mesh networks with renewable energy supplies. *IEEE JOURNAL ON SELECTED AREAS IN COMMUNICATIONS*, 32(2):345–355, FEBRUARY 2014.

[235] Mohamed Saad. Joint optimal routing and power allocation for spectral efficiency in multihop wireless networks. *IEEE TRANSACTIONS ON WIRELESS COMMUNICATIONS*, 13(5):2530–2539, MAY 2014.

[236] Yulong Zou, Jia Zhu, and Rui Zhang. Exploiting network cooperation in green wireless communication. *IEEE TRANSACTIONS ON COMMUNICATIONS*, 61(3):999–1010, MARCH 2013.

[237] Silvia Boiardi, Antonio Capone, and Brunilde Sansò. Energy-aware planning and management of wireless mesh networks. *IEEE Global Communications Conference, GLOBECOM'12*, pages 3049 – 3055, Anaheim, California, DECEMBER 2012.

[238] Vijay Raghunathan, Saurabh Ganeriwal, Curt Schurgers, and Mani Srivastava. Energy efficient wireless packet scheduling and fair queuing. *ACM Transactions on Embedded Computing Systems (TECS)*, 3(1):3–23, FEBRUARY 2004.

[239] Jing Yang and Sennur Ulukus. Optimal packet scheduling in an energy harvesting communication system. *IEEE TRANSACTIONS ON COMMUNICATIONS*, 60(1):220–230, JANUARY 2012.

[240] Elif Uysal-Biyikoglu, Balaji Prabhakar, and Abbas El Gamal. Energy-efficient packet transmission over a wireless link. *IEEE/ACM TRANSACTIONS ON NETWORKING*, 10(4):487–499, AUGUST 2002.

[241] Feng Shan, Junzhou Luo, and Xiaojun Shen. Optimal energy efficient packet scheduling with arbitrary individual deadline guarantee. *Computer Networks*, 75, PART A:351–366, DECEMBER 2014.

[242] Murtaza A. Zafer and Eytan Modiano. A calculus approach to energy-efficient data transmission with quality-of-service constraints. *IEEE/ACM TRANSACTIONS ON NETWORKING*, 17(3):898–911, JUNE 2009.

[243] K. Tutuncuoglu and A. Yener. Optimum transmission policies for battery limited energy harvesting nodes. *IEEE Transactions on Wireless Communications*, 11(3):1180–1189, March 2012.

[244] Xiaojing Chen, Xin Wang, and Yichuang Sun. Energy-harvesting powered transmissions of bursty data packets with strict deadlines. *IEEE International Conference on Communications, ICC'14*, pages 4060–4065, Sydney, Australia, JUNE 2014.

[245] Xiaojing Chen, Xin Wang, and Xiaolin Zhou. Energy-harvesting powered transmissions of delay-limited data packets. *IEEE Global Communications Conference, GLOBECOM'14*, pages 2550–2555, Austin, TX, DECEMBER 2014.

[246] Kian Hedayati and Izhak Rubin. A robust distributive approach to adaptive power and adaptive rate link scheduling in wireless mesh networks. *IEEE TRANSACTIONS ON WIRELESS COMMUNICATIONS*, 11(1):275 – 283, JANUARY 2012.

[247] Pan Li, Nicola Scalabrino, Yuguang Fang, Enrico Gregori, and Imrich Chlamtac. How to effectively use multiple channels in wireless mesh networks. *IEEE TRANSACTIONS ON PARALLEL AND DISTRIBUTED SYSTEMS*, 20(11):1641 – 1652, NOVEMBER 2009.

[248] G.711. Pulse code modulation (pcm) of voice frequencies. `http://www.itu.int/rec/T-REC-G.711/e`. [Online Available].

[249] Vern Paxson and Sally Floy. Wide-area traffic: The failure of poisson modeling. *IEEE/ACM TRANSACTIONS ON NETWORKING*, 3(3):226 – 244, JUNE 1995.

[250] Wei Wang, Xin Liu, and Dilip Krishnaswamy. Robust routing and scheduling in wireless mesh networks under dynamic traffic conditions. *IEEE TRANSACTIONS ON MOBILE COMPUTING*, 8(12):1705 – 1717, DECEMBER 2009.

[251] P. Gupta and P. R. Kumar. Critical power for asymptotic connectivity. *Proceedings of the 37th IEEE Conference on Decision and Control*, 1:1106–1110, Tampa, FL, 1998.

[252] Fei Xing and Wenye Wang. On the critical phase transition time of wireless multihop networks with random failures. *Proceedings of the 14th ACM international conference on Mobile computing and networking, MobiCom'08*, pages 175 – 186, San Francisco, California, USA, 2008.

[253] Lei Sun and Wenye Wang. Understanding blackholes in large-scale cognitive radio networks under generic failures. *Proceedings of IEEE INFOCOM*, pages 728 – 736, Turin, APRIL 2013.

[254] Piyush Gupta and P. R. Kumar. The capacity of wireless networks. *IEEE TRANSACTIONS ON INFORMATION THEORY*, 46(2):388 – 404, MARCH 2000.

[255] Rahul Vaze. Percolation and connectivity on the signal to interference ratio graph. *Proceedings of IEEE INFOCOM*, pages 513 – 521, Orlando, FL, MARCH 2012.

[256] Tarun Joshi, Anindo Mukherjee, Younghwan Yoo, and Dharma P. Agrawal. Airtime fairness for ieee 802.11 multirate networks. *IEEE TRANSACTIONS ON MOBILE COMPUTING*, 7(4):513 – 527, APRIL 2008.

[257] Tao Han and N. Ansari. Powering mobile networks with green energy. *IEEE Wireless Communications*, 21(1):90–96, February 2014.

[258] R.P. Cox and H.D. Miller. *The Theory of Stochastic Processes, Chapter 5, pp. 203-251.* Taylor & Francis, 1977.

[259] William Feller. Diffusion processes in one dimension. *Transactions of the American Mathematical Society*, pages 1–31, 1954.

[260] Tadeusz Czachórski, Tomasz Nycz, and Ferhan Pekergin. Transient states of priority queues - a diffusion approximation study. *Fifth Advanced International Conference on Telecommunications, AICT '09*, pages 44–51, Venice, MAY 2009.

[261] Erol Gelenbe. On approximate computer system models. *Journal of the ACM*, 22(2):261–269, APRIL 1975.

[262] Toshikazu Kimura, Katsuhisa Ohno, and Hisashi Mine. Diffusion approximation for gi/g/1 queueing systems with finite capacity: I-the first overflow time. *J. of the Oprerations Research Society of Japan*, 22:41–68, 1979.

[263] Feng Shan, Junzhou Luo, Weiwei Wu, Minming Li, and Xiaojun Shen. Discrete rate scheduling for packets with individual deadlines in energy harvesting systems. *IEEE JOURNAL ON SELECTED AREAS IN COMMUNICATIONS*, 33(3):438–451, MARCH 2015.

[264] Alan V. Oppenheim and A. S. Willsky. *Signals and Systems, Chapter 2, pp. 74-174.* Prentice Hall, second edition, 1997.

[265] Will E. Leland, Murad S. Taqqu, Walter Willinger, and Daniel V. Wilson. On the self-similar nature of ethernet traffic (extended version). *IEEE/ACM TRANSACTIONS ON NETWORKING*, 2(1):1–15, FEBRUARY 1994.

[266] Zafer Sahinoglu and Sirin Tekinay. On multimedia networks: self-similar traffic and network performance. *IEEE Communications Magazine*, 37(1):48–52, JANUARY 1999.

[267] CISCO. Class-based weighted fair queueing and weighted random early detection. `http://www.cisco.com/c/en/us/td/docs/ios/12_0s/feature/guide/fswfq26.html`. [Online Available].